Aalto University
School of Engineering

Sebastian Muuronen

Seismic design of industrial bolted concentric brace connections

Master's Thesis submitted for examination for the degree of Master of Science in Technology.

Espoo 27.5.2019
Supervisor: Asst. Prof. Jarkko Niiranen
Advisor: D.Sc. Jussi Jalkanen

Aalto University
School of Engineering

Aalto University, P.O. BOX 11000, 00076 AALTO
www.aalto.fi

Abstract of master's thesis

Author Sebastian Muuronen

Title of thesis Seismic design of industrial bolted concentric brace connections

Master programme Building Technology **Code** ENG27

Thesis supervisor Asst. Prof. Jarkko Niiranen

Thesis advisor(s) D.Sc. Jussi Jalkanen

Date 27.5.2019 **Number of pages** 92 + 16 **Language** English

Abstract

In this thesis, the design of bolted concentric brace connections used in industrial structures located in seismic areas is studied. The dynamic nature of earthquake loads on structures induces multifaceted issues in the structural design of members and their connections. The structural requirements stipulated by three seismic design codes, Eurocode 8, AISC 341 and NCh2369 are discussed and compared to each other.

Different bolted connection designs of diagonal braces in concentrically braced frames are compared. They are evaluated in six performance categories: mass, cost, ease of design, ease of installation, mechanical simplicity and customer preference. By utilizing 3D models of the connections, their mass is calculated, and their cost is estimated by a feature-based costing method. The other aspects of the connections are evaluated via a survey targeting experienced structural designers. The strength of the connections was verified by using a software utilizing component-based finite element method.

Large differences in cost and weight are found between the different connection options. Generally, the connections of wide flange I-profile diagonal braces were found to be less expensive than the connections of hollow rectangular braces. However, special design consideration regarding the installation is required for connections featuring multiple different-sized I-profile braces and beams. Connections of diagonal braces featuring a hollow rectangular profile were found to be somewhat more flexible in terms of design and different brace sizes, although they were heavier and more expensive than their counterparts. Thus, no single ideal brace connection solution was found that could be employed in all industrial projects. The selection of a connection type depends on the most important criteria in a given project, as is outlined in the conclusions of this thesis.

Keywords Concentrically braced frame, SCBF, bolted connection, Eurocode 8, AISC 341, NCh2369, CBFEM

Aalto-yliopisto
Insinööritieteiden
korkeakoulu

Aalto-yliopisto, PL 11000, 00076 AALTO
www.aalto.fi

Diplomityön tiivistelmä

Tekijä Sebastian Muuronen		
Työn nimi Teollisuuslaitosten jäykistyssiteiden pulttiliitokset maanjäristysalueella		
Maisteriohjelma Building Technology		**Koodi** ENG27
Työn valvoja Apulaisprofessori Jarkko Niiranen		
Työn ohjaaja(t) TkT Jussi Jalkanen		
Päivämäärä 27.5.2019	**Sivumäärä** 92 + 16	**Kieli** Englanti

Tiivistelmä

Tässä diplomityössä käsitellään maanjäristysalueella sijaitsevien teollisuuslaitosten seinien jäykistyssiteiden pulttiliitosten suunnittelua. Maanjäristyksen aiheuttama dynaaminen kuormitus luo monitahoisia ongelmia rakenneosien ja niiden liitosten suunnitteluun. Kolmen seismisen suunnittelustandardin, Eurokoodi 8, AISC 341 ja NCh2369, asettamia vaatimuksia tarkastellaan ja vertaillaan keskenään.

Erilaisia keskeisesti jäykistettyjen kehien vinositeiden pulttiliitoksia vertaillaan keskenään. Liitosten ominaisuuksia arvioidaan kuudella eri osa-alueella: massa, hinta, suunnittelutyön helppous, asentamistyön helppous, lujuusopillinen yksinkertaisuus ja asiakkaan mielipide. Käyttämällä liitoksista tehtyjä 3D-malleja saadaan laskettua niiden paino, ja niiden hinta-arvio muodostetaan ominaisuusperusteisen kustannusarviointimenetelmän avulla. Liitosten muita ominaisuuksia arvioitiin kokeneille rakennesuunnittelijoille kohdennetun kyselytutkimuksen avulla. Liitosten kestävyys varmistettiin komponenttipohjaista elementtimenetelmää hyödyntävän ohjelmiston avulla.

Vertailtujen liitosten välillä havaittiin merkittäviä eroja niiden hintojen ja painojen välillä. Yleisesti ottaen I-profiilista valmistettujen vinositeiden liitokset olivat halvempia kuin suorakaidepoikkileikkausta hyödyntävien siteiden liitokset. I-profiilia käyttävien siteiden liitosten suunnittelu vaatii kuitenkin erityistä huomiota asennettavuuteen liittyen, kun liitokseen yhdistetään useita erikokoisia vinositeitä ja vaakapalkkeja. Suorakaidepoikkileikkauksisten vinositeiden liitosten havaittiin olevan joustavampia eri profiilikokojen ja suunnittelun suhteen, vaikkakin ne olivat vertailukohtiaan painavampia ja kalliimpia. Näin ollen ei pystytty valitsemaan yhtä sideliitosta, jota voitaisiin käyttää kaikissa tulevissa teollisuuslaitosprojekteissa. Liitostyypin valinta riippuu arviointiin käytetyistä kriteereistä, kuten on esitetty työn johtopäätöksissä.

Avainsanat Keskeisesti jäykistetty kehä, SCBF, pulttiliitos, Eurokoodi 8, AISC 341, NCh2369, CBFEM

Preface

This thesis was completed in cooperation with Sweco Structures Ltd, who also provided the interesting topic. The objective of this thesis was to form a better understanding of the criteria affecting the selection of the bolted brace connection type in the seismic design of concentrically braced frames. Through the analysis of different connection types, their applicability to future projects can be evaluated.

I would like to thank Jussi Jalkanen (D.Sc.) for providing the interesting topic and for advising me with the complex subject. The discussions and insight at challenging parts of the project were invaluable. I present my gratitude for Assistant Professor Jarkko Niiranen for supporting me with the selection of the thesis topic and for his guidance through the process.

I want to thank Jaakko Haapio (D.Sc.) for helping me to utilize his feature-based costing method and for providing me with more up-to-date unit cost data. A special thanks goes to HR Coordinator Laura Nevalainen for helping me to conduct the survey. Furthermore, I would like to thank my coworkers for all their help and input throughout the thesis.

Lastly, I would like to thank my friends and family who have supported me throughout my studies and during the thesis. Your encouragement and assistance have made my studies a lot more enjoyable. The financial support from the Foundation for Aalto University Science and Technology and Sweco Structures Ltd is gratefully acknowledged.

Espoo 27.5.2019

Sebastian Muuronen

Contents

Symbols

A	[mm^2]	cross section area
A^+	[mm^2]	area of the horizontal projection of the tension diagonal cross-section
A^-	[mm^2]	area of the horizontal projection of the compression diagonal cross-section
A_b	[mm^2]	nominal unthreaded body area of the bolt
A_{gv}	[mm^2]	gross area subjected to shear
A_{net}	[mm^2]	net cross section area
A_{nt}	[mm^2]	net area subjected to tension
A_{nv}	[mm^2]	net area subjected to shear
A_s	[mm^2]	tensile stress area of the bolt
$B_{p,Rd}$	[kN]	design punching shear resistance of the bolt head and the nut
$\mathbf{C}$	[Ns/m]	damping matrix
C_u	[kN]	critical buckling force for the first load cycle
C_u'	[kN]	critical buckling force for the second load cycle
E	[N/mm^2]	modulus of elasticity
$F_{b,Rd}$	[kN]	design bearing resistance per bolt
$F_{p,C}$	[kN]	design preload force
$F_{s,Rd}$	[kN]	deign slip resistance per bolt for the ultimate limit state
$F_{s,Rd,ser}$	[kN]	design slip resistance per bolt for the serviceability limit state
$F_{t,Ed}$	[kN]	design tensile force per bolt for the ultimate limit state
$F_{t,Ed,ser}$	[kN]	design tensile force per bolt for the serviceability limit state
$F_{t,Rd}$	[kN]	design tension resistance per bolt
$F_{v,Ed}$	[kN]	design shear force per bolt for the ultimate limit state
$F_{v,Ed,ser}$	[kN]	design shear force per bolt for the serviceability limit state
$F_{v,Rd}$	[kN]	design shear resistance per bolt shear plane
I	[mm^4]	second moment of area
I_e	[-]	importance factor
$\mathbf{K}$	[N/m]	stiffness matrix
L	[m]	unsupported length of the compressed bar
L_c	[mm]	effective buckling length of member
M	[kNm]	bending moment
$\mathbf{M}$	[kg]	mass matrix
M_b	[Nm]	bending moment at foundation
$M_{c,Rd}$	[kNm]	design bending resistance
M_{Ed}	[kNm]	design bending moment
$M_{j,Rd}$	[kNm]	ultimate limit bending resistance of the connection at 5% plastic strain
M_p	[kNm]	plastic bending moment
N_{cr}	[kN]	elastic critical force for the relevant buckling mode based on the gross cross sectional properties
N_{Ed}	[kN]	design normal force
$N_{Ed,E}$	[kN]	design normal force in the beam or in the column due to seismic actions
$N_{Ed,G}$	[kN]	design normal force in the beam or in the column due to non-seismic actions
$N_{Ed,i}$	[kN]	design normal force in diagonal brace i
$N_{net,Rd}$	[kN]	design plastic resistance of the net cross section at bolt holes

$N_{pl,Rd}$	[kN]	design plastic resistance to normal forces of the gross cross-section
$N_{pl,Rd,i}$	[kN]	design plastic resistance to normal forces of the gross cross-section of diagonal brace i in the system
$N_{u,Rd}$	[kN]	design ultimate resistance to normal forces of the net cross-section at holes for fasteners
P	[kN]	axial force
P_c	[kN]	expected compression resistance
P_M	[kNm]	required flexural strength of a connection
$P_{residual}$	[kN]	expected post-buckling compression resistance
P_v	[kN]	shear force resistance
P_y	[kN]	expected tension resistance
R	[-]	response modification coefficient
R_d	[kN]	design value of resistance for connections
R_{fy}	[kN]	design plastic resistance
$R_{n,b}$	[kN]	bearing resistance of the bolt hole
$R_{n,block}$	[kN]	block shear resistance
$R_{n,t}$	[kN]	tension resistance of the bolt
$R_{n,tear}$	[kN]	tearout resistance of the bolt hole
$R_{n,tv}$	[kN]	resistance to combined tension and shear of the bolt
$R_{n,v}$	[kN]	shear force resistance of the bolt
R_y	[-]	ratio of expected yield stress
S_1	[g]	mapped maximum considered earthquake spectral acceleration
S_a	[m/s^2]	pseudo-acceleration
S_d	[m]	peak deformation
S_{D1}	[g]	design, 5 percent damped, spectral response acceleration parameter at a period of 1 s
S_{DS}	[g]	design, 5 percent damped, spectral response acceleration parameter at short periods
S_j	[MNm/rad]	rotational stiffness of the connection
$S_{j,ini}$	[MNm/rad]	initial rotational stiffness of the connection calculated at 2/3 of limit capacity
$S_{j,P}$	[MNm/rad]	stiffness limit for pinned connection classification
$S_{j,R}$	[MNm/rad]	stiffness limit for rigid connection classification
S_v	[m/s]	pseudo-velocity
T_n	[s]	natural period of vibration
U_{bs}	[-]	block shear calculation parameter
V_b	[N]	shear force at foundation
$V_{eff,1,Rd}$	[kN]	design block tearing resistance
b	[mm]	width
c	[Ns/m]	viscous damping coefficient
d	[mm]	nominal bolt diameter
d_0	[mm]	hole diameter for a bolt
d_m	[mm]	mean of the across points and across flats dimensions of the bolt head or the nut, whichever is smaller
e	[-]	Euler's number
e_1	[mm]	end distance from the center of a fastener hole to the adjacent end of any part, measured in the direction of load transfer

e_2	[mm]	end distance from the center of a fastener hole to adjacent edge of any part, measured at right angles to the direction of load transfer
f_{cre}	[N/mm^2]	critical buckling stress using expected yield stress
f_e	[N/mm^2]	elastic buckling stress
f_{nt}	[N/mm^2]	nominal tensile stress of the bolt
f'_{nt}	[N/mm^2]	nominal tensile stress modified to include the effects of shear stress, of the bolt
f_{nv}	[N/mm^2]	nominal shear stress of the bolt
f_{rv}	[N/mm^2]	required shear stress resistance of the bolt
f_s	[N]	equivalent static force
f_u	[N/mm^2]	ultimate strength
f_{ub}	[N/mm^2]	ultimate tensile strength of the bolt
f_y	[N/mm^2]	yield strength
g	[m/s^2]	standard acceleration due to gravity
h	[mm]	height
i	[-]	imaginary unit
i	[-]	index
k	[N/m]	spring stiffness coefficient
k_1	[-]	bearing resistance calculation parameter
k_2	[-]	bearing resistance calculation parameter
k_{cr}	[-]	effective buckling length factor
k_s	[-]	slip resistance calculation parameter
l_s	[mm]	total connection length
m	[kg]	mass
n	[-]	a given number or the number of friction surfaces
p	[N]	external dynamic force
$\mathbf{p}$	[N]	external dynamic force vector
p_1	[mm]	spacing between centers of fasteners in a line in the direction of load transfer
p_2	[mm]	spacing measured perpendicular to the load transfer direction between adjacent lines of fasteners
q	[-]	behavior factor
r	[mm]	radius of gyration
t	[s]	time
t_p	[mm]	plate thickness
u	[m]	displacement
$\mathbf{u}$	[m]	displacement vector
$\bar{\mathbf{u}}$	[m]	displacement eigenvector
$\dot{u}$	[m/s]	velocity
$\dot{\mathbf{u}}$	[m/s]	velocity vector
$\ddot{u}$	[m/s^2]	acceleration
$\ddot{u}_g$	[m/s^2]	ground acceleration
$\ddot{\mathbf{u}}$	[m/s^2]	acceleration vector
x	[m]	position coordinate along the length of the brace
Δ	[m]	transverse displacement at brace midlength
Ω	[-]	multiplicative factor on axial force from the analysis due to the design seismic action, for the design of the non-dissipative members in concentric or eccentric braced frames

α_b	[-]	bearing resistance calculation parameter
α_d	[-]	bearing resistance calculation parameter
α_v	[-]	bolt shear resistance calculation parameter
γ_I	[-]	importance factor
γ_{M0}	[-]	partial safety factor for resistance of cross sections
γ_{M2}	[-]	partial safety factor for resistance of cross sections in tension to fracture or resistance of bolts
γ_{M3}	[-]	partial safety factor for slip resistance for the ultimate limit state
$\gamma_{M3,ser}$	[-]	partial safety factor for slip resistance for the serviceability limit state
γ_{ov}	[-]	overstrength factor
δ	[m]	axial deformation
ζ	[-]	damping ratio
$\bar{\lambda}$	[-]	non-dimensional slenderness
λ_1	[-]	rotation stiffness parameter for the first end of the compressed bar
λ_2	[-]	rotation stiffness parameter for the second end of the compressed bar
μ	[-]	slip factor
φ	[-]	resistance factor
ϕ	[mrad]	rotation
ϕ_c	[mrad]	rotation capacity
χ	[-]	reduction factor for the relevant buckling mode
ω_n	[1/s]	natural circular frequency

Abbreviations

2D	two-dimensional
3D	three-dimensional
AISC	American institute of steel construction
ANSI	American national standards institute
ASD	allowable stress design
CBF	concentrically braced frame
CBFEM	component-based finite element method
DCH	high ductility class
DCL	low ductility class
DCM	medium ductility class
DOF	degree-of-freedom
FEM	finite element method
HSS	hollow structural section
LRFD	load and resistance factor design
MDOF	multi-degree-of-freedom
N/A	not applicable
OCBF	ordinary concentrically braced frame
SCBF	special concentrically braced frame
SDOF	single-degree-of-freedom
PGA	peak ground acceleration

1 Introduction

1.1 *Background*

Earthquakes are some of the most destructive natural phenomena. On average, they cause ten thousand deaths and billions of dollars in economic losses annually (Elnashai & Di Sarno 2008). Therefore, the protection of human life and mitigation of financial losses are key issues in the design of structures in seismic areas.

The topic of design of structures against the effects of earthquakes is relatively well researched. Regional design codes have been stipulated to ensure adequate seismic performance of structures located in areas vulnerable to earthquakes. Those design codes have been updated throughout the years based on research and empirical evidence to further increase the safety of structures.

A common structural system used to resist lateral forces in a steel structure is the concentrically braced frame (see Figure 1). Such frames feature diagonal bracing members which stiffen the frame making it act as a truss. The behavior of the bracing members and their connections in earthquakes is a complex subject which has given rise to considerable amount of research on the topic. Furthermore, specific requirements are made to such structures in the design codes.

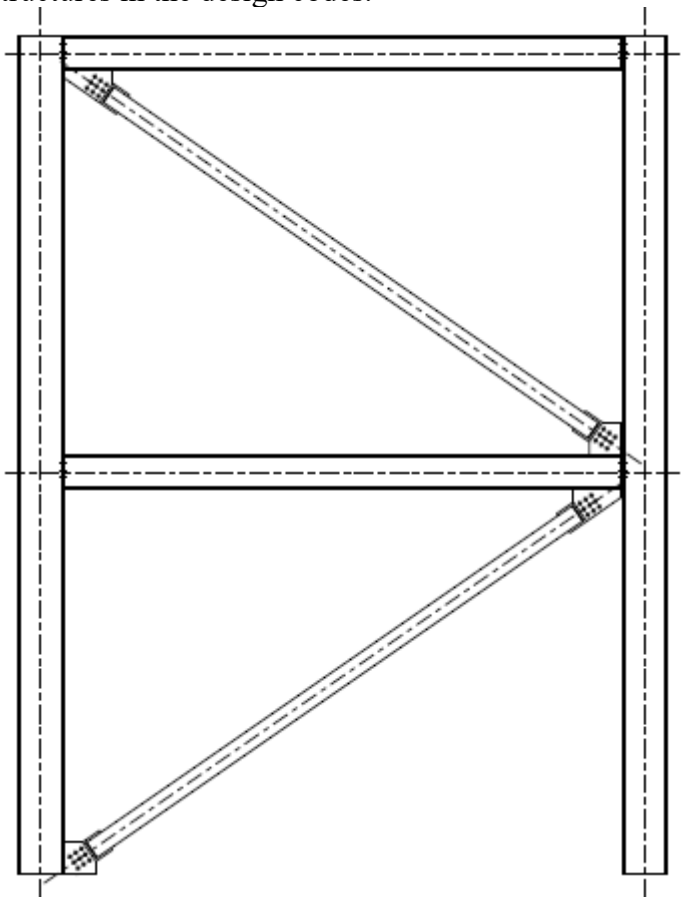

Figure 1. A steel concentrically braced frame featuring bolted gusset plate connections.

One of the most important features of earthquake-resistant structures is ductility. In this context, ductility refers to the capacity of the structure to deform before fracture or collapse.

To ensure sufficient ductility, the bracing members and their connections need to demonstrate adequate deformation capacity and avoid brittle failure. A large share of the research on the topic has concentrated on welded gusset plate connections, as those are commonly used in countries utilizing the American design code. A relatively smaller portion of the research has concentrated on bolted connections which are commonly used in other markets.

Many factors must be considered in the design of bolted concentric brace connections in seismic areas. Therefore, the structural design is laborious and time-consuming, which directly increases the cost of a building project. Furthermore, as the connections must transmit large forces, they tend to be large, heavy and expensive. The regulations in the different design codes are also somewhat dissimilar, which makes the design especially complicated in instances where the use of multiple clashing design codes is required. Relatively few research articles dealing with the cost and design aspects of seismic brace connections were found in the process of writing this thesis.

1.2 *Objectives and scope*

The main objective of this thesis is to establish a generic design solution for a bolted concentric brace connection to be used in seismic regions. While one solution might not be ideal for all scenarios, the pros and cons of different types of connections are compared. The aim of this research is to clarify the design criteria used in the selection of the connection type, and to emphasize the influence of the connection type on the performance of the structure.

The optimal connection would fulfill the regulations stipulated in many different design codes, would be easy to design and economical to manufacture. Oftentimes, the overall cost of a steel structure is evaluated based on its weight which has therefore become a performance criterion in itself. As the connection type affects the types of brace profiles that can be used, they are evaluated together as a whole in this thesis. Using I-profile braces is generally considered a less optimal solution in terms of material usage compared to hollow structural sections, but their connections are presumed to be simpler and more economical. The accuracy of this argument is discussed in this thesis.

The background information and general theory of seismic design is covered. The regulations of three different design codes regarding the design of concentrically braced frames are introduced and compared. By using the presented information, different brace connection design options are evaluated. Different aspects of their performance are investigated with the goal of finding a universal connection to be used in future projects.

The focus of this thesis is strictly limited to the behavior of concentrically braced frames only. Furthermore, diagonal braces and their bolted connections are discussed in more detail compared to columns and beams and their connections. Brace configurations where braces intersect each other (X-configuration) or a beam (V- or inverted V-configuration) are not discussed in depth. More novel solutions such as buckling restrained concentrically braced frames or base isolation structures are not covered.

2 Literature review

The relevant theoretical background and prerequisite information are presented in this chapter. First, the characteristics of earthquakes and basic structural dynamics principles are introduced. Next, the design and analysis methods used in seismic structural design are briefly discussed. Most of the theoretical background concentrates on the behavior of steel structures in earthquakes, after which the design requirements set in design codes are examined.

2.1 *Earthquake characteristics*

Earthquakes are manifested as shaking of the surface of the Earth, resulting from sudden release of energy in the Earth's crust. There are multiple different mechanisms and causes for earthquakes, but from the engineering point of view the most interesting ones are tectonic earthquakes. Therefore, this chapter is limited to earthquakes caused by tectonic plate movement. (Elnashai & Di Sarno 2008, p. 1.)

Tectonic plates are about 100 km thick, solid rock slabs which form the Earth's crust and a part of the upper mantle. The crust has a variable thickness of 25–60 km under continents and 4–6 km under oceans. The upper part of the mantle is composed of a relatively warm and soft layer of dense silicate rocks, which causes movements in the crust by convection currents. The velocity of the crust's movement is only about 1 to 10 cm per year, but it causes high stresses between tectonic plates moving differentially to one another. (Elnashai & Di Sarno 2008, p. 1.)

The stresses are mostly concentrated on tectonic plate boundaries, and that's where most earthquakes happen (Figure 2) due to brittle fracturing of the plates. Earthquakes are, however, not limited to tectonic plate boundary areas, as local small magnitude earthquakes can happen virtually anywhere and cause significant damage. High stresses from tectonic plate boundaries can be transmitted across the plates, where release of energy happens at locally weak zones of the crust. (Elnashai & Di Sarno 2008, pp. 1–5, Sucuoğlu & Akkar 2014, p. 8.)

Strong earthquakes occur relatively rarely. However, the frequency of occurrence of earthquakes that might influence a structure during its lifetime should be estimated. Current design codes deal with this uncertainty by utilizing probabilistic analysis. The acceptable level of damage in a building during an earthquake of certain strength can be determined, which affects the strictness of the design requirements. (Elnashai & Di Sarno 2008, Sucuoğlu & Akkar 2014, pp. 53–60.) This performance-based design ideology is discussed in chapter 2.5.

Earthquakes cause earth vibrations in both horizontal and vertical planes. However, in the design of buildings the horizontal component of ground acceleration is often the most significant. Horizontal acceleration of the ground causes lateral forces in the buildings, which generate high stresses in the lateral bracing system of the building. Moreover, the building's response to rapidly changing accelerations is highly dynamic, and therefore very different from ordinary static loads.

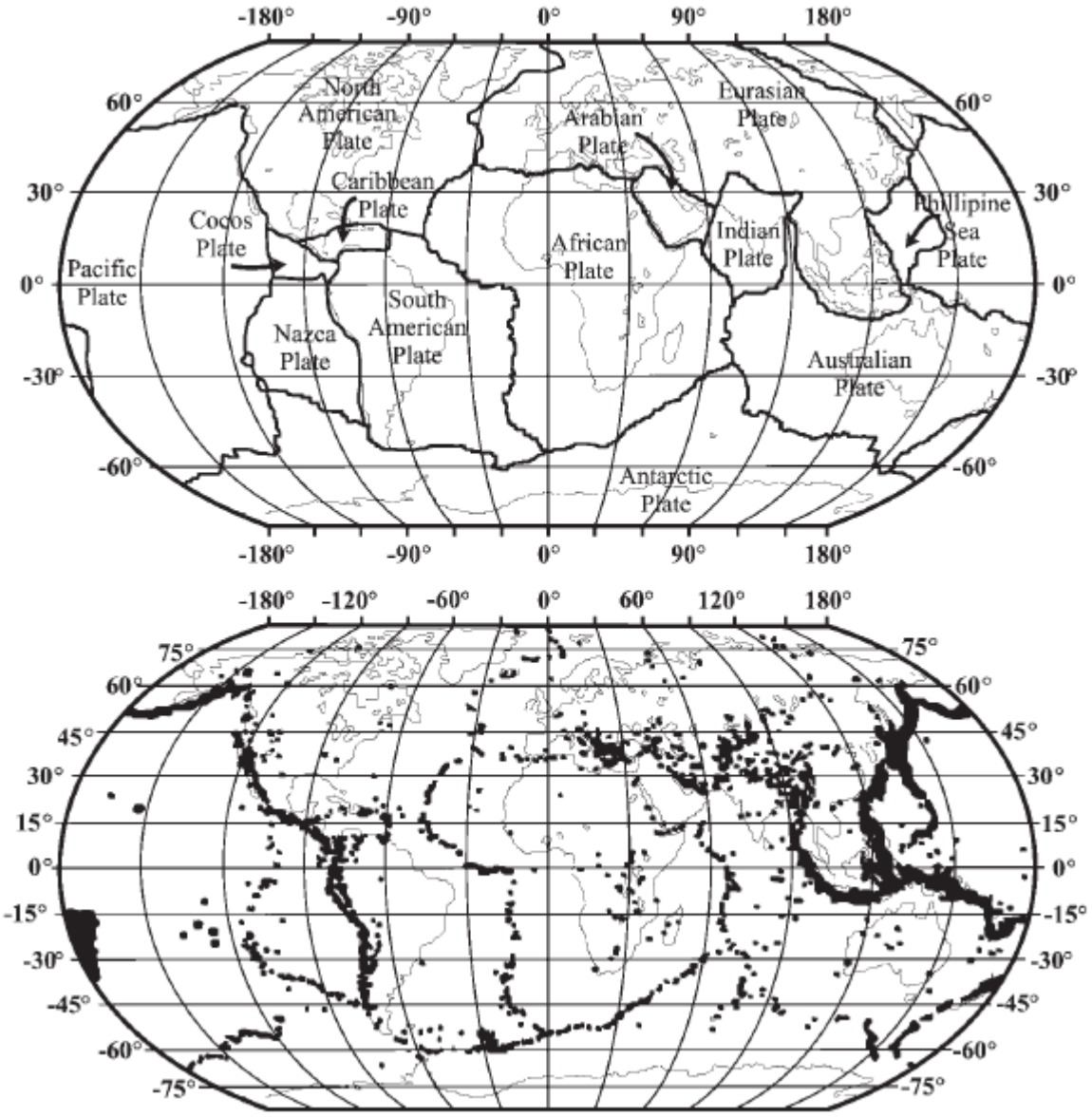

Figure 2. Tectonic plates (top) and worldwide earthquake distribution (bottom) (Elnashai & Di Sarno 2008, p. 3).

2.2 *Structural dynamics*

Earthquakes subject structures to rapidly changing accelerations which create dynamic forces. The structure's response to seismic loading is dynamic, and dynamic expressions are needed to capture this behavior in a mathematical representation. The basic principles of dynamics of structures are introduced in this chapter.

2.2.1 Single-degree-of-freedom systems

The nature of dynamic systems is studied by considering a simplified single-degree-of-freedom (SDOF) system. In this context, the degrees of freedom refer to the number of independent displacement variables needed to represent the total displacement of all the masses relative to their original position. The classical representation of a SDOF system is a mass-spring-damper system shown in Figure 3a. Displacement is denoted with letter u, and its differentiation with respect to time is marked with the overdot notation. Therefore, $\dot{u}$ and

$\dot{u}$ denote the velocity and the acceleration of the mass, respectively. (Chopra 2011, pp. 7–20, Duggal 2013, p. 55.)

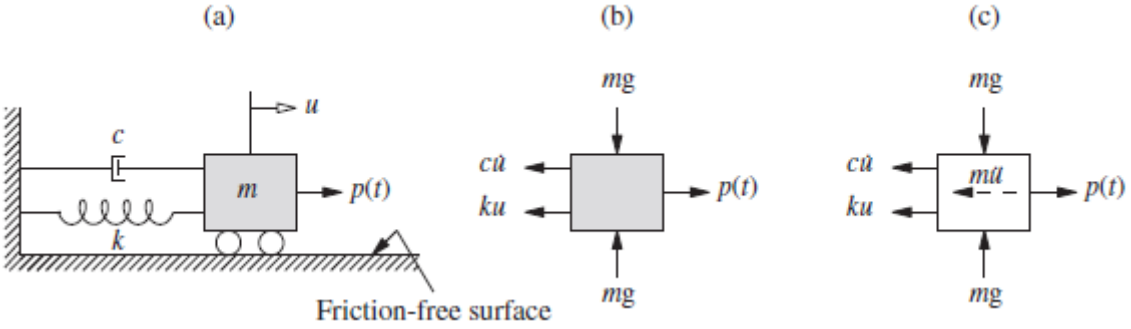

Figure 3. Mass-spring-damper representation of a SDOF system (Chopra 2011, p. 20)

The system consists of a rigid mass resting on a frictionless surface. The mass is connected to the adjacent wall by a linear elastic spring and a linear viscous damper. The horizontal displacement of the mass is examined when it is subjected to an external excitation force. Equilibrium of forces on the mass is shown in Figure 3b. If the sum of external forces does not equal zero, the mass starts accelerating, and its inertial force is added to the equation (Figure 3c). The effect of these forces can be considered by utilizing Newton's second law of motion which states that the sum of external forces equals the mass of the system times its acceleration in the direction of the force resultant. The resulting dependence is shown in equation 1. (Chopra 2011, pp. 19–20, Duggal 2013, pp. 55–56.)

$$m\ddot{u}(t) + c\dot{u}(t) + ku(t) = p(t) \tag{1}$$

where
m is the mass of the system [kg]
c is the viscous damping coefficient [Ns/m]
k is the spring stiffness coefficient [N/m]
$p(t)$ is the external dynamic force at time t [N]

The mass-spring-damper representation can be used to describe a simple structural system. Consider a one-story frame structure, where all mass is concentrated at the roof level (Figure 4). The stiffness of the system is provided by the massless frame elements (columns and a beam) and all its damping is provided by a linear viscous damper. The mass, stiffness and damping of an actual structural system is provided by all its members. However, in this idealized system these components are separated. With these simplifications, it is now possible to study the dynamic response of the structural system with equation 1. (Duggal 2013, p. 55.)

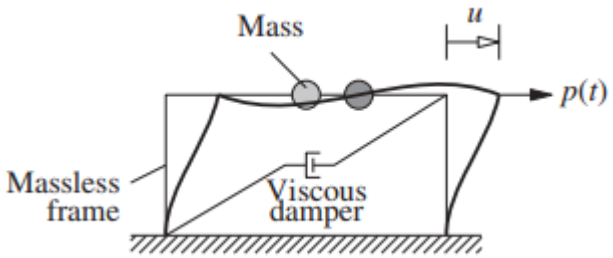

Figure 4. SDOF representation of a single-story frame structure (adapted from Chopra 2011, p. 7).

If the viscous damper and the external excitation force are removed from the system, its free vibration can be studied. Initial displacement and velocity are given to the mass at time zero, which causes the system to oscillate harmonically (Figure 5). The governing equation for the displacement of the system is given below (equation 2) and plotted to Figure 5. The derivation of equation 2 is shown by Chopra (2011, pp. 39–40, 46).

$$u(t) = u(0)cos\omega_n t + \frac{\dot{u}(0)}{\omega_n} sin\omega_n t \tag{2}$$

where

$$\omega_n = \sqrt{\frac{k}{m}} \tag{3}$$

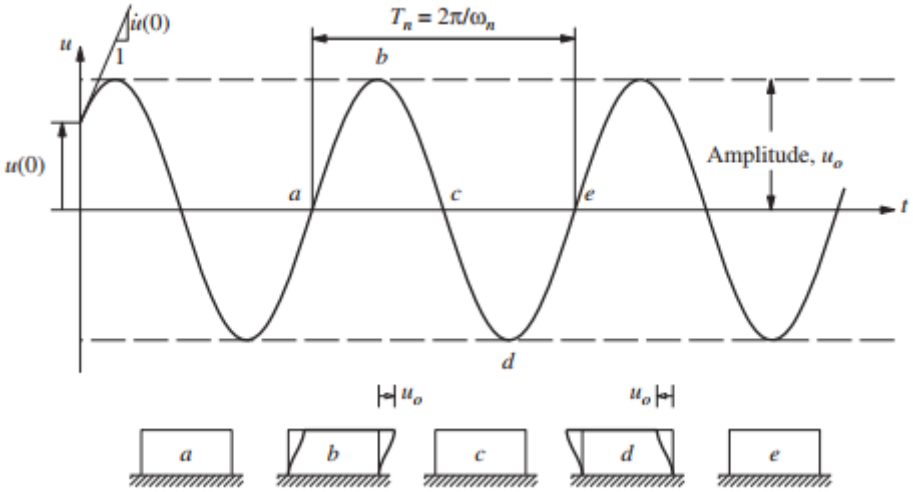

Figure 5. Free vibration of an undamped SDOF system (Chopra 2011, p. 40).

The time it takes for the undamped system to complete one full cycle of free vibration is denoted as T_n [s]. It is called the natural period of vibration of the system, and it is related to the natural circular frequency of the system, ω_n [1/s], as shown in equation 4. (Chopra 2011, p. 41, Duggal 2013, p. 58.)

$$T_n = \frac{2\pi}{\omega_n} \tag{4}$$

When external excitation force is set to zero in equation 1, and it is divided by mass, the equation gets the form given in equation 5. The equation now contains a new variable, ζ [-] which denotes the damping ratio. In other words, it shows the fraction of the system's damping in relation to the critical damping. A comparison of free vibration of critically damped, underdamped and overdamped systems are shown in Figure 6. (Chopra 2011, p. 48, Duggal 2013, p. 60.)

$$\ddot{u} + 2\zeta\omega_n\dot{u} + \omega_n^2 u = 0 \tag{5}$$

where

$$\zeta = \frac{c}{2m\omega_n} \tag{6}$$

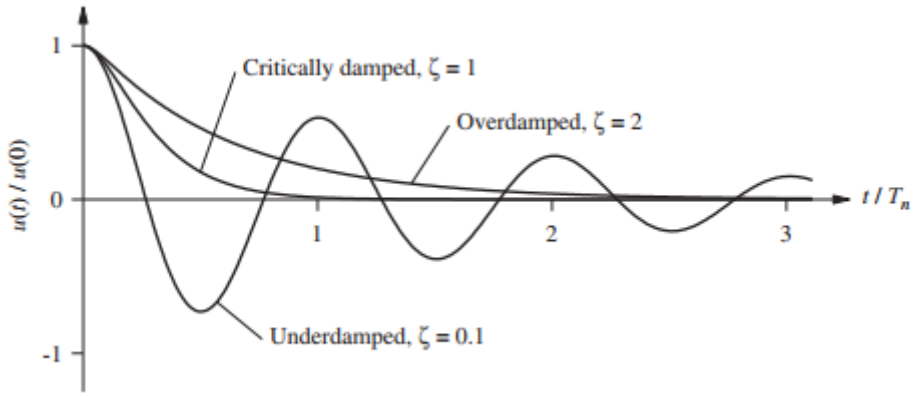

Figure 6. Free vibration damped systems (Chopra 2011, p. 49)

Undamped systems in free vibration will retain the amplitude of motion without needing any excitation apart from the initial disturbance. Therefore, damped systems will tend towards zero displacement. Critically damped and overdamped systems will stop vibrating before completing even one full cycle of motion. Underdamped systems will continue oscillating until amplitude is eventually reduced to zero. The rate at which free vibration decays depends on the damping ratio (Figure 7). Buildings are underdamped structures, with damping ratios typically less than 0.1 (Chopra 2011, p. 49, Duggal 2013, pp. 60–61.)

When ground acceleration is used as the external excitation in equation 5, the resulting equation is

$$\ddot{u} + 2\zeta\omega_{\mathrm{n}}\dot{u} + \omega_{\mathrm{n}}^2 u = -\ddot{u}_{\mathrm{g}}(t) \tag{7}$$

where $\ddot{u}_{\mathrm{g}}(t)$ is ground acceleration [m/s^2]

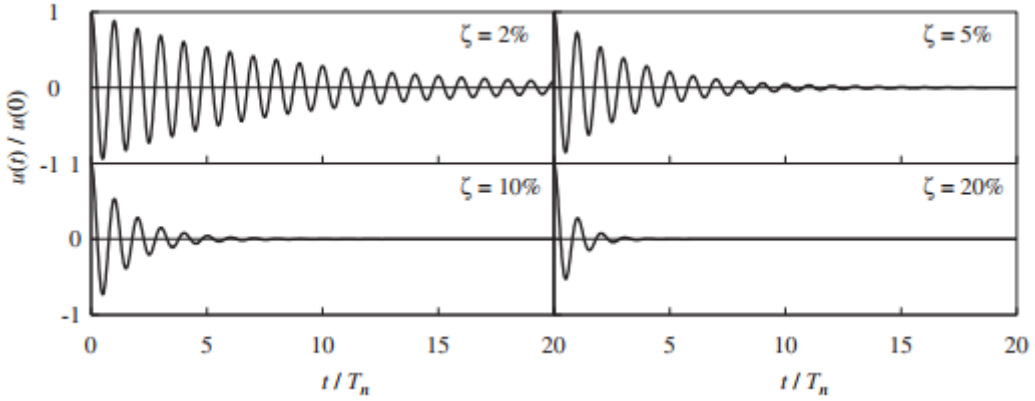

Figure 7. Free vibration of underdamped systems with different damping ratios (Chopra 2011, p. 51).

It is evident in equation 7 that at any given time t the displacement response of the system $u(t)$ is only dependent on its natural frequency ω_{n} and damping ratio ζ. This means that any system with equal natural frequency and damping ratio will have an equal displacement response, regardless of its mass or stiffness. Since natural period T_{n} is related to ω_{n} by relation shown in equation 4, it can also be used to determine system response. (Chopra 2011, p. 203.)

2.2.2 Multi-degree-of-freedom systems

Since real structures are rarely simple enough to be represented by SDOF systems, more advanced models are needed. Multi-degree-of-freedom (MDOF) systems are based on the same ideology as SDOF systems, but as the name states, there are multiple degrees of freedom to solve.

MDOF systems can be represented with a similar mass-spring-damper system as SDOF systems. A simple two-degree-of-freedom system is represented by a mass-spring-damper configuration in Figure 8a. Any finite number of degrees of freedom could be added to this system to represent an MDOF system. As is evident in Figure 8, the two system masses are linked together by the spring and the viscous damper. Therefore, their displacements, velocities and accelerations are dependent on each other. (Chopra 2011, pp. 350–351.)

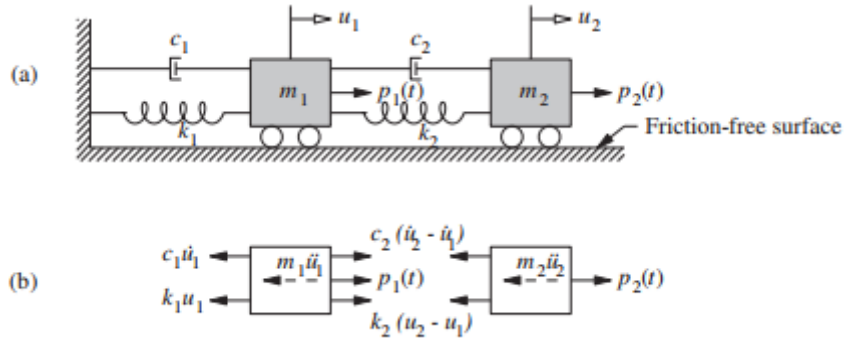

Figure 8. Two-degree-of-freedom representation of an MDOF system (a) and free-body diagrams (b) (Chopra 2011, p. 351).

An MDOF system has multiple degrees of freedom which are coupled, and therefore must be solved simultaneously. The number of ordinary differential equations needed to solve the response of the system equals the number of independent degrees of freedom. Therefore, the equations of motion are often given in a matrix representation shown in equation 8. (Chopra 2011, p. 350, Strømmen 2014, pp. 281–282.)

$$\mathbf{M}\ddot{\mathbf{u}}(t) + \mathbf{C}\dot{\mathbf{u}}(t) + \mathbf{K}\mathbf{u}(t) = \mathbf{p}(t) \tag{8}$$

where **M** is the mass matrix [kg]
C is the damping matrix [Ns/m]
K is the stiffness matrix [N/m]
p(t) is the excitation force vector [N]
ü is the acceleration vector [m/s^2]
u̇ is the velocity vector [m/s]
u is the displacement vector [m]

The vibration of a point mass in an MDOF system is not necessarily harmonic with the vibration of the other point masses in the system, and therefore the overall frequency of motion of the system cannot be determined. It is however possible to initiate free vibrations in an MDOF system by introducing deflections in the DOFs in such a way, that it will vibrate harmonically, maintaining the initial deflected shape. An MDOF system will have multiple deflected shapes which will initiate harmonic vibrations (see Figure 9). These shapes are referred to as natural modes of vibration. In fact, the number of natural modes of vibration

will always be equal to the number of degrees of freedom (Chopra 2011, p. 405, Strømmen 2014, p. 11.)

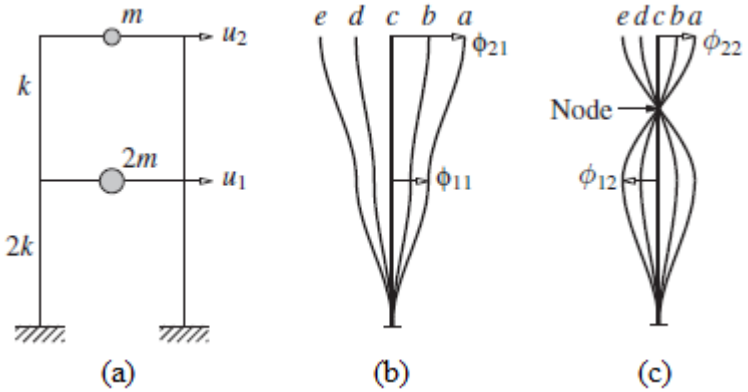

Figure 9. Free vibration of an undamped system in its first two natural modes of vibration. (a) two-story frame; (b) deflected shapes at time instants a, b, c, d and e in the first natural mode; (c) deflected shapes at time instants a, b, c, d and e in the second natural mode (adapted from Chopra 2011, pp. 405–406).

An MDOF system has multiple (n) natural modes of vibration, all of which have a unique natural period of vibration T_n. Therefore, the natural frequency ω_n is determined for each natural mode separately. The natural mode with the longest natural period is referred to as the first natural mode. (Chopra 2011, pp. 405–406.) The natural modes of a system are often solved by numerical methods using finite element software.

Free vibrations of an undamped MDOF system can, however, be presented simply as

$$\mathbf{M}\ddot{\mathbf{u}}(t) + \mathbf{K}\mathbf{u}(t) = \mathbf{0} \tag{9}$$

To find the free vibration response, the harmonic response is assumed in the form

$$\mathbf{u}(t) = \bar{\mathbf{u}}\mathrm{e}^{\mathrm{i}\omega t} \tag{10}$$

where $\bar{\mathbf{u}}$ is a constant displacement vector (eigenvector) to be solved [m]
e is the Euler's number [-]
i is the imaginary unit [-]

Substituting the solution presented in equation 10 into equation 9 results in a generalized discrete eigenvalue problem

$$(\mathbf{K} - \omega^2\mathbf{M})\bar{\mathbf{u}} = \mathbf{0} \tag{11}$$

Non-trivial solutions for the equation can be found when

$$\det(\mathbf{K} - \omega^2\mathbf{M}) = 0 \tag{12}$$

which gives n eigensolutions, i.e., eigenvalue-eigenvector pairs

$$(\omega_i, \bar{\mathbf{u}}_i), i = 1, \dots, n \tag{13}$$

for stiffness and mass matrices of size n x n.

2.3 *Seismic design and analysis*

The characteristics of an earthquake (ground acceleration, velocity, displacement) can be measured. Plots containing information on ground acceleration, velocity and displacement are called time histories. Time history data can be used to evaluate the characteristics of a specific earthquake. However, simply knowing the ground-motion characteristics does not give information on the dynamic response of different structures. The dynamic response of individual systems can be evaluated for a given ground motion (Figure 10). As separate plots have to be constructed for each system, the comparison between systems can be cumbersome. Therefore, diagrams called response spectra are used to describe the dynamic response of all possible linear SDOF systems to a certain component of ground motion (Chopra 2011, p. 207).

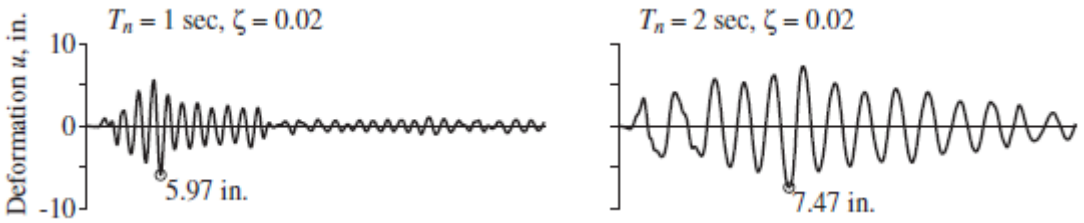

Figure 10. Deformation response of two SDOF systems to El Centro earthquake (1940) ground motion (adapted from Chopra 2011, p. 205).

The shape of the response spectra is influenced by many factors, including the magnitude of the earthquake, source mechanism, distance from source, wave travel path and soil conditions. It is often hard to determine all factors affecting the earthquake and the dynamic response of structures. Therefore, seismic design codes often recommend response spectra that are dependent only on peak ground-motion parameters and the soil condition. (Elnashai & Di Sarno 2008, p. 130.)

A response spectrum is usually plotted for the peak value of a response quantity, such as displacement, as a function of the natural vibration period T_n (Figure 11). Since the dynamic response of a linear SDOF system is also dependent on its damping ratio, as shown in equation 7, separate plots must be created for different damping ratios. (Chopra 2011, p. 207.)

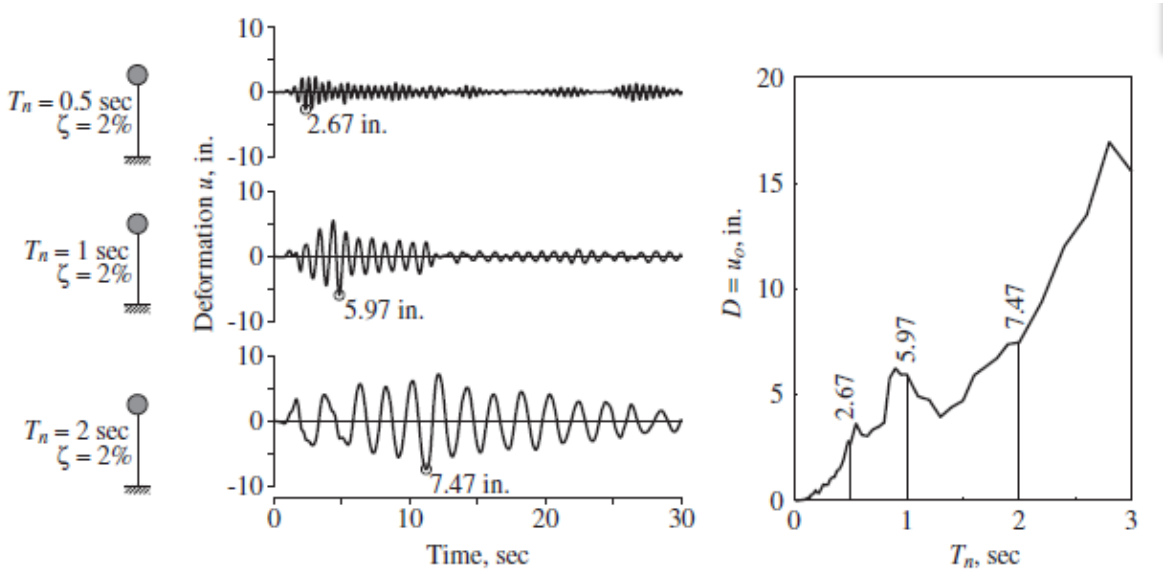

Figure 11. Deformation response spectrum (right) constructed from SDOF system response peak values (left) (adapted from Chopra 2011, p. 209).

The deformation response history of a system can be used to determine the forces affecting the system at a given time instant. One method for such an analysis is the equivalent static force method shown in Figure 12 and expressed mathematically in equation 14. The reactions at foundation, i.e., the base shear $V_b(t)$ [kN] and the base overturning moment $M_b(t)$ [kNm], are calculated at each time instant separately via static analysis. (Chopra 2011, p. 206.)

$$f_s(t) = m\omega_n^2 u(t) \tag{14}$$

where $f_s(t)$ is the equivalent static force at time t [N]

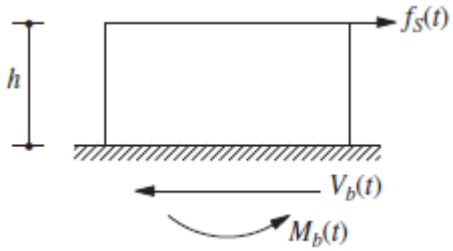

Figure 12. Equivalent static force and reactions at foundation at time t (Chopra 2011, p. 206).

As can be interpreted from equation 14, only the deformation response spectrum is needed to determine peak internal forces and peak deformations in the structural system. However, two related spectra called pseudo-velocity and pseudo-acceleration response spectra can be useful in seismic design. (Chopra 2011, p. 208.) The names of the spectra are intended to show that they do not in fact describe the actual velocity and acceleration of a structure at a time t but are instead related directly to the deformation response spectrum. This is because the deformation response spectrum contains only peak values of deformations for systems with different periods of natural vibration, instead of the response of an individual structure. (Tapan 2009, p. 143.)

Peak deformation S_d [m], pseudo-velocity S_v [m/s] and pseudo-acceleration S_a [m/s^2] are related by the following equation

$$S_a = \omega_n S_v = \omega_n^2 S_d \tag{15}$$

As is evident from the relation, pseudo-velocity and pseudo-acceleration spectra contain no additional information over the deformation response spectrum. However, pseudo-velocity spectrum is directly related to the kinetic energy stored in the structure, and pseudo-acceleration spectrum is related to the peak equivalent static force. Therefore, all three spectra can be used simultaneously for quick assessment of the dynamic response of a structure. (Chopra 2011, p. 212, Tapan 2009, p. 143.)

When designing new structures in seismic areas, the severity of future earthquakes must be somehow estimated. Using ground-motion data from a recorded past earthquake in design is not sufficient, as future earthquakes might be very different. For example, the dominant frequencies might be dissimilar, causing vastly different response spectra. Generally, the response spectra used in design should be representative of past earthquakes in the area. The design spectrum is therefore based on statistical analysis and normalization of past earthquakes. (Chopra 2011, pp. 230–231.) However, the design spectra also include features that are decided by code committees and other parties, making them not entirely based on measurable data (Elnashai & Di Sarno 2008, p. 151).

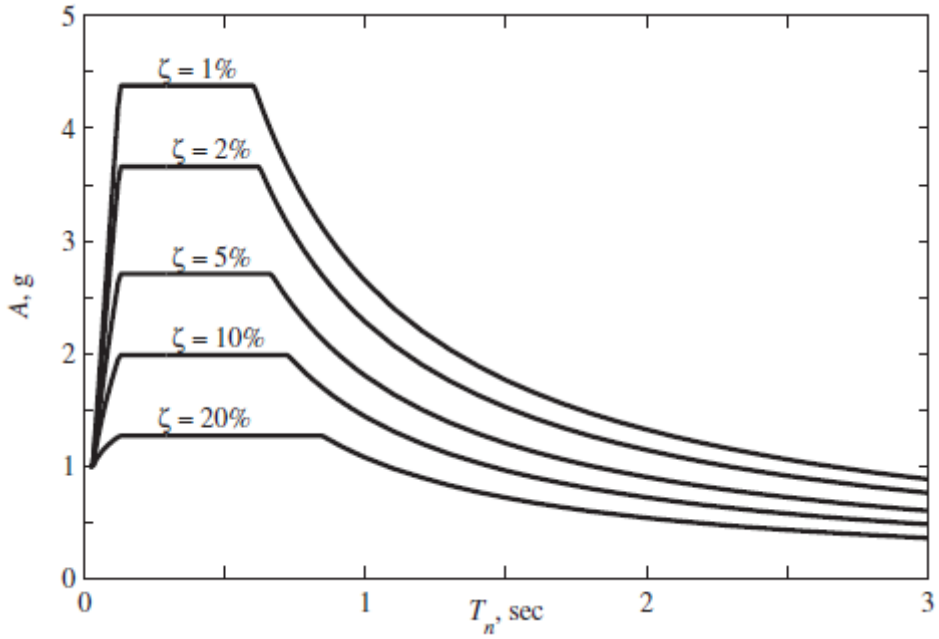

Figure 13. Example of a pseudo-acceleration design spectrum (Chopra 2011, p. 238).

The elastic design spectrum is used to estimate the peak response of structures that stay fully elastic during the earthquake (Chopra 2011, p. 238). Elastic design spectrum is often plotted for pseudo-acceleration (Figure 13), as it can be readily used to estimate peak forces. The elastic design spectrum can also be used to estimate peak response of an MDOF system by considering each of its natural mode separately. It should be noted that structures rarely remain completely elastic in strong earthquakes. Therefore, the design forces suggested by the elastic design spectrum can often be reduced (Bruneau et al. 2011, pp. 312–313).

2.4 *Characteristics of steel structures in seismic applications*

A structure exhibiting a fully elastic response to an earthquake experiences strong forces, that might be difficult to combat in elastic design. In such cases, the magnitude of forces encountered in seismic design can easily govern the design process. However, the forces considered in seismic design can be significantly smaller than those encountered in the elastic response of the structure. This is possible due to the highly nonlinear material properties of yielding steel. Predetermined parts of the structural system are designed to yield at lower forces and dissipate seismic energy as heat through a hysteretic behavior. Hysteretic behavior of single braces is presented in chapter 2.4.2. Through yielding of designated elements in the structure, the rest of the system experiences lower forces and can remain elastic. This design principle is referred to as capacity design. (Bruneau et al. 2011, p. 502.)

2.4.1 Concentrically braced frames

Concentrically braced frames (CBF) are a type of braced frame structure, where both ends of the brace join at the end points of other framing members to form a truss (Sabelli et al. 2013). Concentrically braced frames should not be confused with eccentrically braced frames, which are based on another structural concept and require different design steps. Some variations of concentrically and eccentrically braced frames are shown in Figure 14.

CBFs are expected to dissipate energy in earthquakes through hysteretic behavior of their bracing members. In simpler terms, the axially loaded braces are expected to yield in tension, and buckle in compression (Figure 15). If the earthquake is modeled as a purely horizontal, reversing cyclic load, each diagonal brace will go through successive cycles of buckling followed by tension yielding. Their connections must be designed to withstand this type of loading and repetitive yielding to ensure that no plastic deformations happen in members carrying gravity loads, i.e., beams and columns. (Bruneau et al. 2011, pp. 502–503, Lumpkin et al. 2012, Shen et al. 2017.)

The compression strength of a diagonal brace is degraded through repetitive buckling, which causes it to buckle at lower compression forces during successive load cycles. This causes a higher percentage of the lateral load to be carried by diagonal braces in tension instead. Early seismic design practice preferred the use of less slender braces to mitigate strength degradation in buckling. However, it was later found that such stocky braces would be more susceptible to low-cycle fatigue induced brittle failure. The more recent ideology therefore prefers the use of more slender braces, relying more on the tensile braces to dissipate energy. (Bruneau et al. 2011, pp. 503–504, Fell 2008, p. 242.)

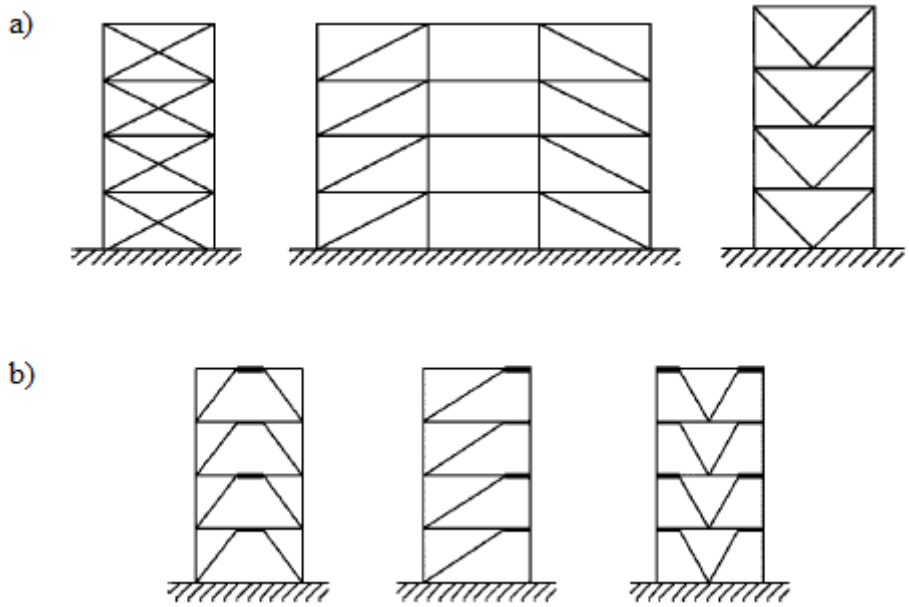

Figure 14. Examples of concentrically (a) and eccentrically (b) braced frames (adapted from SFS-EN 1998-1 2004, p. 142).

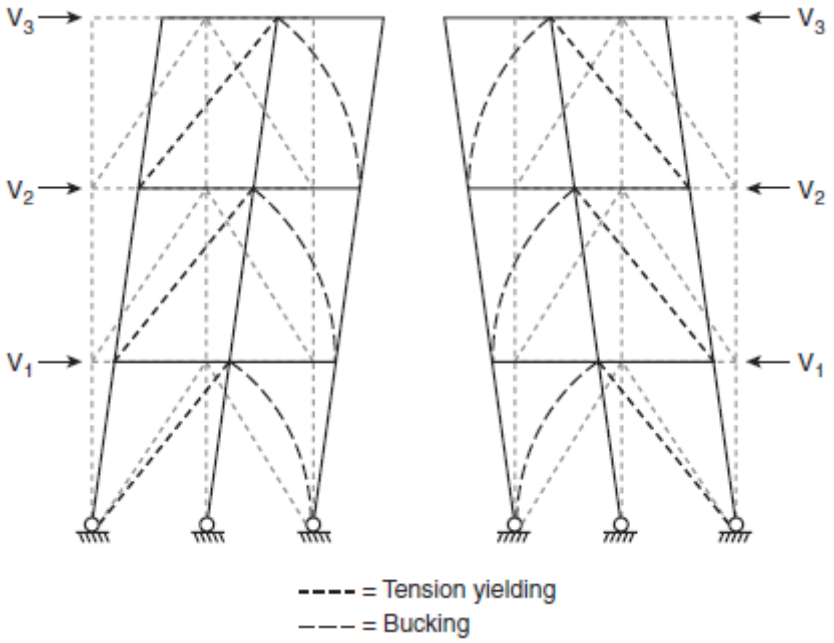

Figure 15. Brace yielding and buckling under lateral load V (Bruneau 2011, p. 502).

Different concentric brace configurations utilize different load paths. For example, the V-braced frame (Figure 14a, right) transfers vertical forces to the beams, which must be considered together with gravity loads in design. This behavior is not found in configurations where the diagonal braces connect directly to the columns. However, irrespective of brace configuration, the redistribution of forces in the frame must be recognized, as braces weaken in cyclic loading (Bruneau 2011, p. 506). Columns supporting the braces and beams intersected by the braces have also been shown to develop early yielding due to the brace forces, and therefore a higher level of ductility is required from them (Shen et al. 2017).

Modeling the brace connections as either pinned or fixed is somewhat inaccurate. Therefore, more accurate analytical models have been proposed. Hsiao et al. (2012) proposed a modeling approach for gusset plate connections, which includes nonlinear rotational springs combined with multiple rigid end zones and fully nonlinear beam-column elements for all members (Figure 16). The model provides accurate estimates of compressive capacity of the brace and its post-buckling deformation, as well as the distribution of deformation between stories of multi-story frames. Typical fixed-end brace models tend to significantly overestimate the compressive strength of the brace and the deterioration of resistance in post-buckling deformation. Similarly, pinned-end brace models significantly underestimate the compressive resistance of the brace. (Hsiao et al. 2012.) Nevertheless, pinned-end and fixed-end models are widely used in the structural design industry due to their simplicity.

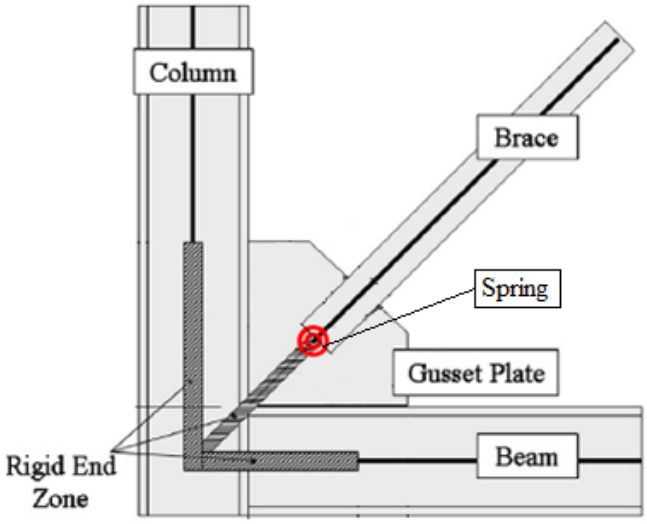

Figure 16. Improved analytical model for CBF gusset plate connections featuring rigid end zones and nonlinear rotational springs (adapted from Hsiao et al. 2012).

2.4.2 Hysteresis of bracing members

The way in which axially loaded braces can dissipate energy is shown in Figure 17. The sample brace is simply supported, and it is loaded axially. The horizontal axis of the graph shows axial deformation δ [mm], and the vertical axis shows the applied axial force P [kN]. In addition, transverse displacement at brace midlength is denoted with Δ [m]. Tensile axial force is taken as positive and compressive axial force as negative. Similarly, the corresponding axial deformations are taken as positive for lengthening and negative for shortening. Critical buckling force is shown with C_u and C_u' for the first and second load cycles, respectively. Points O and A-G are used in the diagram to distinguish important parts of the cycle. (Bruneau 2011, pp. 506–507.)

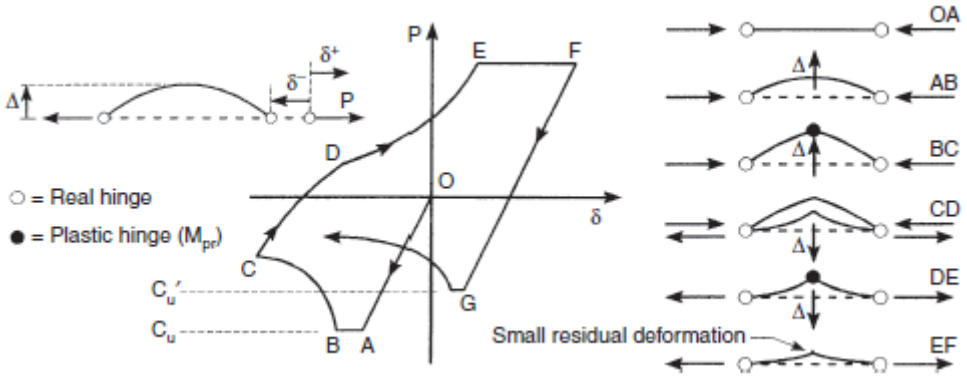

Figure 17. Hysteresis curve of a brace under cyclic axial loading (Bruneau 2011, p. 506).

The idealized model in Figure 17 shows how the brace compresses in a linear elastic fashion along line OA. The brace buckles at point A, as compressive force P reaches value C_u. As the brace buckles, additional axial shortening takes place with no further increase in compressive force (segment AB). As the transverse displacement increases, the brace is subjected to growing bending moment. The bending moment at any point x along the length of the brace is calculated according to equation 16. As the compressive force P is constant along the length of the brace at any given time, the maximum bending moment is located at brace midlength. (Bruneau 2011, p. 507.)

$$M(x) = \Delta(x) * P \tag{16}$$

where x is the position coordinate along the length of the brace [m]
$M(x)$ is the bending moment at point x [kNm]
$\Delta(x)$ is the transverse displacement at point x [m]
P is the axial force [kN]

When a bilinear elastic-perfectly plastic material model is assumed for the brace, plastic moment will eventually be reached at midlength (point B). As the moment cannot be higher than the plastic moment, any further increase in transverse displacement must be accompanied by a decrease in compression force (segment BC). The nonlinear path from point B to point C is a consequence of bending moment and axial force interaction, where decreasing axial force increases the bending moment capacity of the brace. As the brace is unloaded, residual axial deformation is retained, along with a kink due to the plastic rotations. (Bruneau 2011, p. 507.)

After unloading the brace is subjected to a tensile force. The brace starts extending but will again develop a plastic hinge at midlength (point D) due to the axial force and transverse displacement. The rotations at the plastic hinge are now acting in reverse direction, reducing the transverse displacement. Therefore, the tensile axial force is increasing while the bending moment remains constant at the plastic hinge (segment DE). Increasing tensile force will reduce the magnitude of the transverse displacement, until the brace reaches its tension yielding capacity, after which the axial force remains constant, while the brace is axially elongated (segment EF). It is not possible to completely remove the kink before tension yielding happens, since the theoretical force required to completely straighten the brace tends to infinity. (Bruneau 2011, pp. 507–508.)

Upon unloading the brace will shorten elastically, but it will retain some axial deformation, along with transverse displacement. As the brace is subjected to another load cycle, it will behave in a similar manner as before. However, having retained some of the deformation, the brace will buckle at a smaller compressive force: $P = C_u$' (point G). The shape of the hysteresis curve will remain similar in successive load cycles but buckling will happen at lower forces (shorter segment OA), and the elastic buckling plateau (segment AB) shortens. (Bruneau 2011, p. 508.)

Energy dissipation capacity of a brace is determined by the shape of the hysteretic curve. The larger the surface area enclosed inside the curve, the more energy the brace dissipates as heat. More slender braces will buckle with lower compression forces, leaving their energy dissipation capacity in compression quite limited. Less slender, stocky braces will have a higher energy dissipation capacity in compression but might not always be the optimal choice due to low-cycle fatigue, as discussed in chapter 2.4.1. (Chen & Tirca 2013, Fell 2008, p. 242.)

2.4.3 Brace connections

As explained before, the bracing members of a CBF are expected to successively yield and buckle when subjected to strong earthquake loads. Therefore, the connections between the braces and the frame should be able to resist such forces. Large transverse displacements in the frame and brace buckling will also require relatively large clearance in the joint area to allow unrestricted member rotations. (Tamboli 2016, p. 329.)

Connections are needed to join structural elements together in the entire frame. The scope of this thesis is limited to connections joining diagonal braces to the intersection of columns and beams. Thus, brace configurations such as the V-brace (Figure 14a, right) connecting diagonal braces to the middle of the beams are not further discussed. Furthermore, only bolt connections are covered in detail.

A typical solution for joining diagonal braces to the other framing members is the gusset plate connection (Figure 18). The gusset plate is typically welded to the beam and the column, and either bolted or welded to the diagonal brace. Gusset plate connections are used because they are easier to design and construct than fully restrained brace end connections. However, the design of gusset plate connections meeting all seismic criteria is strenuous, and research has shown that they might not show intended behavior in an earthquake. (Roeder et al. 2011.)

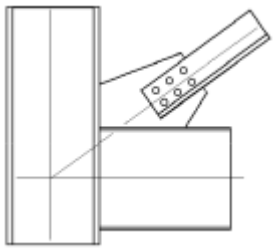

Figure 18. Typical bolted gusset plate brace connection (Roeder et al. 2006).

In simplified terms, the brace connection must be designed such that it retains its strength in cyclic earthquake loading, and that the connection does not fail before the brace. There are numerous failure mechanisms through which a connection can fail. Failure mechanisms exhibiting ductile behavior instead of sudden, brittle failure are preferred. Current design

codes require that a connection has sufficient strength in all relevant failure mechanisms, in order to promote more favorable failure mechanisms, such as brace fracture. (Roeder et al. 2011.) This type of design ideology promotes the idea that certain predetermined elements of a structural system endure inelastic deformations to preserve elasticity in the rest of the system.

Brace post-buckling hysteretic behavior is typically chosen as the primary energy dissipation method, while the connections are expected to remain elastic. Braces buckling out of the plane of the frame require significant rotation capacity from a gusset plate connection. This is accounted for in some design standards by providing a nominal clearance in the gusset plate. The current design ideology is based on capacity design principles but does not necessarily ensure sufficient system ductility and inelastic deformation capacity (Roeder et al. 2006, Roeder et al. 2008). The effects of frame distortions resulting from large story drifts are also generally neglected in design codes and therefore rarely considered in connection design (Thornton & Muir 2009).

Roeder et al. (2011) have proposed a balanced design procedure for braced frame connections to ensure adequate seismic performance. The balanced design procedure is based on the principle of balancing various yield mechanisms in the system, to maximize ductile yielding and drift capacity of the frame. The procedure utilizes complementary yielding mechanisms such as gusset plate yielding together with the primary yield mechanism, brace buckling. The higher degree of control in failure mechanism hierarchy is expected to reduce the occurrence of unintended failure modes. Despite the promising research and test results, the balanced design procedure is not widely used in practice. This is partly because balancing of failure mechanisms is deemed complex and somewhat uncertain. (Lehman et al. 2004, Roeder et al. 2005, Roeder et al. 2011.)

Control of plastic hinge location in the brace is essential, as it affects the effective buckling length of the brace used in design. The type of the connection greatly affects the location of plastic hinge. Particularly, connections should be designed such that a plastic hinge forms at a predetermined location. It is often advantageous to allow free rotation at the brace ends to encourage plastic hinge formation at the brace midlength only. If multiple plastic hinges are formed near the joint area, i.e., in the gusset plates and at the brace ends, brace buckling length is uncertain. Therefore, hinge type connections allowing free rotations can be advantageous compared to fixed end moment resisting connections. (Duggal 2013, pp. 436–437.) Furthermore, braces where significant yielding occurs before buckling might have a reduced fracture life due to the induced inelastic rotation in the middle of the brace (Nascimbene et al. 2012).

Connection geometry also affects the brace behavior in cyclic loading. For instance, in many cases in-plane buckling of the brace is more desirable than out-of-plane buckling, to prevent damage to adjacent nonstructural elements (Bruneau 2011, p. 544). However, a typical gusset plate connection shown in Figure 18 shows much greater bending moment resistance in the in-plane direction compared to the out-of-plate direction and will therefore facilitate out-of-plane buckling of the brace. Out-of-plane bending resistance of the connection can be increased by additional stiffeners. Figure 19 shows a welded gusset plate connection utilizing a knife plate to prevent out-of-plane buckling. The design allows yielding of the knife plate, effectively forming a hinge at the brace end (Hsiao 2012, pp. 49–51). Similar design solutions can be made with bolt connections as well. It should be noted that the buckling

behavior of the brace is also affected by brace cross section shape. A brace will buckle easier around the weak axis of its cross section, per minimum energy principle.

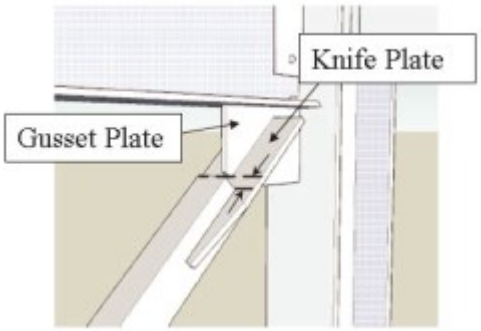

Figure 19. Gusset plate connection promoting in-plane brace buckling (adapted from Hsiao 2012, p. 51).

The multitude of possible failure mechanisms, the necessity of brace buckling behavior control and the high design forces make design of brace connections laborious. Furthermore, the requirement of stiffeners makes the manufacturing of the connection more expensive and requires more material. While manufacturing of one connection might not be a major cost, recurrent complex connections in a structure can quickly add up the expenses. According to Nazarko (2018, p. 54), the weight of connection plates and loose parts can be over 10% of the total weight of an industrial boiler plant steel frame in a typical project. Moreover, the time taken in detail design will also directly increase the cost of the project. Therefore, minimizing material, manufacturing and design costs in connection design is desirable. An optimized diagonal brace connection solution is sought in the latter part of this thesis.

2.5 *Design code requirements for concentrically braced frames*

Concentrically braced frames are stiff structures capable of resisting large lateral loads. With special design and detailing CBFs can be used to resist seismic loads. They are able to sustain relatively large inelastic deformations while retaining their load carrying capacity. (Roeder et al. 2011.) Modern seismic design codes are based on decades of research and practical observations and are used to provide seismic safety in structures (Bruneau 2011, p. 309). To overcome the challenges of seismic design, one must consider a large variety of phenomena related to earthquakes. Design standards strive to simplify the design process and ensure safety by mandating minimum structural requirements.

While seismic design standards have the common goal of providing structural safety in earthquakes, they might have somewhat different approaches. The following chapters briefly describe the ideologies and requirements represented in three seismic design codes used in different parts of the world. The perspective of the following chapters is on concentrically braced frames, especially on diagonal brace connections, although some general background information is introduced as well.

In some scenarios, it is necessary to use several design codes simultaneously, while fulfilling all necessary requirements. Such a case is presented by Peña et al. (2017), where an industrial steel structure was designed to independently meet with both American and Chilean seismic design code provisions. In the aforementioned situation, it is vital to recognize the similarities and differences in design codes, in order to meet their demands. Comparisons between the European, American and Chilean seismic design approach are made in chapter 2.5.4.

2.5.1 Eurocodes

EN 1998-1 (2004), more commonly known as Eurocode 8 part 1, contains general rules, seismic actions and rules for buildings. The same design code is used for both industrial and residential buildings. Its purpose is to ensure that in the event of an earthquake human lives are protected, damage is limited and important civil protection structures, such as hospitals, remain operational. However, due to the random nature of earthquakes, such objectives can only be fulfilled with a certain probability. (SFS-EN 1998-1 2004, p. 15.) Values of many coefficients might be chosen nationally in corresponding National Annexes. For simplicity, the suggested default values are used in this thesis when possible.

Eurocode 8 sets fundamental requirements that all structures in seismic regions shall meet. First is the no-collapse requirement, which states that a structure shall not collapse locally or globally in a strong earthquake with an expected return period of 475 years. The second one is the damage limitation requirement which states that the structure shall not be damaged such that the costs would be disproportionately high in comparison with the cost of the structure, in a moderate earthquake with an expected return period of 95 years. The length of the return period can be determined in National Annexes, and it is also affected by the importance factor of the structure. (SFS-EN 1998-1 2004, p. 29.)

The importance factor, γ_I, is used to classify buildings by their perceived societal importance. The need for importance classes arises when available resources are balanced with the fundamental purpose of protecting human lives. Effectively, the importance classes are multipliers that determine the strength of the design earthquake and thereby affect their theoretical return period. Descriptions of importance classes and the recommended values of importance factors are shown in Table 1. (SFS-EN 1998-1 2004, pp. 29–30.) The importance class of a new structure should be discussed with the client.

Table 1. Importance classes and earthquake return periods for buildings (adapted from SFS-EN 1998-1 2004, p. 53).

Importance class	Buildings	γ_I	Return period (yrs.)
I	Buildings of minor importance for public safety, e.g. agricultural buildings, etc.	0.8	243
II	Ordinary buildings, not belonging in the other categories	1.0	475
III	Buildings whose seismic resistance is of importance in view of the consequences associated with a collapse, e.g. schools, assembly halls, cultural institutions, etc.	1.2	821
IV	Buildings whose integrity during earthquakes is of vital importance for civil protection, e.g. hospitals, fire stations, power plants, etc.	1.4	1303

The hazard of a seismic zone is determined by the National Authorities and described in terms of peak ground acceleration (PGA). The value of PGA corresponds with the reference seismic action with a return period of 475 years mentioned before. Ground conditions affect seismic ground accelerations, and therefore PGA is determined for a rock-like surface categorized as type A in the Eurocode. The ground conditions at the design site are then used to modify the reference PGA value. (SFS-EN 1998-1 2004, p. 35.)

Elastic response spectrum (described in chapter 2.3) is then constructed based on the ground type. Default values for coefficients determining the shape of the response spectrum are given for each ground type, making this a straightforward process. By default, a viscous damping ratio of 5% is assumed. Horizontal seismic action is described by two orthogonal components, represented by the same response spectrum. A separate response spectrum is constructed for the vertical component. Alternatively, seismic action can be represented by recorded or simulated accelerogram data fulfilling specific criteria. (SFS-EN 1998-1 2004, pp. 36–43.)

Eurocode 8 also sets basic principles to guide conceptual design. The goal of such guidance is to facilitate design that satisfies the fundamental requirements within acceptable costs. The guiding principles are listed below, although not further elaborated here:

- structural simplicity
- uniformity, symmetry and redundancy
- bi-directional resistance and stiffness
- diaphragmatic behavior at story level
- adequate foundation. (SFS-EN 1998-1 2004, p. 45.)

Eurocode 8 provides two alternative design concepts for steel structures, concept A and concept B. Concept A anticipates low-dissipative structural behavior, indicating that capacity design is not employed, allowing the use of linear elastic global analysis. Thus, any additional seismic requirements set by Eurocode 8 are not necessary in the design of members and connections. However, earthquake induced forces in a completely elastic structure might easily grow excessive, and therefore concept A is recommended only for low seismicity zones. In concept B, the inelastic dissipative behavior of the structure is taken into account, and therefore the design forces can be reduced. However, ductility criteria set by Eurocode 8 must be met where applicable, which makes design more demanding. (SFS-EN 1998-1 2004, pp. 137–138.)

The energy dissipation capacity of a structure is characterized by behavior factor q [-]. A higher behavior factor is used for more ductile structures which benefit from hysteretic energy dissipation. The behavior factor is used to reduce the accelerations given by elastic response spectrum, thus giving a new design spectrum. Using the behavior factor is a way to avoid explicit inelastic structural analysis in the design, by utilizing the reduced elastic design spectrum instead. (SFS-EN 1998-1 2004, pp. 31, 41.) Due to its better applicability for strong earthquakes, this chapter will concentrate on concept B.

Structures can be assigned in different ductility classes which will in turn affect the design criteria. Structural ductility classes are named DCL, DCM and DCH which stand for low, medium and high ductility classes, respectively. Selecting high ductility class for a structure will result in lower design forces, but it also imposes stricter member design and detailing criteria. Effects of ductility class on design concept and behavior factor are shown in Table 2.

Somewhat different design criteria are determined for different structural types, such as moment resisting frames, concentrically braced frames and eccentrically braced frames. The design of these structures is based on the same common principles, but a different design approach is taken in some design steps depending on the type of the structure. For simplicity,

only concentrically braced frames are discussed from here on. Upper limits for behavior factors of concentrically braced frames are shown in Table 3.

Table 2. Structural ductility classes and their effect on design concept and behavior factor (adapted from SFS-EN 1998-1 2004, p. 137).

Structural ductility class	Design concept	Range of reference values of behavior factor q
DCL (Low)	Concept A	$\leq$ 1.5 - 2
DCM (Medium)	Concept B	$\leq$ 4 (also limited by Table 3)
DCH (High)	Concept B	only limited by Table 3

Table 3. Upper limit values of behavior factors for concentrically braced frames (adapted from SFS-EN 1998-1 2004, p. 143).

CBF brace configuration	q upper limit, DCM	q upper limit, DCH
Diagonal bracings	4	4
V-bracings	2	2.5

Eurocode 8 allows dissipative zones to be located in either the structural members or in their connections. If dissipative zones are in the connections, the connected members must have sufficient overstrength to allow for the cyclic yielding of the connections. Similarly, when dissipative zones are in the structural members, the connections must have sufficient overstrength. (SFS-EN 1998-1 2004, p. 145.) The use of dissipative connections is permitted for diagonal brace connections in concentrically braced frames, if two conditions are satisfied. First, the connections shall have an elongation capacity consistent with the global deformations. Second, connection deformations are taken into account in global drift analysis using non-linear static pushover analysis or non-linear time history analysis. (SFS-EN 1998-1 2004, p. 152.) As such, the use of non-dissipative connections allows for more simple design.

In structural analysis, all gravity loads are considered to be resisted by beams and columns without the help of bracing members. The diagonals are taken into account in elastic analysis by considering the diagonal bracings in tension only, except for V bracings, where both compression and tension diagonals are accounted for. This means that for non-V configurations the compression strength of the diagonals is ignored in elastic analysis. Taking the compression diagonals into account in any type of concentric bracing is allowed in non-linear analysis, when both pre-buckling and post-buckling states are considered, and background information justifying the model representing the behavior of diagonals is provided. (SFS-EN 1998-1 2004, p. 151.)

The cross section class of dissipative members in compression or bending is limited. Eurocode cross section classes for steel members are determined in Eurocode 3 (EN 1993-1-1 2005, pp. 40–44). To ensure local ductility and to prevent local buckling, the cross section width-thickness ratio (b/t_p) is restricted. The required cross section class of a member in compression or bending is affected by its ductility class and behavior factor. This dependence is shown in Table 4. (SFS-EN 1998-1 2004, p. 145.)

Table 4. Cross section class requirements for dissipative members in bending or compression (SFS-EN 1998-1 2004, p. 145).

Ductility class	Reference value of behavior factor q	Required cross-section class
DCM	$1.5 < q \leq 2$	class 1, 2 or 3
DCM	$2 < q \leq 4$	class 1 or 2
DCH	$q > 4$	class 1

For dissipative members in tension, their design plastic resistance $N_{\mathrm{pl,Rd}}$ should be less than the design ultimate resistance of the net section at fasteners holes $N_{\mathrm{u,Rd}}$ (SFS-EN 1998-1, p. 145, SFS-EN 1993-1-1 2005, p. 49). This limitation is made to ensure that the brace does not fracture at the bolt connection before it starts to yield, thus ensuring ductile behavior. This is expressed in equation 17.

$$N_{\mathrm{pl,Rd}} = \frac{A f_{\mathrm{y}}}{\gamma_{\mathrm{M0}}} < N_{\mathrm{u,Rd}} = \frac{0.9 A_{\mathrm{net}} f_{\mathrm{u}}}{\gamma_{\mathrm{M2}}} \tag{17}$$

where A is the cross section area [mm^2]
f_{y} is the material yield strength [N/mm^2]
γ_{M0} is the partial safety factor for cross sectional resistance, recommended value 1.00 [-]
A_{net} is the net area of a cross section [mm^2]
f_{u} is the material ultimate strength [N/mm^2]
γ_{M2} is the partial safety factor for cross sectional tension fracture resistance, recommended value 1.25 [-]

The diagonal braces shall be placed in such a way that the structure exhibits similar horizontal deflection characteristics in both directions. This requirement should be met at each floor. This requirement can be met by installing equal amount of similar diagonal braces such that their inclination is mirrored to each other, at each floor. The concept is shown in equation 18, and further explained in Figure 20. (SFS-EN 1998-1 2004, p. 150.)

$$\frac{|A^+ - A^-|}{A^+ + A^-} \leq 0.05 \tag{18}$$

where A^+ is the area of the horizontal projection of the tension diagonal cross section [mm^2]
A^- is the area of the horizontal projection of the compression diagonal cross section [mm^2]

Non-dimensional slenderness, as defined in EN 1993-1-1 (2005) clause 6.3.1.2(1) (see equation 19), of diagonal bracings is limited based on their configuration. In frames with X bracings (Figure 14a, left), non-dimensional brace slenderness shall be between 1.3 and 2.0, and for other diagonal or V bracings non-dimensional slenderness should be less than or equal to 2.0. For structures with two stories or fewer, no limitations are given to non-dimensional slenderness. (SFS-EN 1998-1 2004, p. 152.)

$$\bar{\lambda} = \sqrt{\frac{Af_y}{N_{cr}}} \tag{19}$$

where N_{cr} is the elastic critical force for the relevant buckling mode based on the gross cross sectional properties [kN]

The yield resistance of the gross cross section of the diagonals, $N_{pl,Rd}$ (defined in equation 17), should be larger than or equal to the applied design axial force, N_{Ed}. Additionally, frames with V bracings should verify the compression resistance of diagonal bracings according to Eurocode 3. To enable homogeneous energy dissipation in all diagonals, it should be checked that the maximum overstrength of a diagonal, Ω_{max}, does not exceed the minimum overstrength, Ω, of a diagonal in the system by more than 25%. (SFS-EN 1998-1 2004, p. 152.) The definition of the diagonal overstrength is given in equation 20.

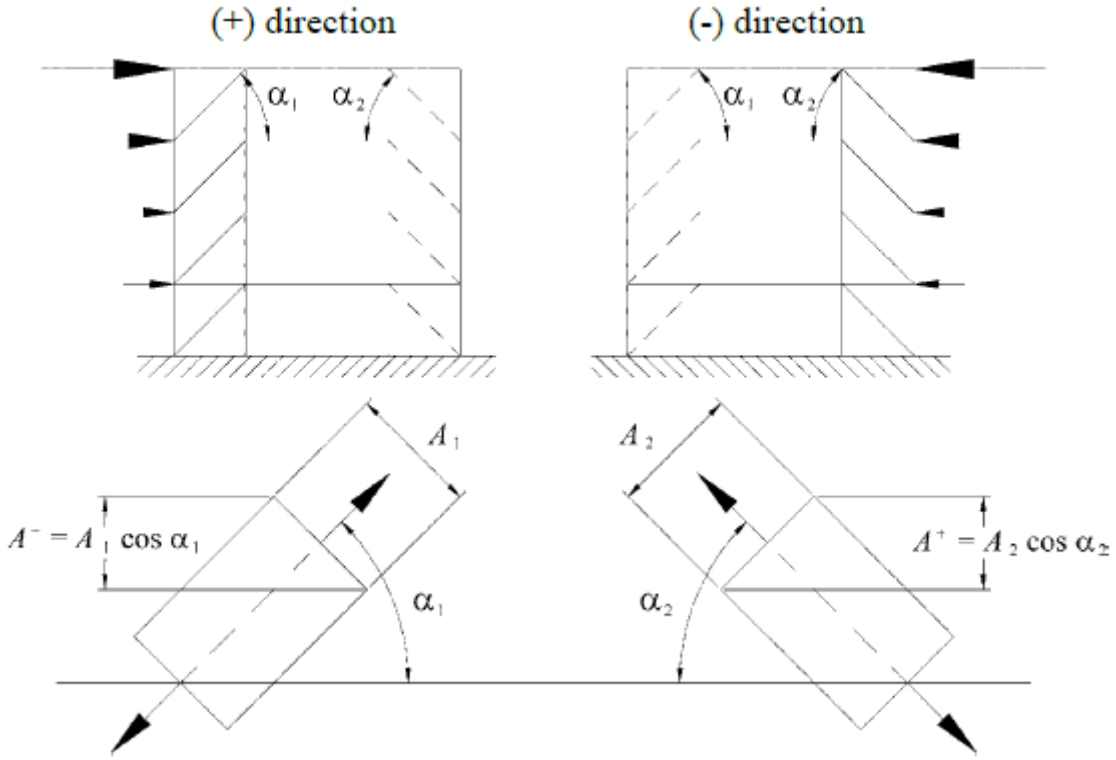

Figure 20. Determining horizontal projections of diagonal braces (SFS-EN 1998-1 2005, p. 151).

$$\Omega = \min\left(\frac{N_{pl,Rd,i}}{N_{Ed,i}}\right) \tag{20}$$

where $N_{pl,Rd,i}$ is the design plastic resistance of diagonal brace i in the system [kN]
$N_{Ed,i}$ is the corresponding design axial force for diagonal brace i [kN]
i is the index used to go through each diagonal brace in the system [-]

In addition to regular design checks, beams and columns in a concentrically braced frame should pass an additional design check presented in equation 21. Beams in frames with V-bracings should also be able to resist effects caused by the connected braces, not further

elaborated here. Tensile and compressive forces transmitted to the columns by diagonal bracings should be considered as well. (SFS-EN 1998-1 2004, pp. 152–153). The design check is used to verify that the beams and columns have sufficient buckling resistance in the earthquake. Preventing the buckling of beams and columns is essential, as global and local collapse must be avoided.

$$N_{\mathrm{pl,Rd}}(M_{\mathrm{Ed}}) \geq N_{\mathrm{Ed,G}} + 1.1\gamma_{\mathrm{ov}}\Omega N_{\mathrm{Ed,E}} \tag{21}$$

where $N_{\mathrm{pl,Rd}}(M_{\mathrm{Ed}})$ is the design buckling resistance of the beam or in the column according to EN 1993, taking into account the interaction effect of design bending moment M_{Ed} introduced by seismic design situation [kN]
$N_{\mathrm{Ed,G}}$ is the design axial force in the beam or in the column due to non-seismic actions [kN]
$N_{\mathrm{Ed,E}}$ is the axial force in the beam or in the column due to seismic actions [kN]
γ_{ov} is the overstrength factor, with a recommended value of 1.25 [-]

Non-dissipative connections shall have such overstrength that they will be able to resist the forces transmitted by the dissipative brace. For fillet welds and bolted non-dissipative connections, the overstrength requirement is expressed in equation 22. (SFS-EN 1998-1 2004, pp. 145–146.) The resistance of a member or a connection represents the strength of its weakest component under the applied load.

$$R_{\mathrm{d}} \geq 1.1\gamma_{\mathrm{ov}}R_{\mathrm{fy}} \tag{22}$$

where R_{d} is the resistance of the connection according to Eurocode 3 [kN]
$R_{\mathrm{fy}} = N_{\mathrm{pl,Rd}}$ is the plastic resistance of the connected dissipative member [kN]

Bolted connections where bolts are subjected to shear forces should belong to category B or C according to Eurocode 3 part 1-8. Category B friction connections are slip-resistant at serviceability limit state, meaning that design serviceability shear load should not exceed the design slip resistance. Category C connections are slip-resistant at ultimate limit state, meaning that the design ultimate shear load should not exceed the design slip resistance. Friction surfaces in category B and C bolted connections shall belong to either class A or B as defined in EN 1090-2 (2018, p. 64). For bolt connections in tension, category E preloaded bolts shall be used. High-strength bolt grades 8.8 and 10.9 are allowed for all bolted connections. For bolted shear connections, the design shear resistance of the bolts should be higher than 1.2 times the design bearing resistance. (SFS-EN 1998-1 2004, p. 146, SFS-EN 1993-1-8 2005, p. 21.) Design criteria for connections in categories B, C and E are summarized in Table 5.

Table 5. Design criteria for different categories of bolted connections (adapted from SFS-EN 1993-1-8 2005, p. 22, SFS-EN 1998-1 2004, p. 146).

Category	Criteria
B: shear connection, slip-resistant at serviceability	$F_{v.Ed,ser} \leq F_{s,Rd,ser}$ $F_{v,Ed} \leq F_{v,Rd}$ $F_{v,Ed} \leq F_{b,Rd}$ $1.2F_{b,Rd} \leq F_{v.Rd}$
C: shear connection, slip-resistant at ultimate	$F_{v,Ed} \leq F_{s,Rd}$ $F_{v,Ed} \leq F_{b,Rd}$ $F_{v,Ed} \leq N_{net,Rd}$ $1.2F_{b,Rd} \leq F_{v.Rd}$
E: tension connection, preloaded	$F_{t,Ed} \leq F_{t,Rd}$ $F_{t,Ed} \leq B_{p,Rd}$

where $F_{v,Ed,ser}$ is the design shear force per bolt for the serviceability limit state [kN]
$F_{s,Rd,ser}$ is the design slip resistance per bolt at the serviceability limit state [kN]
$F_{v,Ed}$ is the design shear force per bolt for the ultimate limit state [kN]
$F_{v,Rd}$ is the design shear resistance per bolt shear plane [kN]
$F_{b,Rd}$ is the design bearing resistance per bolt [kN]
$F_{s,Rd}$ is the design slip resistance per bolt at the ultimate limit state [kN]
$N_{net,Rd}$ is the design plastic resistance of the net cross section at bolt holes [kN]
$F_{t,Ed}$ is the design tensile force per bolt for the ultimate limit state [kN]
$F_{t,Rd}$ is the design tension resistance per bolt [kN]
$B_{p,Rd}$ is the design punching shear resistance of the bolt head and the nut [kN]

A slip-resistant connection can be subjected to both shear force and tensile force simultaneously. The tensile force will counteract the bolt preloading force, reducing the slip resistance of the connection. Design slip resistance per bolt is given for category B and C connections below in equations 23a and 23b, respectively. In the absence of applied tensile force, zero will be used in its place. (SFS-EN 1993-1-8 2005, p. 31.)

$$F_{s,Rd,ser} = \frac{k_s n \mu \left(F_{p,C} - 0.8F_{t,Ed,ser}\right)}{\gamma_{M3,ser}} \quad (23a)$$

$$F_{s,Rd} = \frac{k_s n \mu \left(F_{p,C} - 0.8F_{t,Ed}\right)}{\gamma_{M3}} \quad (23b)$$

where k_s is a parameter given in Table 6 [-]
n is the number of friction surfaces [-]
μ is the slip factor obtained either by testing or by Table 7 when applicable [-]
$F_{p,C}$ is the preloading force (see equation 24) [kN]
$F_{t,Ed,ser}$ is the design tensile force per bolt for the serviceability limit state [kN]
$\gamma_{M3,ser}$ is the partial safety factor for slip resistance at serviceability limit state, recommended value 1.1 [-]
γ_{M3} is the partial safety factor for slip resistance at ultimate limit state, recommended value 1.25 [-]

Table 6. Values of parameter k_s (SFS-EN 1993-1-8 2005, p. 30).

Description	k_s
Bolts in normal holes	1.0
Bolts in either oversized holes or short slotted holes with the axis of the slot perpendicular to the direction of load transfer	0.85
Bolts in long slotted holes with the axis of the slot perpendicular to the direction of load transfer	0.7
Bolts in short slotted holes with the axis of the slot parallel to the direction of load transfer	0.76
Bolts in long slotted holes with the axis of the slot parallel to the direction of load transfer	0.63

Table 7. Slip factor, μ, for pre-loaded bolts (adapted from SFS-EN 1993-1-8 2005, p. 31).

Class of friction surfaces according to EN 1090-2	Slip factor μ
A	0.5
B	0.4

The preloading force to be used in equations 23a and 23b is defined below in equation 24 (SFS-EN 1993-1-8 2005, p. 30).

$$F_{p,C} = 0.7 f_{ub} A_s \tag{24}$$

where f_{ub} is the ultimate tensile strength of the bolt [N/mm^2]
A_s is the tensile stress area of the bolt [mm^2]

Shear resistance per shear plane of the bolt is determined as (SFS-EN 1993-1-8 2005, p. 27)

$$F_{v,Rd} = \frac{\alpha_v f_{ub} A}{\gamma_{M2}} \tag{25}$$

where γ_{M2} is the partial safety factor for resistance of bolts, recommended value 1.25 [-]
if the shear plane passes through the threaded portion of the bolt:
$A = A_s$ [mm^2]
α_v = 0.6 or 0.5 (for bolt grades 8.8 and 10.9, respectively)
if the shear plane passes through the unthreaded portion of the bolt:
A is the gross cross section of the bolt [mm^2]
α_v = 0.6

Bearing resistance for bolts in normal holes is determined in equation 26. The bearing resistance shall be multiplied by 0.8 for bolts in oversized holes, and by 0.6 for bolts in slotted holes perpendicular to the direction of force transfer. When using countersunk bolts, the bearing resistance should be based on a plate thickness equal to the thickness of the connected plate minus half the depth of the countersinking. Symbols for bolt spacing are shown in Figure 21. Symbols p_1 [mm] and p_2 [mm] stand for the bolt spacing in the direction of load transfer and perpendicular to the direction of load transfer, respectively. Symbols e_1

[mm] and e_2 [mm] stand for bolt edge distance in the direction and perpendicular to the direction of load transfer, respectively. Symbol d_0 [mm] stands for bolt hole diameter. (SFS-EN 1993-1-8 2005, p. 27.)

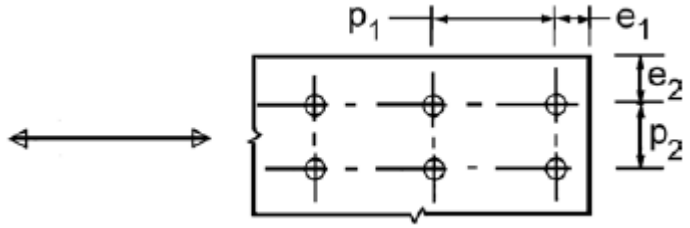

Figure 21. Symbols for spacings of bolts (adapted from SFS-EN 1993-1-8 2005, p. 24).

$$F_{\mathrm{b,Rd}} = \frac{k_1 \alpha_{\mathrm{b}} f_{\mathrm{u}} d t_{\mathrm{p}}}{\gamma_{\mathrm{M2}}} \tag{26}$$

where α_{b} is the smallest of α_{d}, $\frac{f_{\mathrm{ub}}}{f_{\mathrm{u}}}$ or 1.0 [-]

in the direction of load transfer:

- for end bolts: $\alpha_{\mathrm{d}} = \frac{e_1}{3d_0}$
- for inner bolts: $\alpha_{\mathrm{d}} = \frac{p_1}{3d_0} - \frac{1}{4}$

perpendicular to the direction of load transfer:

- for edge bolts: k_1 is the smallest of $2.8\frac{e_2}{d_0} - 1.7$, $1.4\frac{p_2}{d_0} - 1.7$ or 2.5
- for inner bolts: k_1 is the smallest of $1.4\frac{p_2}{d_0} - 1.7$ or 2.5

d is the nominal bolt diameter [mm]
t_{p} is the plate thickness [mm]

The design plastic resistance of the net cross section is determined by equation 27 (SFS-EN 1993-1-1 2005, p. 49).

$$N_{\mathrm{net,Rd}} = \frac{A_{\mathrm{net}} f_{\mathrm{y}}}{\gamma_{\mathrm{M0}}} \tag{27}$$

Tension resistance of the bolts is given in equation 28. For the determination of tension resistance of countersunk bolts, the angle and the depth of countersinking should conform with the reference standards listed in chapter 1.2.4 of Eurocode 3 part 1-8. (SFS-EN 1993-1-8 2005, pp. 9, 27.)

$$F_{\mathrm{t,Rd}} = \frac{k_2 f_{\mathrm{ub}} A_{\mathrm{s}}}{\gamma_{\mathrm{M2}}} \tag{28}$$

where $k_2 = 0.63$ for countersunk bolts [-]
$k_2 = 0.9$ otherwise [-]

Punching shear resistance is given by (SFS-EN 1993-1-8 2005, p. 27)

$$B_{\mathrm{p,Rd}} = \frac{0.6\pi d_{\mathrm{m}} t_{\mathrm{p}} f_{\mathrm{u}}}{\gamma_{\mathrm{M2}}} \tag{29}$$

where d_m is the mean of the across points and across flats dimensions of the bolt head or the nut, whichever is smaller [mm]
t_p is the thickness of the plate under the bolt or the nut [mm]

In addition to design checks made for single bolts, block tearing of the connection (Figure 22) must also be precluded. Block tearing consists of a shear failure at the row of bolt holes along the shear face accompanied by a tensile failure along the row of bolt holes along the tension face of the bolt group. For a symmetric bolt group subject to concentric loading, the design block tearing resistance, $V_{\text{eff},1,\text{Rd}}$, is determined in equation 30.

$$V_{\text{eff},1,\text{Rd}} = \frac{f_u A_{nt}}{\gamma_{M2}} + \frac{\left(\frac{1}{\sqrt{3}}\right) f_y A_{nv}}{\gamma_{M0}} \tag{30}$$

where A_{nt} is the net area subjected to tension [mm^2]
A_{nv} is the net area subjected to shear [mm^2]

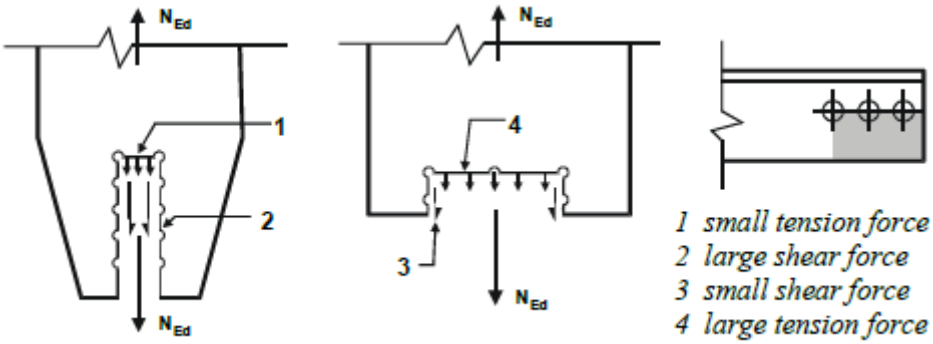

Figure 22. Block tearing of bolted connections (adapted from SFS-EN 1993-1-8 2005, p. 32).

The adequacy of the connection design should be supported by experimental evidence based on either tests or existing data. Complementary rules on acceptable connection design might also be provided in the relevant National Annexes. The experimental evidence shall support design by showing that the strength and ductility of members and connections is sufficient under cyclic loading. The experimental evidence is necessary for connections in or adjacent to dissipative zones. (SFS-EN 1998-1, p. 146.)

2.5.2 American design codes

ANSI/AISC 341-16 (2016), hereafter referred to as AISC 341, is a design standard governing the design, fabrication and erection of structural steel members and connections in seismic force-resisting systems. It is used in structural design together with ASCE 7 and AISC 360 design standards, which determine minimum design loads and specifications for structural steel buildings, respectively. In many occasions, AISC 341 refers to ASCE 7 or AISC 360 for specifications and design requirements.

ASCE/SEI 7-10 (2010) determines an importance factor, I_e, which is used to scale design lateral forces, based on the risk category of the structure. Risk categories are used to classify buildings and structures according to the risk to human life, health and welfare associated

with their damage. Risk categories are defined from I to IV, ranking from low risk to high risk. Examples of buildings and structures in each class are shown in Table 8.

Table 8. Risk categories of buildings and structures (adapted from ASCE/SEI 7-10 2010, p. 2).

Risk category	Buildings and structures	I_e (-)
I	Buildings and other structures that represent a low risk to human life in the event of failure	1.00
II	All buildings and other structures not belonging to other categories	1.00
III	Buildings and other structures, the failure of which could - pose a substantial risk to human life - cause a substantial economic impact	1.25
IV	Buildings and other structures - designated as essential facilities - the failure of which could cause a substantial hazard to the community	1.50

Site class, defined from A to F alphabetically, is used to form the elastic design spectrum (referred to as spectral response acceleration in the standard). Site class is based on soil conditions, and it is classified according to chapter 20 of ASCE 7-10 (2010). Table values are given for a set of parameters based on site class, which are then used in simple formulas to determine the elastic design response spectrum (Figure 23). S_{DS} and S_{D1} are design spectral response acceleration parameters at short periods and one-second periods, respectively. (ASCE/SEI 7-10 2010, pp. 65–67.)

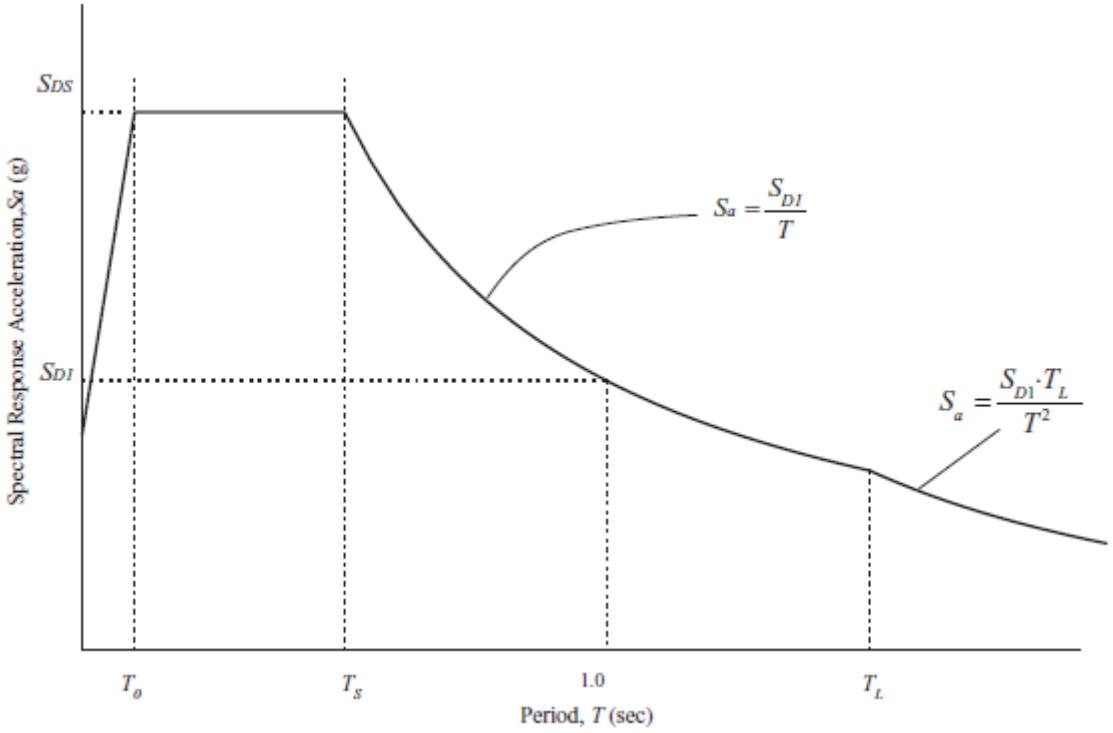

Figure 23. Elastic design response spectrum (ASCE/SEI 7-10 2010, p. 66).

Seismic design category is assigned for each structure or building. It is affected by the spectral accelerations S_{DS} [g] and S_{D1} [g], or for very strong ground motion, by the mapped maximum considered earthquake spectral acceleration S_1 [g]. Another factor in determining seismic design category is the risk category defined above. (Charney 2015, p. 8.) Specific values and criteria for seismic design category classification are determined in section 11.6 of ASCE 7. Seismic design category, also classified from A to F alphabetically, affects the design provisions. Special seismic provisions defined in AISC 341 are not necessary for structures in seismic design category A, are optional for categories B and C, and are mandatory for categories D, E and F. Generally, structures in areas of high seismic risk belong to categories D, E or F. (ANSI/AISC 341-16 2016, p. 171.)

The energy dissipation capacity of a structure is quantified with the response modification coefficient R [-]. It is used in design to reduce the design forces suggested by the elastic design spectrum. The response modification coefficient is determined separately for different structural systems in table 12.2-1 of ASCE 7-10 (2010). The American standards make a distinction between ordinary concentrically braced frames (OCBF) and special concentrically braced frames (SCBF), the latter of which are preferred in seismic design due to their stable inelastic performance and energy dissipation capacity. Only certain brace configurations are permitted for SCBF (see Figure 24), and they require special ductile detailing. (Bruneau 2011, pp. 504–505.) However, due to their improved seismic performance over OCBFs, the rest of this chapter concentrates on SCBFs.

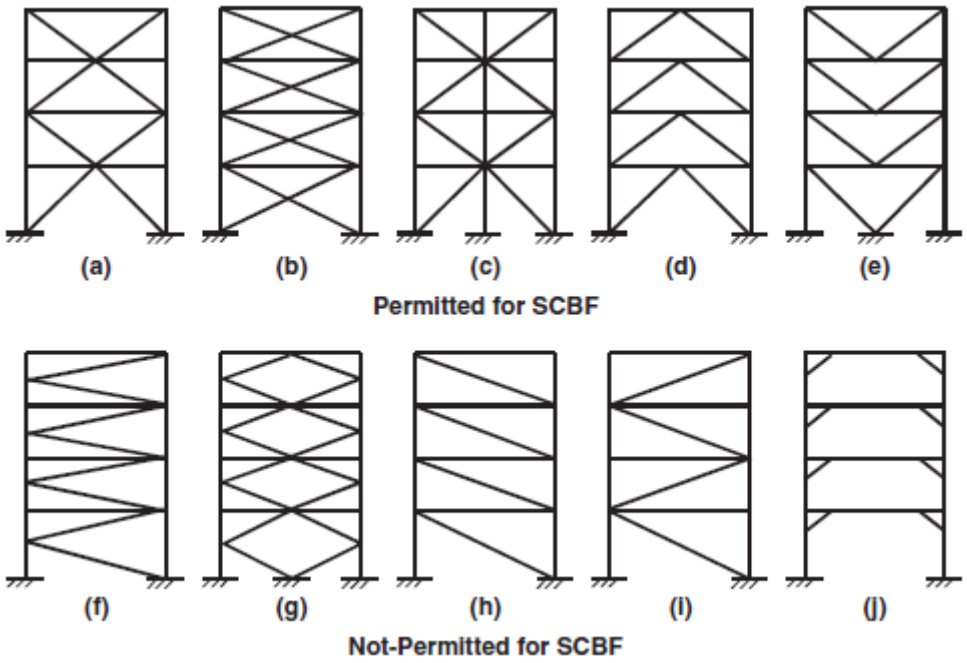

Figure 24. Allowed and disallowed brace configurations for SCBF (Bruneau 2011, p. 505).

Separate and specific design rules are given in ASCE 7-10 for the so-called nonbuilding structures which include all self-supporting structures that carry gravity loads and that might be required to resist the effects of an earthquake. Such structures include many industrial structures, such as industrial boiler plants. Seismic design procedures are given for specific nonbuilding structures, including the selection of the structural analysis method, the section of the seismic force-resisting system, and the selection of the response modification coefficient R. (ASCE/SEI 7-10 2010, pp. 139–143.) Thus, the design of industrial structures might differ from the design of residential buildings.

In structural analysis of SCBFs, the magnitude of the horizontal seismic load effect shall be taken as the largest force determined from the following analyses. In the first analysis, all braces are assumed to resist forces corresponding to their expected strength in compression or tension. In the second analysis, tension braces remain the same as in the first analysis, but compression braces are only assumed to resist forces corresponding to their post-buckling strength. A third analysis is performed for multi-tiered braced frames (braced frame divided into tiers by intermediate horizontal struts), where the braces are assumed to yield and buckle progressively starting from the weakest to the strongest. (ANSI/AISC 341-16 2016, p. 63.)

Braces are not expected to carry gravity loads, and as such they will be designed purely for resisting lateral loads in the system. Braces transmit forces to the beams and columns, and thus increase the load they must carry. In seismic analysis, AISC 341 instructs that the forces transmitted by the braces are based on their expected strength. The expected strength of tensile braces is based on their expected tensile yield strength, P_y [kN] (equation 31), while the expected strength of compression braces, P_c [kN], is the lesser of its expected yield strength (equation 32a) and its buckling strength (equation 32b). The expected post-buckling strength of compression braces, $P_{residual}$ [kN], shall be taken as 0.3 times the expected strength in compression (equation 34). As many structural steels are in practice stronger than their specified minimum strength, their expected strength is corrected with factor R_y. (ANSI/AISC 341-16 2016, p. 63, ANSI/AISC 360-16 2016, p. 35)

$$P_y = R_y f_y A \tag{31}$$

where R_y is the ratio of expected yield stress of the material [-]

$$P_c = R_y f_y A \tag{32a}$$

$$P_c = \frac{1}{0.877} f_{cre} A \tag{32b}$$

where f_{cre} is the critical stress defined in equations 33a and 33b [N/mm^2]

$$when\ \frac{L_c}{r} \leq 4.71\sqrt{\frac{E}{f_y}}$$

$$f_{cre} = \left(0.658^{\frac{R_y f_y}{f_e}}\right) R_y f_y \tag{33a}$$

where L_c is the effective length of the member [mm]
$r = \sqrt{I/A}$ is the radius of gyration [mm]
I is the second moment of area of the cross section about relevant axis [mm^4]
E is the modulus of elasticity of steel [N/mm^2]
f_e is the elastic buckling stress of the relevant buckling mode [N/mm^2]

$$when\ \frac{L_c}{r} > 4.71\sqrt{\frac{E}{f_y}}$$

$$f_{cre} = 0.877 f_e \tag{33b}$$

$$P_{\text{residual}} = 0.3P_{\text{c}} \tag{34}$$

Along a given structural line, the braces shall be deployed such that at least 30% but no more than 70% of the total horizontal force along the line is resisted by members in tension (ANSI/AISC 341-16 2016, p. 64). Examples of acceptable and unacceptable brace layouts based on this requirement are shown in Figure 25. The aim of such limitation is to ensure balanced lateral force resistance in both horizontal directions. It should however be noted, that the requirement considers design forces in braces determined by elastic analysis, instead of expected member strengths in seismic design.

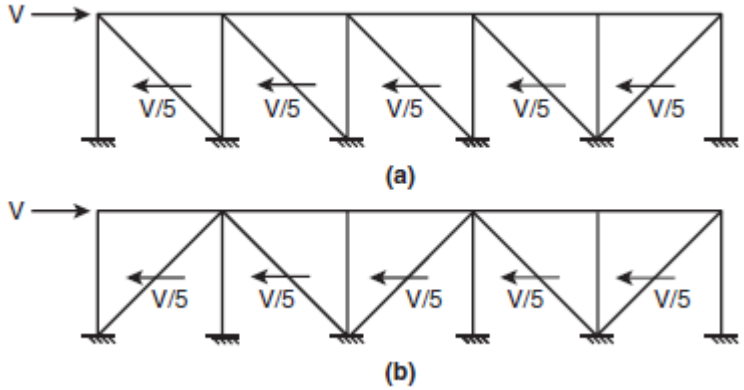

Figure 25. Unacceptable (a) and acceptable (b) brace layouts (adapted from Bruneau 2011, p. 539)

Columns, beams and braces in SCBFs shall satisfy the requirements set for highly ductile members in section D1.1 of AISC 341. Structural steel sections shall have their flanges continuously connected to the web or webs of the cross section. Additionally, members must comply with the width-to-thickness ratio limits set in table D1.1 of AISC 341. (ANSI/AISC 341-16 2016, pp. 13–17, 66) Such limitations are used to ensure that the members have sufficient ductility and rotation capacity, so that yielding can happen before local buckling of plate or shell parts of the section.

The slenderness ratio, defined as L_c/r [-], shall be less than or equal to 200 for the braces. The radius of gyration used in the expression shall be the governing (smallest) radius of gyration for the member. The brace effective net area shall not be less than the brace gross area. Where this requirement is not fulfilled (e.g. cross section at bolt holes) reinforcement must be applied. The reinforcement can be done by welding additional plates to the profile to increase the net section area. The yield strength of the reinforcements shall be at least equal to that of the braces, and the reinforcement connection shall have sufficient strength. (ANSI/AISC 341-16 2016, pp. 66–67)

Specific design rules are to be applied for beam-to-column connections, column splices, brace connections and certain welds. However, only brace connections are studied in detail here. The required strength in tension, compression and flexure shall be verified independently for the connection. All bolts shall be installed as pre-tensioned high-strength bolts, and friction surfaces shall satisfy the requirements for slip-critical connections. (ANSI/AISC 341-16 2016, pp. 25, 68.)

Brace connections shall have tensile strength larger than or equal to the lesser of the expected yield strength (equation 31) of the brace in tension, and the maximum load effect transferable

to the brace by the system. The latter of the two must be determined by global analysis of the system and is not commonly used in design in practice. Local connection failure mechanisms such as block shear rupture must be precluded. Bolt slip, however, is not considered critical, if bearing failure and block shear rupture are precluded, and therefore it is not required to be checked in design. The required compressive strength of the connection shall be equal to the expected brace strength in compression (the lesser of equations 32a and 32b). (ANSI/AISC 341-16 2016, pp. 68–69.)

Brace connections experience significant flexural forces as the compression braces buckle. Therefore, the connection must either be rigid enough to withstand this bending moment or have sufficient rotation capacity to allow for rotation of the brace end. Inelastic rotation of the connection is permitted. Where rigid connections are used, the required flexural strength of the connection, P_M [kNm], shall be as defined in equation 35. (ANSI/AISC 341-16 2016, p. 69.)

$$P_{\mathrm{M}} = 1.1 R_{\mathrm{y}} M_{\mathrm{p}} \tag{35}$$

where M_p is the plastic bending moment of the brace about the critical buckling axis [kNm]

Where braces are designed for out-of-plane buckling behavior, the welds that attach a gusset plate directly to a beam flange or a column flange shall have available shear strength, P_v [kN], as shown in equation 36.

$$P_{\mathrm{v}} = 0.6 R_{\mathrm{y}} f_{\mathrm{y}} t_{\mathrm{p}} l_{\mathrm{s}} \tag{36}$$

where t_p is the thickness of the gusset plate [mm]
l_s is the total joint length [mm]

General rules for connections are given in AISC 360, and they must be followed in design of SCBF connections as well (ANSI/AISC 341-16 2016, p. 59). Allowed bolt types, pretension forces, hole dimensions, edge spacings and such can be found in chapter J of AISC 360-16 (2016) and are not listed here. However, relevant design checks for bolted brace connections shall be introduced. Two parallel design philosophies are included in AISC 360: allowable stress design (ASD) and load and resistance factor design (LRFD). Due to its closer resemblance to the Eurocode, only LRFD checks will be presented here. Design tensile and shear strength of single bolts can be determined from equation 37 (ANSI/AISC 360-16 2016, p. 131).

$$\varphi R_{\mathrm{n}} = \varphi f_{\mathrm{n}} A_{\mathrm{b}} \tag{37}$$

where $\varphi = 0.75$ is the LRFD resistance factor [-]
R_n is the tensile resistance, $R_{n,t}$, or shear resistance, $R_{n,v}$, of a bolt [kN]
f_n is the nominal tensile stress, f_{nt}, or shear stress, f_{nv}, of the bolt [N/mm^2]
A_b is the nominal unthreaded body area of a bolt [mm^2]

The available tensile strength of a bolt subjected to combined tension and shear shall be determined from equation 38 (ANSI/AISC 360-16 2016, pp. 133–134):

$$\varphi R_{\mathrm{n,tv}} = \varphi f'_{\mathrm{nt}} A_{\mathrm{b}} \tag{38}$$

where $R_{n,tv}$ is the resistance to combined shear and tension of the bolt [kN]
f'_{nt} is the nominal tensile stress modified to include the effects of shear stress, defined in equation 39 [N/mm^2]

$$f'_{nt} = 1.3f_{nt} - \frac{f_{nt}}{\varphi f_{nv}} f_{rv} \leq f_{nt} \tag{39}$$

where f_{rv} is the required shear stress resistance of the bolt [N/mm^2]

The force that can be resisted by a bolt might be limited by the bearing strength at the bolt hole. The effective strength of an individual bolt can be taken as the lesser of the shear strength of the bolt and the bearing strength at bolt hole. The total strength of a bolt group is taken as the sum of the effective strengths of individual bolts. (ANSI/AISC 360-16 2016, p. 133.)

Bolt holes shall be standard holes or short-slotted holes perpendicular to the applied load in bolted connections where the load is transferred by bolts in shear. Oversized holes and short-slotted holes are permitted in connections where the load is transferred by bolts in tension, but not in shear. The strength of bolted connections using standard holes or short-slotted holes shall be calculated as that for bearing-type connections (connections where the design forces are transmitted by bolt shear or bearing). Bolt hole bearing and tearout strengths are given in the following equations (equations 40 and 41, respectively), where deformation at the bolt hole at service load is not a design consideration, as is permitted when the required connection strength is based upon the expected strength of a member. (ANSI/AISC 341-16 2016, pp. 24–25, ANSI/AISC 360-16 2016, pp. 135–136.)

$$\varphi R_{n,b} = \varphi 3.0 d t_p f_u \tag{40}$$

where $R_{n,b}$ is the bearing resistance at the bolt hole [kN]
f_u is the specified minimum tensile strength of the connected material [N/mm^2]

$$\varphi R_{n,tear} = \varphi 1.5 l_c t_p f_u \tag{41}$$

where $R_{n,tear}$ is the tearout resistance of the bolt hole [kN]
l_c is the clear distance, in the direction of the force, between the edge of the hole and the edge of the adjacent hole or the edge of the material [mm]

Design block shear strength along a shear failure plane and a perpendicular tension failure plane is defined with equation 42.

$$\varphi R_{n,block} = \varphi(0.60 f_u A_{nv} + U_{bs} f_u A_{nt}) \leq \varphi\left(0.60 f_y A_{gv} + U_{bs} f_u A_{nt}\right) \tag{42}$$

where $R_{n,block}$ is the block shear resistance [kN]
A_{nv} is the net area subject to shear [mm^2]
U_{bs} = 1, when the tension stress is uniform, and U_{bs} = 0.5 when the tension stress is nonuniform [-]
A_{nt} is the net area subject to tension [mm^2]
A_{gv} is the gross area subject to shear [mm^2]

2.5.3 Chilean design codes

The Chilean standard for earthquake-resistant design of industrial structures and facilities, NCh2369.Of2003, is reviewed in this section. It is of interest due to its different design philosophy compared to the Eurocode or AISC. NCh2369 is a specification which references NCh433 for general rules of seismic design of buildings. Specific rules for the design of steel structures are provided in NCh427, however, historically AISC 360 has been allowed to be used instead (Soules et al. 2016, Appendix A, p. 42). This chapter is based on the English translations of NCh2369.Of2003 and NCh433.Of96 from Appendices B and A from Soules et al. (2016), respectively. Detailed design of steel structures is often done according to AISC 360-10, and therefore the Chilean steel detailing provisions are not presented here.

The basic objectives of NCh2369 are to protect human life, and to allow for continuity of operation in industry. To ensure the fulfillment of these objectives, structural systems shall be designed such that the behavior of their resistant elements and their connections is ductile, and instability and fragile failure is prevented. Structures shall also provide multiple earthquake-resistant structural lines. Additionally, simple and clearly identifiable structural systems are preferred. (Soules et al. 2016, Appendix B, pp. 17–18.)

Structures and equipment are classified according to their importance. Based on the importance class, an importance coefficient, I_e, shall be given. Examples of structures and equipment in each category, and their effect on importance coefficient are given in Table 9.

Structures shall be analyzed considering the earthquake loads in at least two perpendicular directions. Vertical effects of the earthquake shall be considered in situations where it implies significant design considerations, described more specifically in clause 5.11 of NCh2369.Of2003. Horizontal actions can be considered independently of each other in most cases. When calculating seismic mass of the structure for inertial force effects, the vertical service loads shall be reduced based on the likelihood of their simultaneous occurrence with the design earthquake. (Soules et al. 2016, Appendix B, pp. 22–25.)

Table 9. Importance categories and corresponding importance coefficients (adapted from Soules et al. 2016, Appendix B, pp. 20–21).

Importance category	Structures and equipment	I_e (-)
C1	Critical structures and equipment based on any one of the following reasons: a) Vital, must be kept in operation so to control fire, render health, etc. b) Dangerous, failure implies hazard of fire, explosion or poisoning c) Essential, failure generates standstills and serious production losses	1.20
C2	Normal structures and equipment, not belonging to category C1	1.00
C3	Minor or provisional structures and equipment, not belonging to category C1 or C2	0.80

The importance factor, I_e, is used to directly scale the base shear force suggested by static elastic analysis, or alternatively the accelerations from the design spectrum. Other factors affecting the design seismic forces are the natural vibration period of the structure, foundation soil type, seismic zone, damping ratio and response modification factor. It should be noted that damping ratios other than 5% are possible by default. In fact, according to

NCh2369.Of2003, industrial steel structures have a damping ratio of only about 2–3%. (Soules et al. 2016, Appendix B, pp. 27–40.)

Chile is divided into three seismic zones. Each seismic zone has an accompanying value of maximum effective acceleration which is used in seismic load calculations. The soil type at the site also affects the response spectrum, with harder soils amplifying shorter periods vibrations. Additionally, a response modification factor is used to take the inelastic response of the structure into account. Structures designed to remain elastic will have a maximum response modification factor, R, of 1, while steel structures typically have a response modification factor of 3–5. The response modification factor is used to reduce the seismic loads experienced by the structure. (Soules et al. 2016, Appendix B, pp. 35–46.)

Braced frame configurations where diagonal bracings that only resist tensile forces are not allowed, except in light steel bays which are not discussed here. Every resistant line shall include diagonal braces in both directions, such that at least 30% of the shear load is resisted by tensile braces in either direction. The elements of vertical earthquake-resistant systems under compression shall have their width-to-thickness ratios limited by values in table 8.1 of NCh2369. Additionally, the slenderness ratio L_c/r of all members should be less than $1.5\pi\sqrt{E/F_y}$. (Soules et al. 2016, Appendix B, p 54.)

The diagonal bracings in an X-configuration shall be connected at the point of intersection. The connected point can be assumed to act as an out-of-plane lateral support when determining the buckling length of the brace, if one of the braces is continuous. When V-bracings or inverted V-bracings are used, the beams shall be designed continuous over the intersection point, and they shall resist all vertical loads without the help of the bracings. The bracings on the other hand must be able to resist the self-weight loads and the beam-induced live loads plus the seismic loads amplified by a factor of 1.5. Bracings in K-configuration (Figure 24 f) are not allowed. (Soules et al. 2016, Appendix B, pp. 54–55.)

The maximum stress in compressed diagonal bracings due to the design earthquake actions must not exceed 80% of its resistant capacity. However, if the earthquake-induced stresses in the bracings are less than one third of those caused by the governing load combination, no such limitation is applied. Furthermore, in those cases the limitations concerning brace slenderness, width-to-thickness ratios and V-bracings might also be waived. (Soules et al. 2016, Appendix B, p. 55.) It should however be noted that the design forces reduced by the response modification factor R do not accurately represent the forces experienced by the braces in an actual earthquake, and as such yielding of the braces might happen.

Bolts used in all connections must be exclusively of high-strength material. The diagonal brace connections shall be designed to resist forces equal to the tensile capacity of the brace gross cross section. Bolted connections shall be slip-critical, with a bolt pretension equal to 70% of the tensile strength of A325 or A490 bolts. However, the connection strength might be calculated as that corresponding to bearing-type connections. Contact surfaces in connections shall be mechanically cleaned and not painted. (Soules et al. 2016, Appendix B, p. 56.)

2.5.4 Comparisons and differences

All the design codes covered in the above three sections share the same common goal of protecting human life in the event of an earthquake. Being targeted for industrial

applications, NCh2369 has additional interest in facilitating continuity of operation. The European and American design standards share many common design methods and ideologies, although they too have their differences. However, the Chilean design code, although partly based on the American code, differs from the other two quite significantly in the design of braced frames. Comparison for some parts of the design codes concerning the design of concentrically braced frames is presented in Table 10.

In Eurocode 8 and AISC 341 braced frames are designed to behave in a similar fashion under seismic loading. Columns and beams are designed to stay elastic, while diagonal bracings are allowed to successively buckle in compression and yield in tension to dissipate energy. NCh2369 does not allow compression braces to reach stress levels higher than 80% of their strength in a design earthquake, theoretically leaving them elastic under the load. Thus, no energy dissipation is expected to happen in the braces through buckling under compression and yielding under tension. Such an assumption only applies to the design procedure, though, and might not be representative of real brace behavior.

The above difference in design approach does not mean that the Chilean code does not utilize capacity design principles. Due to the higher stiffness in the braced frame structure, a structure designed per the Chilean code will experience higher horizontal base shear loads. Additionally, the LRFD load combinations obtained from the Chilean code will be amplified by a factor of 1.4, while this value is 1.0 in ASCE 7-10 (Peña et al. 2017). Therefore, the foundation is designed for higher loads and allowed to develop inelastic deformations, which allows for energy dissipation. For this reason, NCh2369 stresses the importance of ductility in the foundation connections.

Each of the three discussed seismic design codes classify structures based on their importance. The importance class will then determine an importance factor which will be used to scale the design seismic loads such that more important structures are designed for more severe earthquake loads. Each design code presents the horizontal earthquake action via an elastic design response spectrum, although the formulas in the Chilean code do not make it very apparent. The formulas used to calculate base shear in NCh2369 are based on an empiric elastic response spectrum which is comparable to the elastic response spectra used in the other two standards (Soules et al. 2016, Appendix B, pp. 106–108).

Default damping ratio for all steel structures is 5% in both Eurocode 8 and AISC 341 but only 2–3% in NCh2369. The damping ratios presented in the Chilean standard are specifically geared towards industrial structures, and verified through empirical evidence (Soules et al. 2016, Appendix B, p. 104). Structures designed by using NCh2369 will experience stronger lateral loads than structures designed using Eurocode 8 or AISC 341. However, as the latter two design codes require a higher level of structural ductility, special detailing is also needed. Therefore, it is possible that in some cases the structure designed per the Chilean code might even be lighter, despite the need for larger lateral load resistance (Peña et al. 2017). However, in many industrial structure projects the opposite has been found to be true.

Table 10. Comparison of seismic design practice for CBFs.

	Eurocode 8	AISC 341	NCh2369
Behavior factor or equivalent	diagonal bracings: $q = 4$ V-bracings (DCH): $q = 2.5$	OCBF: $R = 3.25$ SCBF: $R = 6$	braced frames: $R = 5$
Braces considered in elastic analysis	diagonal bracings: tension only V-bracings: compression + tension	tension + compression OR + 0.3*compression	tension + compression
Brace design strength	tension: Af_y/γ_{M0} compression: Af_y/γ_{M0} or $\chi Af_y/\gamma_{M1}$ †	tension: $R_y f_y A$ compression: $R_y f_y A$ or $\frac{1}{0.877} f_{cre} A$	tension: N/A compression: stress max 80% of capacity
Tension brace net section resistance	$\frac{Af_y}{\gamma_{M0}} < \frac{0.9 A_{net} f_u}{\gamma_{M2}}$	$A \leq A_{net}$	N/A
Brace slenderness	X-bracings: $1.3 \leq \sqrt{\frac{Af_y}{N_{cr}}} \leq 2.0$ other: $\sqrt{\frac{Af_y}{N_{cr}}} \leq 2.0$	$\frac{L_c}{r} \leq 200$	$\frac{L_c}{r} \leq 1.5\pi \sqrt{\frac{E}{f_y}}$
Compression brace cross section limits	for $2 < q \leq 4$: Class 1 or 2	width-to-thickness limits	width-to-thickness limits
Compression-tension brace distribution	$\frac{\lvert A^+ - A^- \rvert}{A^+ + A^-} \leq 0.05$	at least 30% tension braces in either load direction	at least 30% tension braces in either load direction
Maximum brace overstrength	$\Omega_{max} \leq 1.25\Omega$	N/A	N/A
Additional requirements for beams and columns	$N_{pl,Rd}(M_{Ed}) \geq N_{Ed,G} + 1.1\gamma_{ov}\Omega N_{Ed,E}$	N/A	$\frac{L_c}{r} \leq 1.5\pi \sqrt{\frac{E}{f_y}}$
Connection tensile strength requirement	$1.1\gamma_{ov} R_{fy}$	$R_y f_y A$	$f_y A$
Bolted connections	slip-resistant, preloaded 8.8 or 10.9 bolts	preloaded high-strength bolts	preloaded high-strength bolts

†) Uniform member buckling resistance according to EN 1993-1-1 clause 6.3.1.1(3)

Concentrically braced frames are divided into two groups in the ASIC 341, with SCBFs having more stringent design and detailing rules to ensure high levels of ductility. The behavior factor, or response modification coefficient, of all SCBFs is the same regardless of brace configuration. Similarly, NCh2369 assigns behavior factors based on resistant system type, disregarding brace configuration. On the contrary, Eurocode 8 recommends different behavior factors based on brace configuration. Furthermore, the behavior factor given by Eurocode 8 might be affected by adopted design philosophy, namely the ductility class of the structure, depending on brace configuration (see Table 3). Thus, Eurocode 8 expects CBFs with diagonal bracings to be more ductile than V-braced frames (Costanzo & Raffaele 2017).

The design codes strive to mitigate local buckling effects of the braces, as it can lead to stress concentrations and subsequent crack propagation in the material. Local buckling prevention can be done by increasing the wall thickness, i.e., limiting the width-to-thickness ratio of the cross section. Each design code under consideration proposes different width-to-thickness ratio limits. Comparison is made for two test braces to display these differences. The first test subject is a rectangular hollow structural section (HSS) diagonal brace under pure compression. The chosen material is ASTM A500/A500M Gr. C which has a minimum specified yield stress of 345 MPa, elastic modulus of 200 GPa, and $R_y = 1.3$. The second test subject is a hot-rolled I-shape diagonal brace under pure compression. The material is ASTM A572/A572M Gr. 50 which has a minimum specified yield stress of 345 MPa, elastic modulus of 200 GPa, and $R_y = 1.1$. (ANSI/AISC 341-16 2016, p. 5). A comparison of width-to-thickness limits for the rectangular HSS brace is shown in Figure 26. Width-to-thickness limits for the flanges and height-to-thickness limits for the web of the I-shape brace are compared in Figure 27 and Figure 28, respectively.

The formulae used to calculate the width-to-thickness ratios are shown in Table 11. The most severe requirements for rectangular HSS braces are imposed for SCBFs designed according to AISC 341, while the diagonal brace designed according to NCh2369 has the most relaxed limitation. The high width-to-thickness ratios permitted by NCh2369 are understandable, as braces are not allowed to reach over 80% of their compressive stress capacity anyway. However, the difference between the limits of Eurocode class 1 and AISC highly ductile members is quite drastic, considering that cross sections in either class are expected to be able to reach their full plastic capacity.

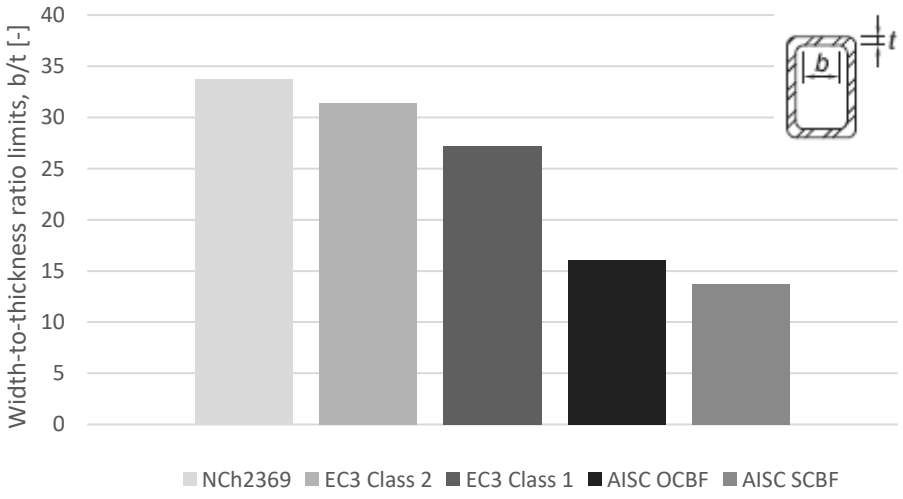

Figure 26. Width-to-thickness ratio limits for a rectangular HSS diagonal brace.

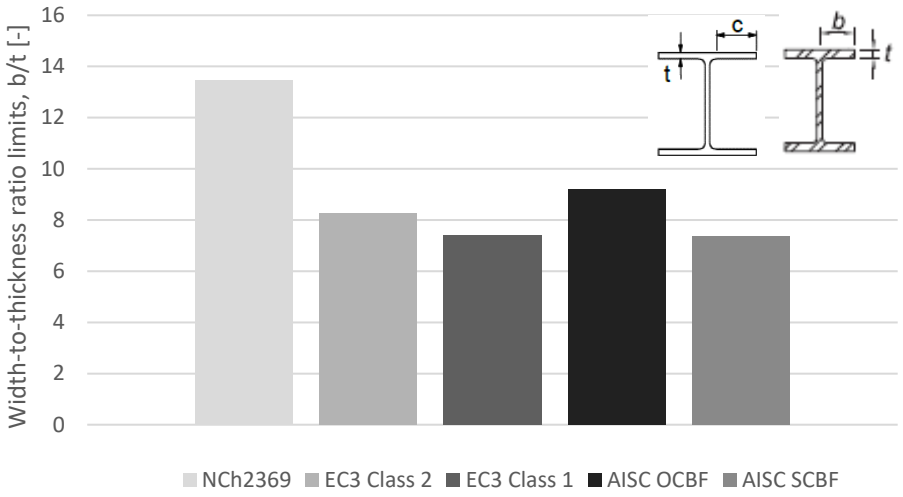

Figure 27. Width-to-thickness ratio limits for flanges of a I-shape diagonal brace.

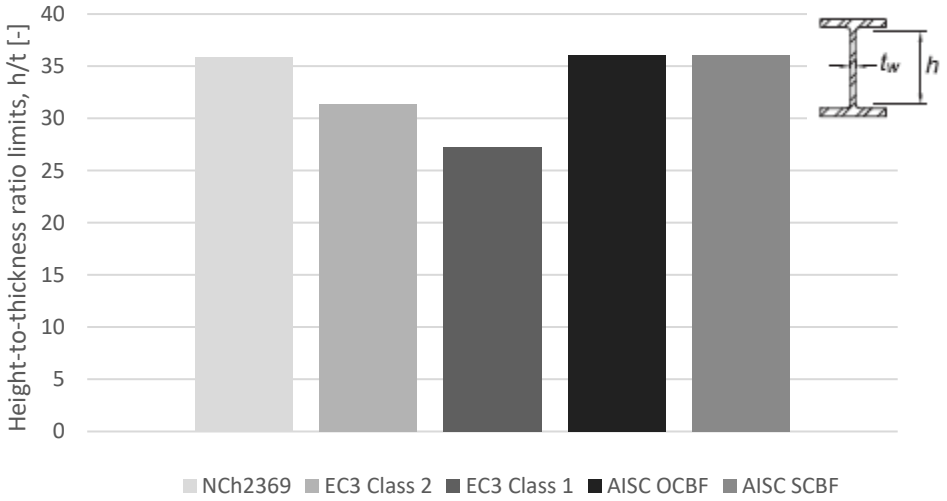

Figure 28. Height-to-thickness ratio limits for the web of a I-shape diagonal brace.

One possible explanation for such a difference in rectangular HSS width-to-thickness limitations between Eurocode and AISC 341 might be in the reported poor low-cycle fatigue performance of rectangular HSS braces. Research has shown that local strain concentrations might occur in rectangular HSS braces, and crack propagation from the corners of the section might lead to fracture, especially with higher width-to-thickness ratios (Sabelli et al. 2013, pp. 7–8, Bruneau et al. 2011, p. 528, Fell 2008, p. 242). While AISC 341 stipulates stricter width-to-thickness limits than those presented in AISC 360 for general steel members in compression, Eurocode 8 settles for the cross section classes defined in Eurocode 3. There is only little difference in width-to-thickness ratio limits for the I-shape profile between Eurocode and AISC. It should be noted though, that the flange length used in Eurocode does not include the fillet and it is therefore shorter than that used in the other two standards. Consequently, the flange width-to-thickness limits presented in Figure 27 are not directly comparable between the standards.

Table 11. Width-to-thickness ratio limits for a diagonal brace under pure compression.

	Eurocode 3 ∗	AISC 341 †	NCh2369 ‡
Rectangular HSS	Class 1: $\frac{b}{t} \leq 33\sqrt{\frac{235\ MPa}{f_y}}$ Class 2: $\frac{b}{t} \leq 38\sqrt{\frac{235\ MPa}{f_y}}$	Highly ductile (SCBF): $\frac{b}{t} \leq 0.65\sqrt{\frac{E}{R_y f_y}}$ Moderately ductile (OCBF): $\frac{b}{t} \leq 0.76\sqrt{\frac{E}{R_y f_y}}$	$\frac{b}{t} \leq 1.40\sqrt{\frac{E}{f_y}}$
Rolled I-shape, flange	Class 1: $\frac{c}{t} \leq 9\sqrt{\frac{235\ MPa}{f_y}}$ Class 2: $\frac{c}{t} \leq 10\sqrt{\frac{235\ MPa}{f_y}}$	Highly ductile (SCBF): $\frac{b}{t} \leq 0.32\sqrt{\frac{E}{R_y f_y}}$ Moderately ductile (OCBF): $\frac{b}{t} \leq 0.40\sqrt{\frac{E}{R_y f_y}}$	$\frac{b}{t} \leq 0.56\sqrt{\frac{E}{f_y}}$
Rolled I-shape, web	Class 1: $\frac{h}{t} \leq 33\sqrt{\frac{235\ MPa}{f_y}}$ Class 2: $\frac{h}{t} \leq 38\sqrt{\frac{235\ MPa}{f_y}}$	Highly ductile (SCBF): $\frac{h}{t} \leq 1.57\sqrt{\frac{E}{R_y f_y}}$ Moderately ductile (OCBF): $\frac{h}{t} \leq 1.57\sqrt{\frac{E}{R_y f_y}}$	$\frac{h}{t} \leq 1.49\sqrt{\frac{E}{f_y}}$

∗) SFS-EN 1993-1-1 2005, pp. 42–43.
†) ANSI/AISC 341-16 2016, pp. 14–15.
‡) Soules et al. 2016, Appendix B, pp. 60–61.

Limits for global brace slenderness are shown in Table 10. Direct comparison between the standards is not straightforward, as each utilize different presentations for slenderness. Interestingly, the American standard is the only one that does not contain material properties in the slenderness limit but rather gives a single value for all braces. Comparison between the slenderness limits is however possible, with some modifications. First, Euler's classical presentation of critical buckling force (equation 43) is substituted into the Eurocode expression for non-dimensional slenderness (equation 19), and the terms are rearranged:

$$N_{\mathrm{cr}} = \frac{\pi^2 EI}{(k_{\mathrm{cr}} L)^2} \tag{43}$$

where k_{cr} is the effective buckling length factor ($L_c = k_{\mathrm{cr}}L$)
L is the unsupported length of the compressed bar

$$\bar{\lambda} = \sqrt{\frac{Af_y}{N_{\mathrm{cr}}}} = \sqrt{\frac{Af_{\mathrm{y}}L_{\mathrm{c}}^2}{\pi^2 EI}} = \frac{1}{\pi}\sqrt{\frac{f_{\mathrm{y}}}{E}}\frac{L_{\mathrm{c}}}{\sqrt{I/A}} \leq 2.0 \tag{44}$$

By expressing the radius of gyration with *r*, and rearranging the inequality, an expression for diagonal brace slenderness more alike the other two is obtained:

$$\frac{L_{\mathrm{c}}}{r} \leq 2.0\pi\sqrt{\frac{E}{f_{\mathrm{y}}}} \tag{45}$$

The same material properties as in the last example are selected: f_{y} = 345 MPa and E = 200 GPa. Using these values, a direct comparison between the three standards is shown in Table 12. The slenderness limits given by Eurocode 8 and NCh2369 are stricter than that in AISC 341. However, the typical brace slenderness used in American seismic design ranges from about 40 to about 100 (Sabelli et al. 2013). It should be noted, that using steel with lower yield strength will result in less strict slenderness limits in both Eurocode 8 and NCh2369.

Table 12. Brace slenderness limits for f_{y} = 345 MPa, E = 200 GPa.

Eurocode 8	AISC 341	NCh2369
Diagonal or V-brace: $\frac{L_{\mathrm{c}}}{r} \leq 151$ X-brace: $98 \leq \frac{L_{\mathrm{c}}}{r} \leq 151$	$\frac{L_{\mathrm{c}}}{r} \leq 200$	$\frac{L_{\mathrm{c}}}{r} \leq 113$

All three of the discussed design codes stipulate the use of high-strength preloaded bolts in connections. Eurocode 8 specifically requires the connections to be designed as slip-resistant. Both AISC 341 and NCh2369 require connections to be designed as slip-critical but allow design calculations to be made as those for bearing-type connections. This reflects the philosophy that bolt slip is not considered as a critical failure in either AISC 341 or NCh2369 if both bearing resistance and block tear resistance are sufficient. Both Eurocode 8 and AISC 341 account for brace overstrength when determining connection resistance, whereas NCh2369 only requires connection strength equal to the nominal brace yield strength.

3 Proposed bolted diagonal brace connections

In this chapter, a design solution for a bolted diagonal brace connection is sought. The diagonal brace is a part of a concentrically braced frame in an industrial structure. The typical diagonal brace connection used in the United States of America is a welded gusset plate connection that might be stiffened in out-of-plane direction in some cases (Figure 29). Such a connection is simple to design, and it provides sufficient clearance for brace end rotations during cyclic buckling and lengthening of the brace. However, the welds made in imperfect conditions at the construction site require a skilled welder. Many large industrial projects are located in remote areas, where the local labor pool does not include a large number of skilled welders (Krumpen & Carrato 2009). Furthermore, welds joining gusset plates to the frame were found to be generally more vulnerable to fracture than bolted connections in older concentrically braced frames (Sen et al. 2016). Therefore, in many cases bolted connections are preferred.

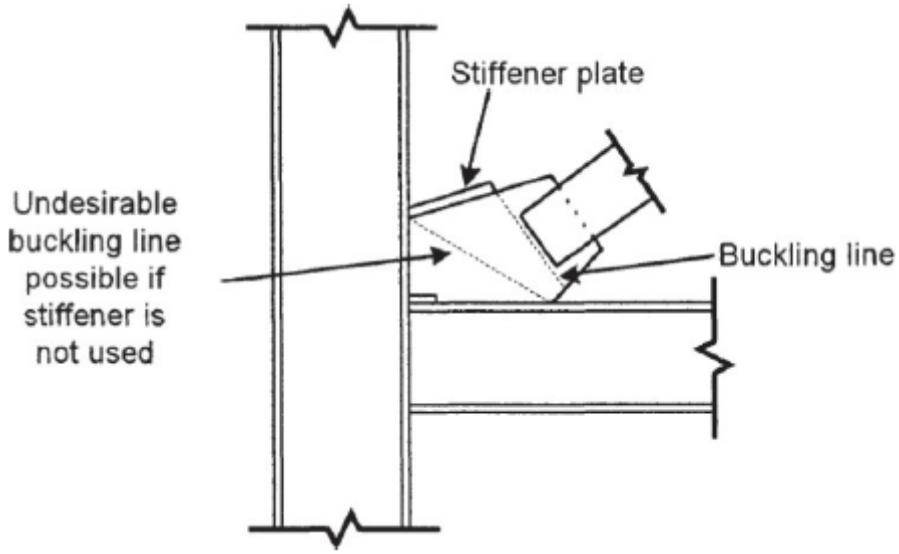

Figure 29. Welded gusset plate connection featuring a stiffener plate to control buckling (Tamboli 2016, p. 354).

Five potential bolted diagonal brace connection designs are evaluated and compared. The effectiveness of the design solution is evaluated by criteria consisting of combined cost of the connection and the brace, their combined weight, ease of design, simplicity of force transfer, ease of installation and possible preference of the customer. The evaluation of the four latter criteria is done by surveying experienced industrial structural engineers at Sweco Structures Ltd. Each of the five connections is modeled such that they join two aligned braces to a column at a 45-degree angle. The centerlines of all members intersect at the same point. Such simplifications are made to ensure unambiguous analysis results by reducing the number of variables. The possibility to connect beams and additional bracing members to the same connection is discussed in section 5.4.

Diagonal braces with a square HSS or a welded box cross section are often used due to their similar flexural stiffness about both of their principal axes. However, using a wide flange I-profile brace might be more cost effective in connection design, resulting in a less expensive solution in overall. Two of the considered connection designs utilize an I-profile cross section, while three are made with a welded box cross section and one with a built-up section of two U-profiles. The cross section size of the I-profile brace is identical to the column, and the dimensions of the welded box profile and the built-up section are selected such that they

have a cross section area equal to that of the I-profile. The dimensions and plate thicknesses of each member are chosen such that they fulfill the strictest local slenderness limitation set in Eurocode 3, ASIC 341 and NCh2369. More accurate information such as part profiles, bolt sizes and weld information are shown in the drawings presented in Appendix 1. The profiles and dimensions of all parts in each connection are also presented in the cost calculation spreadsheets in Appendix 3.

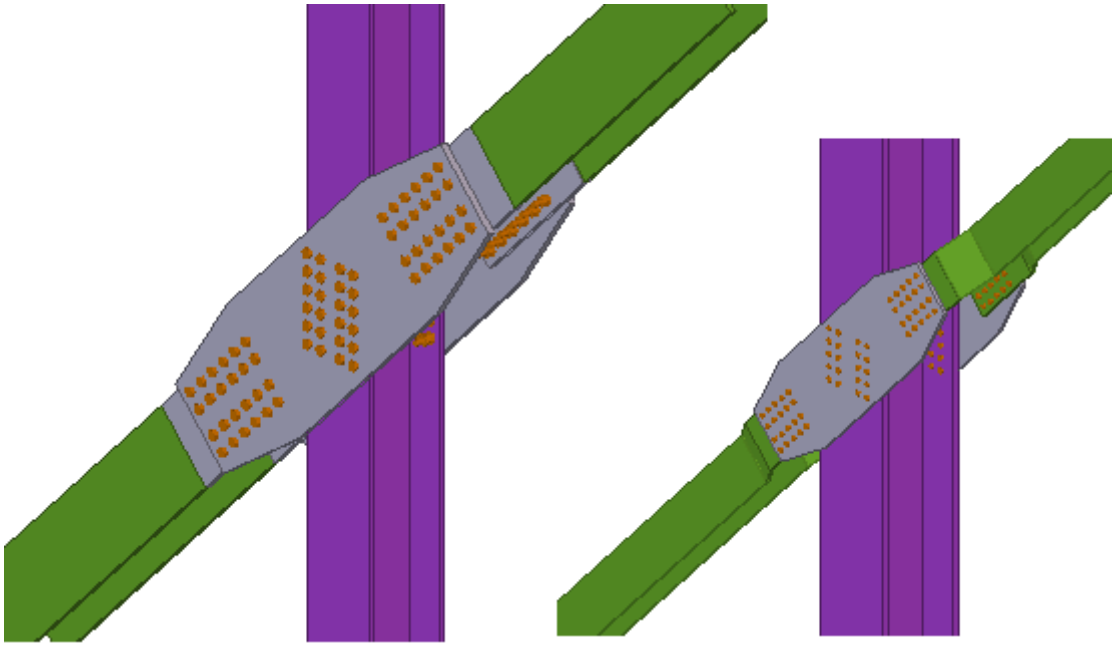

Figure 30. Connections CON1 (left) and CON1s (right).

Each of the five connections is designed for two different brace sizes. The first design case utilizes a large diagonal brace as described in the previous paragraph. The second design case utilizes a brace which has a cross section area equal to about one third of that of the larger brace. The design force used for dimensioning the connections is equal to the nominal tensile yield capacity of the brace. Consequently, the design tensile force in the latter case will also be one third of that in the first case. These variants are made to evaluate the applicability of the connection in different design situations. The connections are named with a prefix “CON” followed by a number. Connection versions containing a smaller brace are distinguished by adding the letter “s” at the end of the name. Similarly, the built-up section is represented with the letter “b”.

The three versions of the first bolted connection, CON1, are shown in Figure 30 and Figure 31. It is a simple design, where the flanges of the brace are bolted to a connection plate which transfers the forces to the column and to the aligned brace. As the brace reaches a tensile force equal to its nominal yield capacity, it will rupture at the net section where the bolt holes are located. To avoid this failure mechanism, the original flanges of the I-profile are cut off and replaced with thicker plates. The plates are then welded to the web and the original flanges of the brace. Where the smaller brace profile is used, its ends are replaced by taller I-profile sections. In the case of the built-up brace the webs are reinforced by welded plates.

The second connection, CON2, is shown in Figure 32. Rectangular slots are cut for cross-plates, which are welded to the welded box brace. Gusset plates aligned with the cross-plates are connected to the brace by sandwich plates. A slot is cut in the web of the column to allow

the vertical gusset plate to pass through it. Slots are cut in the flanges of the column to fit the horizontal gusset plates. The gusset plates are then welded to the column. Reinforcement plates are welded to the webs of the box brace to avoid net section failure of the brace where the cross-plate slots end. CON2s is a smaller version of CON2 with no major differences, other than the horizontal gusset plates which extend through the flanges of the column in the larger version.

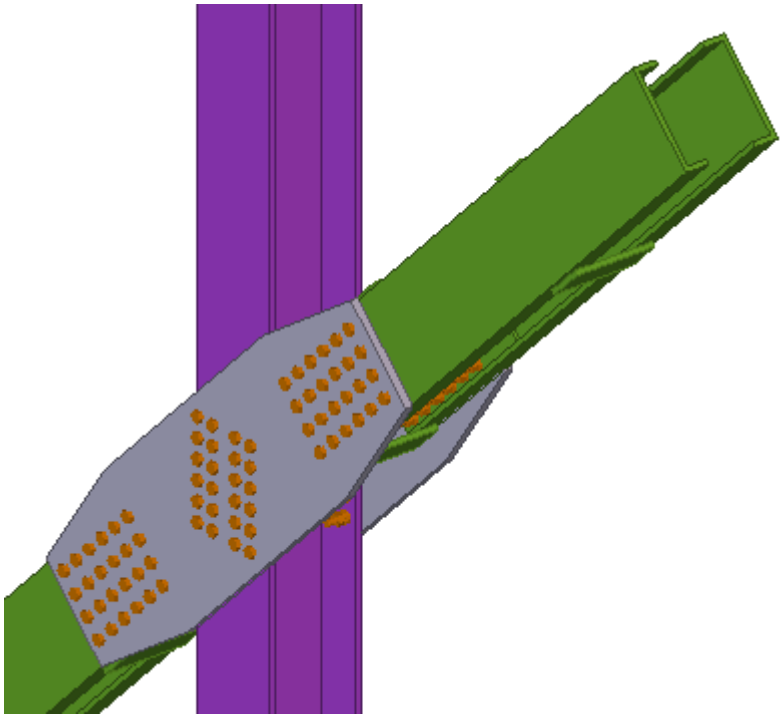

Figure 31. Connection CON1b features a built-up brace cross section.

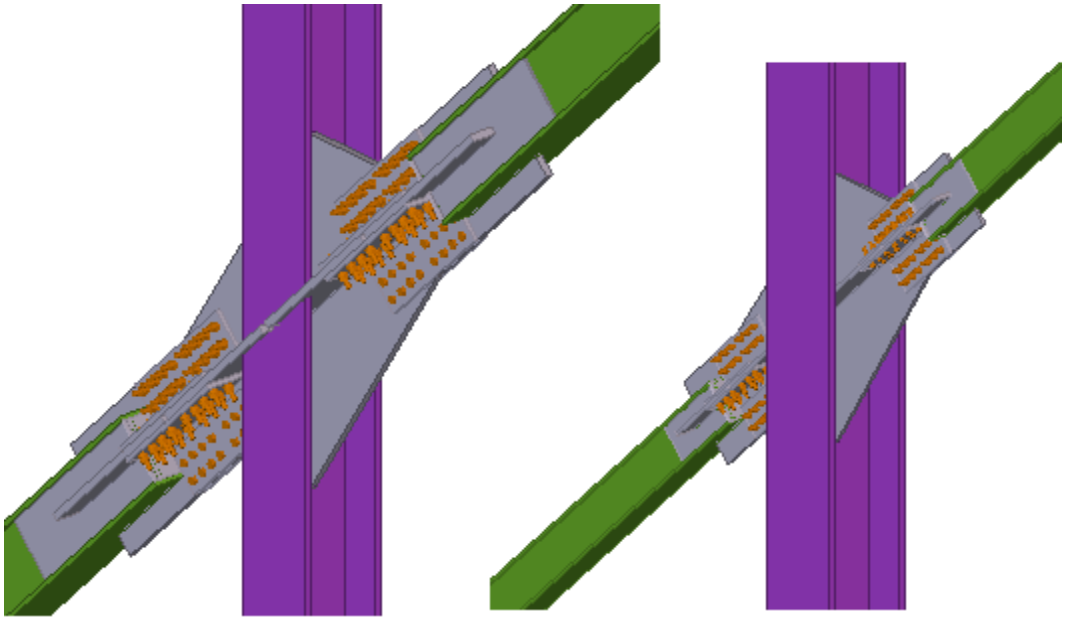

Figure 32. Connections CON2 (left) and CON2s (right).

Connection CON3 is shown in Figure 33. The design is similar to Connection 1, but the reinforcement of the brace ends is done by welding thicker tapered plates to the outside

surfaces of the flanges. The plates are then connected to the column connection plate by sandwich plates. No cutting of the brace profile is necessary in this design. When the smaller brace profile is used taller I-profile sections are welded to its ends. Using a brace member of uniform height possessing the same tensile capacity as the smaller brace would result in impractically narrow flanges.

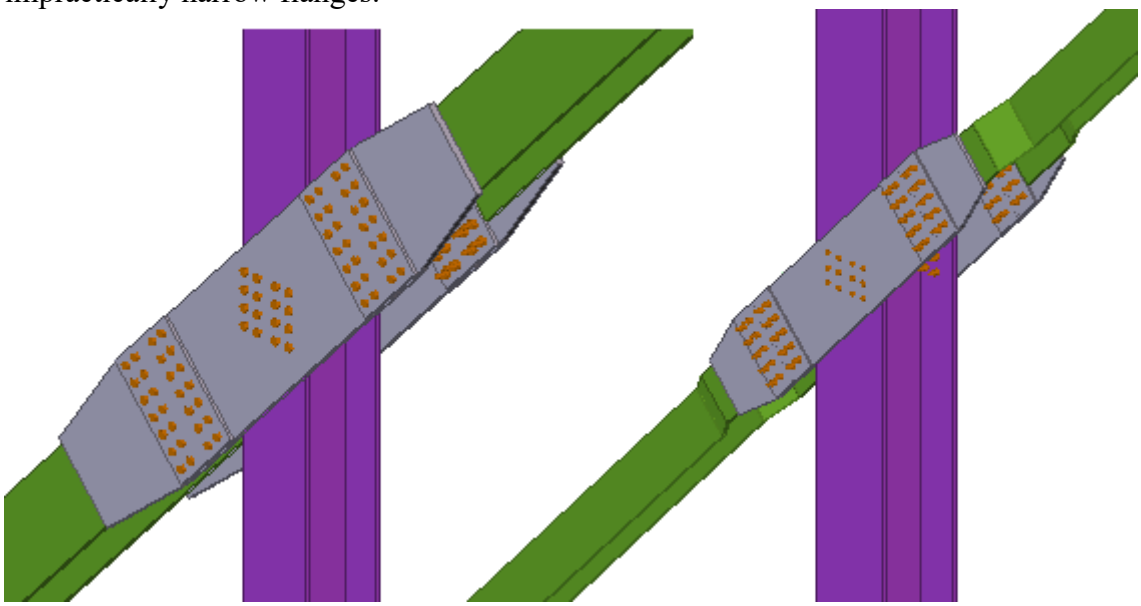

Figure 33. Connections CON3 (left) and CON3s (right).

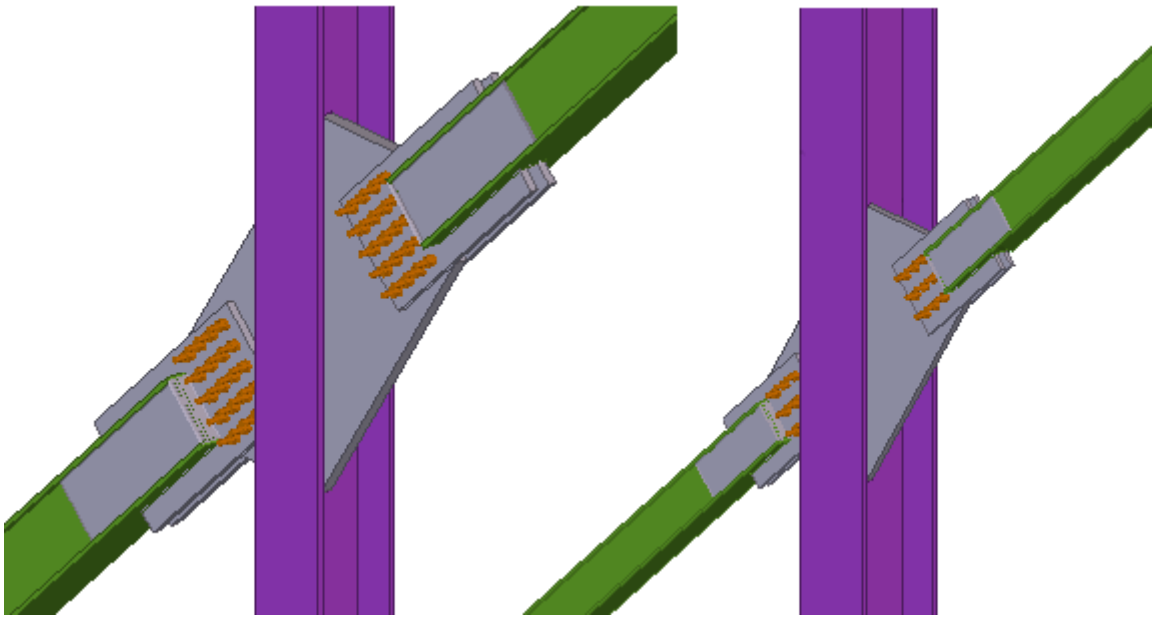

Figure 34. Connections CON4 (left) and CON4s (right).

Connection CON4 (Figure 34) features a single gusset plate penetrating and welded to the web of the column. When high tensile force is transmitted by the brace, the required thickness of the gusset plate reaches impractical dimensions. The gusset plate used in CON4 is 75 mm thick, making it very heavy and its material properties possibly nonhomogeneous along its thickness direction, which is represented by reduced strength properties in the Eurocode (SFS-EN 1993-1-1 2005, p. 26). The braces are connected to the gusset plate via two knife plates which are welded to the brace flanges. Reinforcement plates at brace webs

are necessary due to the large notch cut for the knife plates. A middle end plate is used to connect knife plates to each other at the end of the notch cut. No significant differences are found between CON4 and CON4s.

The final connection to be studied is CON5 (Figure 35). It features connection plates similar to those in CON1 but uses welded box profiles for the braces instead of I-profiles. In order to connect the brace to the connection plates, the flanges of the larger brace are widened and welded to the tapered plates, which are bolted to the connection plates. When a smaller brace profile is used, a simpler solution is to split the brace end with a section of an I-profile which is then welded to the brace webs and bolted to the connection plates.

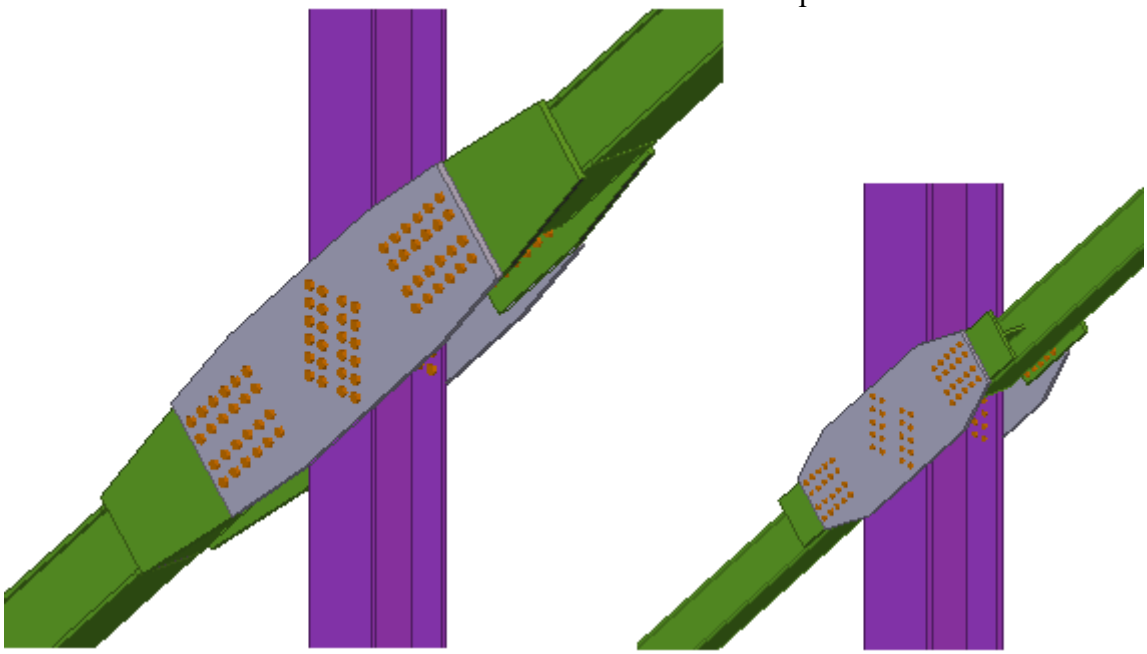

Figure 35. Connections CON5 (left) and CON5s (right).

4 Analysis methods

Each of the connections is designed to withstand a tensile force equal to the nominal yield strength of the brace, i.e., 13440 kN for the larger brace profile, and 4440 kN for the smaller brace profile. Initial dimensioning and design are made according to Eurocode. The strength of the connections is verified in the initial analysis by calculating the resistance of bolts in shear, bearing resistance, slip resistance, net and gross cross section resistance of plates, and the resistance of welds according to Eurocode 3 part 1-8 (SFS-EN 1993-1-8 2005, pp. 20–27, 29–31, 38–45). The connections and members are modeled in Tekla Structures, and further analyzed in IDEA StatiCa utilizing component-based finite element method (CBFEM). A brief theoretical background of CBFEM is presented in section 4.1.

A tensile axial force equal to the nominal yield strength is applied at the end of each brace in the CBFEM model. The column is set as a bearing member, such that its displacements are restricted. The strength of each connection is then verified in the CBFEM model, and modifications to connection geometry are made where necessary. Acceptable utilization ratios for the bolts and welds are set between 90% and 100%. Furthermore, the local plastic membrane strains at each plate are limited to 5%. All steel parts are made of S355 steel, and the bolts are grade 8.8. IDEA StatiCa performs all design checks according to the Eurocodes, and as such includes more design considerations than those included in the initial analysis.

With all the connections having almost equal strength, a direct comparison can be made. A bill of materials is generated for each connection and connected members, barring the columns. The distance between the center nodes of the brace end connections of one brace is selected to be equal to 8 meters. For the connections where the connection plates extend from one brace to another, only a half of the plate mass is considered in mass calculation. Assuming identical connections at each brace end, the total mass can be calculated directly from the 3D model, where the length from the connection center to the farther end of each connected brace is 4 meters.

Bolted connections designed according to Eurocode are slip resistant at either serviceability limit state or at ultimate limit state. If the friction connection between the plates fails, the connection will perform like a bearing-type connection, where shear forces are resisted by the bolts. Thus, the connections are modeled as bearing-type connections to better model their post-slip performance. Interaction of tension and shear forces in the bolts is taken into account. Welds between plates are modeled as solids representing the true geometry of the weld. Full penetration butt welds are assumed to reach strength equal to continuous base material as per clause 6.5.5(2) of Eurocode 8.

The cost estimation of the connections and their connected members is based on the feature-based costing method developed by Haapio (2012). The process of cost calculation is expedited by using JouCO2 & COSTi -spreadsheet tool developed by Research Centre of Metal Structures at Tampere University of Technology. The calculation methods used in the spreadsheet tool are those introduced by Haapio (JouCO2 & COSTi n.d.). The weight of the connection parts is read from the Tekla Structures 3D model, while the weight of the welded profiles is obtained from the spreadsheet tool. The cost estimation procedure is further discussed in section 4.2.

Ease of design, simplicity of force transfer, ease of installation and customer preference are criteria which are evaluated by surveying experienced designers. The goal of the survey is

to evaluate the criteria based on the experience and expertise of the designer. Their knowledge of solutions and issues in previous projects is deemed as a good way to quickly evaluate the criteria, the analysis of which might not otherwise be straightforward. The contents of the survey are presented in section 4.3.

4.1 *Component-based finite element method*

In design standards, joints are analyzed by deconstructing them into their basic components. Each component is then checked with the corresponding design formula to verify its resistance. Design of complex connections using the component method might become cumbersome. Software utilizing the finite element method (FEM) are often used to calculate the stresses of a joint. Combining the FEM results with the design model might not be straightforward, as component-based design checks are still necessary. To expedite this process, a software called IDEA StatiCa is used. It utilizes CBFEM to calculate stresses and to perform appropriate design checks based on the selected design code (Figure 36). Based on published results, CBFEM provides more variability in connection geometry and loading than current simplified component method models (Šabatka et al. 2014). Validation of the method has been done via laboratory testing (Kurejková 2017).

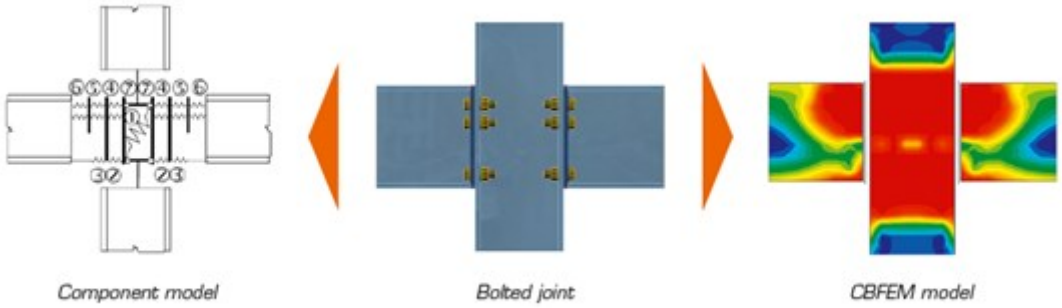

Figure 36. CBFEM combines the component method with finite element analysis (adapted from Theoretical background n.d.).

Theoretical background of the CBFEM utilized by the software is given on their website, on which the rest of this section is based. Webs and flanges of connected members are modeled by using 4-node quadrangle MITC4 shell elements with nodes at each of their corners. Such elements have 6 degrees of freedom per node, and their deformations are divided into the membrane and the flexural components. An elastic-perfectly plastic material model is used (Figure 37 a), and thus the effects of strain-hardening are not modeled. The ultimate strain limit is also set at 5%, as recommended in Eurocode 3 part 1-5, although the limit can be changed in the software settings. (Theoretical background n.d., SFS-EN 1993-1-5 2006, pp. 48–49.)

The mesh generation is automatic for all parts in the connection. The minimum element size is set to 10 mm by default, although this can be controlled by the user. The number of finite elements depends on the part. The default number of finite elements in a member is 8 elements per cross section height (Figure 38, left). The mesh of an end plate is twice as fine by default, as higher accuracy is generally needed for good results (Figure 38, middle). The mesh sensitivity of a T-stub in tension is the highest, with 16 elements used per half of flange width by default (Figure 38, right). For a compressed stiffener the default mesh density is 8 elements per plate width. The default mesh densities are chosen for each part such that the calculated resistance differs only by about 5% from the converged result with a higher

element density (see Figure 39). The default number of elements on edge can, however, be controlled by the user. In this analysis, the default values are used.

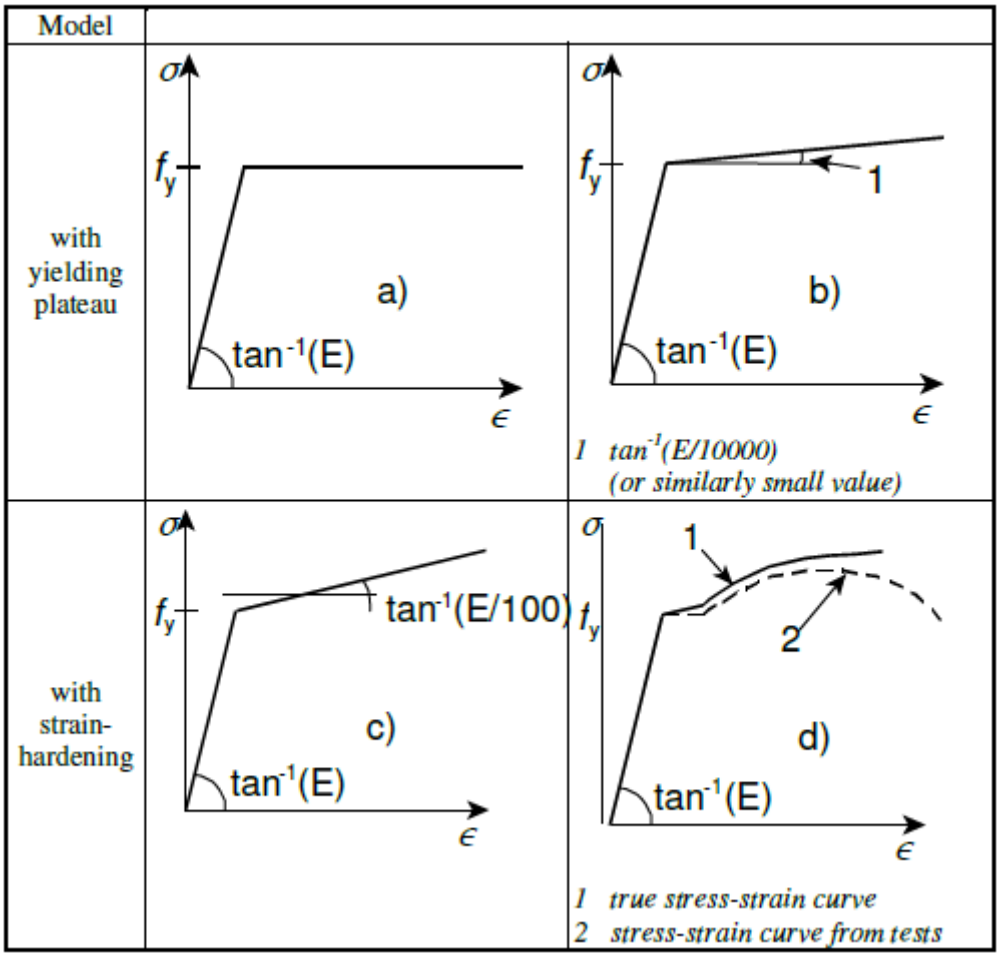

Figure 37. Stress-strain curves for structural steel according to different material models (SFS-EN 1993-1-5 2006, p. 48).

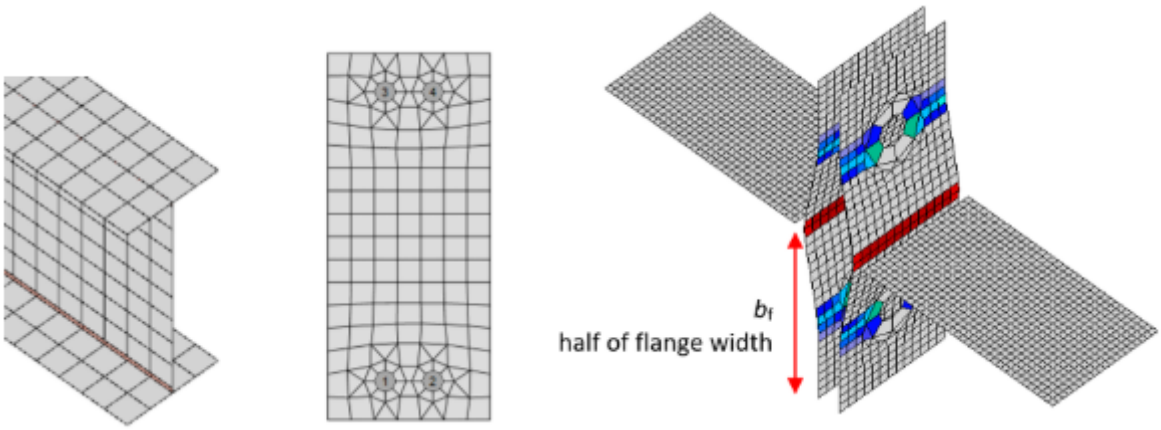

Figure 38. Default mesh size for different parts of a connection (Theoretical background n.d.).

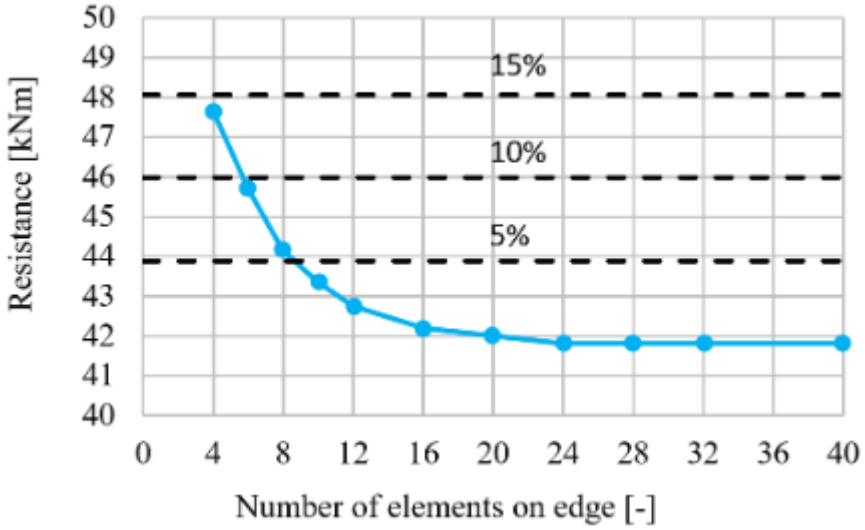

Figure 39. The influence of element density on the bending moment resistance of an open section beam-to-column connection (Theoretical background n.d.).

The finite element nodes of two plates at a weld joint are not directly connected, but instead related to each other by a multi-point force-deformation constraint. By using such an approach, it is possible to connect meshes of different densities. The weld element is modeled as a solid which represents the real geometry of the weld. The welds are elastoplastic, and their plasticity state is controlled by the stresses in the weld throat section. Plastic redistribution of weld stresses is applied in the model by default. However, any residual stresses or initial deformations from the welding process are not simulated.

Bolt behavior in tension, shear and bearing is simulated by interdependent nonlinear springs. As such, interaction of axial force and shear force in the bolts is taken into account. Simulation of slip resistant connections is possible by using preloaded bolts. Bolt tension is transferred to the connected plates which then resist the applied shear forces via friction connection. Contact between plates is modeled by a heuristic penalty method, where the penetration of nodes through other surfaces is prevented by penalty stiffness, leading to the distributed contact force. Where major bolt slip is detected, the design checks of the slip resistant connections fail. In such cases the connection must be remodeled as a bearing-type connection with non-preloaded bolts to perform design checks in post-slip stage.

The software utilizes a geometrically linear model and it is unable to take initial deformations into account. Stability of slender joint components is not realistically simulated, which must be considered in the design. Linear buckling analysis can be performed with the software to estimate the severity of buckling effects. Design of thin walled members is not supported by the software.

Contrary to typical FEM software, no individual boundary conditions are set for the members, i.e., for the beams, columns and braces. Instead, one member is selected as a bearing member, while the other members are referred to as connected members. The plate parts of the connection are simply referred to as plates. Each member will only be two times as long as its cross section height by default, with the rest of its length trimmed out of the model. Thus, the software concentrates on the behavior of the connection instead of its members. The length of a member is automatically increased if it is cut or welded, such that those features can be modeled. In a simplified mode, the bearing member is supported at

both of its ends and cannot be directly loaded. The supports resist translation in all directions at the ends of the bearing member. Such a simplification does not affect the distribution of stresses and internal forces in the connection, but only affects the presentation of deformations. For the purposes of this connection comparison the simplified method is used.

The stiffness of individual connection members can also be analyzed. The analyzed member is selected, and its stiffness is calculated individually, while the other connection members are supported. Thus, the stiffness analysis is only influenced by the selected member and its connection. Loads are applied to the analyzed member to evaluate its stiffness in the relevant direction. The software calculates the member end rotation with different magnitudes of the applied loading. A stiffness diagram is then automatically generated from the data, showing the load-deformation relationship and classification of the connection according to the selected design code.

The linear buckling analysis considers all plate parts of the connection and the members. The first six buckling shapes with the lowest buckling factors are considered. The buckling factor represents the factor by which the applied design load would have to be increased to cause global elastic instability, as defined in the Eurocode (SFS-EN 1993-1-1 2005, p. 30). Thus, the lower values of the bucking factor represent higher susceptibility to global instability inducing buckling. In plastic analysis, a buckling factor larger than 15 means that global instability does not have to be considered in design. For buckling factors smaller than 15, second order global analysis must be performed for the structure. For stiffener plates and column panels in shear, it is not necessary to consider buckling reduction factors if the buckling factor is larger than 3.

4.2 *Feature-based costing method*

The feature-based costing method used to estimate the costs of the proposed connections and braces was developed by Haapio (2012). Its purpose is to allow the designer to compare the costs of different solutions in skeletal steel structures used in industrial, commercial or office buildings. The design concept takes the connection details as well as the structural members into account. The formulae used in the cost calculations can be found in the doctoral thesis by Haapio (2012).

The costing method allows the designer to estimate the costs of the fabrication process in the workshop as well as the costs of transportation and erecting. In this thesis, only the costs related to the fabrication of the connections and the diagonal braces are considered. The feature-based costing method considers each fabrication task individually and utilizes specifically developed formulae to calculate the costs.

The cost functions consist of components for material, labor, equipment investment and maintenance, real estate investment and maintenance, consumables and energy. The cost functions include pre-set values for many parameters based on literature and observations. However, the parameters can be chosen by the designer as suitable in any individual project.

The reliability of the costing method has been evaluated by comparing its results to offers received by five European workshops and results produced by a similar costing method developed in Australia. Through those comparisons, the feature-based costing method has been proven reliable. This costing method provides much more accurate cost estimates than simple mass comparison, which is often used in the industry as an approximate cost estimate.

The feature-based cost estimates are calculated by the JouCO2 & COSTi spreadsheet tool. The tool consists of multiple tab pages which can be used to calculate the individual costs and CO2 emissions of different fabrication processes. The unit prices of real estate, labor, equipment and material are updated to the Finnish year 2015 level from data provided by Haapio, based on literature from Haahtela and Kiiras (2015) and instructions from KH X1-00244 (1998), KH X1-00291 (2001) and KH X1-00379 (2006). The prices for bolts, nuts and washers are selected as those available for workshops ordering large quantities, since the discounts can be significant.

The fabrication costs included in this comparison are material, cutting, deburring, welding, drilling, blasting and assembly by bolts. The costs of painting and weld inspection are ignored, as they might be project dependent variables. The dimensions of the welded profiles and the plate parts are input into their corresponding tab pages in JouCO2 & COSTi, which then produces the total costs of the part. The costs of a welded profile include material, cutting, deburring and beam welding. Each of these sub costs are then documented for each part. Parts requiring additional fabrication processes such as assembly by welding or bolts, drilling, cutting or blasting required separate calculation. Each of the described processes can be calculated in their corresponding tab page, which will then present a breakdown of the costs. The costs are then summed in spreadsheet tables presented in Appendix 3.

4.3 *Specialist survey*

The survey is formulated to collect information and opinions from experienced structural engineers in a concise fashion. Counting all different versions, the total amount of the connections is eleven. However, by grouping the connections based on their working principle, the amount of compared connections can be reduced to five. The survey is conducted via a questionnaire.

The task of the responder is to rank the five compared connections from best to worst based on the given criteria. The responders are shown figures of the different connections displaying the overall geometry (see Figures 30 through 35), however withholding any detailed dimensions. The above-mentioned criteria for ranking are the ease of design, simplicity of the connection, ease of installation and presumed customer's preference. Furthermore, the responder is allowed to give open feedback. The English translation of the questionnaire is shown in Appendix 4.

The responders are chosen from the personnel of Sweco Structures based on their experience in the topic. At the beginning of the questionnaire, the responder is also asked to estimate their familiarity with the subject. Thus, the competence of the responder can be evaluated based on their self-evaluation. No personal data is collected from the responders, and their answers are handled anonymously.

5 Results and discussion

In this chapter, the results from the analysis are presented. The comparison of the connections is made in two groups, with the large connections being evaluated separately from the small versions of the connections. This way, it is easier to select the most suitable connection depending on the design case. Analysis and discussion of the results is also presented in this chapter.

First, the results of the finite element analysis are presented. The design checks according to Eurocode are made for each connection, when the braces are under tension. Bending moment resistance analysis and support classification is made for the different connection types. Finally, the buckling susceptibility of the connections is evaluated.

The weight and estimated cost of each connection is presented in a table format. A direct comparison between the connections can be easily made from the numeric data. Those results are then combined with the data obtained from the survey. The survey results are quantified such that a direct comparison between the connections can be made. The characteristics of the connections are then displayed in radar charts which can be used to evaluate their performance independently in each of the categories.

Other design considerations based on the open feedback from the survey are also addressed. Furthermore, topics not covered by the survey and the cost analysis are discussed. Finally, the reliability of the results is analyzed, and possible error sources are identified.

5.1 *CBFEM analysis*

A summary of the governing utilization ratios is shown in Table 13. Each of the connections passes the design checks made in IDEA StatiCa for the applied load combination. All design checks for different load combinations required by the design codes are not performed at this stage of the analysis. However, the nominal plastic capacity of the brace will likely produce the governing load case for the connection. Furthermore, all connections are designed according to the same criteria.

Table 13. Extreme values of IDEA StatiCa design checks for each connection.

Connection	Plastic strain (%)	Bolt utilization (%)	Weld utilization (%)
CON1	4.1	91.2	98.0
CON1s	4.4	98.3	-
CON2	1.4	96.7	99.5
CON2s	1.3	96.1	98.8
CON3	0.7	99.1	98.7
CON3s	1.0	99.6	98.1
CON4	1.4	97.9	98.2
CON4s	1.2	99.9	99.5
CON5	4.9	95.6	98.8
CON5s	0.7	98.4	99.1

The equivalent stress distributions for each connection type under the applied load are shown in Figure 40 and Figure 41. The results are mostly shown only for the large version of a connection, since the stress distribution in the smaller connection is assumed to be similar to

the larger one. However, as connection CON5s differs from CON5 by a significant amount, their results are displayed separately. The braces in each connection reach their nominal yield stress under the design load, as expected. Stress concentrations can be seen near bolt holes and at fillet weld ends. High stress levels can also be seen at plate cross sections, where their surface area is reduced by bolt holes or cuts. The reinforced brace ends experience lower stresses than the rest of the brace and can therefore remain intact at the net cross section.

The most critically stressed areas of the connections can perhaps be more easily seen by inspecting their plastic membrane strains shown in Figure 42 and Figure 43. Zones subjected to the highest plastic strains also sustain the largest permanent deformations, and thus are most susceptible to rupture. The limit strain of 5% is not exceeded in any of the compared connections.

The largest plastic strains in CON1 are located at the net section of the reinforced flange, at the first bolt row. If the plastic strain needs to be further limited, thicker and wider reinforcement flanges can be used. CON2 shows plastic strains at the plate net cross sections and at the fillet welds. Particularly high weld strains are found at the ends of the vertical cross-plate fillet welds. The 10 mm web reinforcement plates at the brace end also show plastic strains near the end of the notch cut. Plastic strains can also be found at the column flange where the two horizontal gusset plates intersect it. If necessary, this can be avoided by using a continuous horizontal gusset plate that penetrates the column and connects the two braces more directly. Such solutions are usually, however, avoided in order to ensure continuity of the column. Another option would be to cut notches in the horizontal gusset plates and leave the column flanges intact. The plastic strains at CON3 are mostly concentrated at the net cross sections of the sandwich plates. High plastic strains are also found at the fillet welds subject to tension, at the interface of the connection plate and the brace flange.

The plastic membrane strains at CON4 are concentrated at the first bolt row of the knife plates, as expected due to the reduced net cross section area. Larger strains can, however, be found where the knife plates are welded to the flanges of the brace, particularly at the end of the weld. The cross section of the brace is significantly reduced by the notch cut made to accommodate the two knife plates, and therefore stress concentrations can be found near the cut. As stress is transferred from the brace to the knife plates towards the end of the brace, the stresses at the reduced brace end cross section decrease.

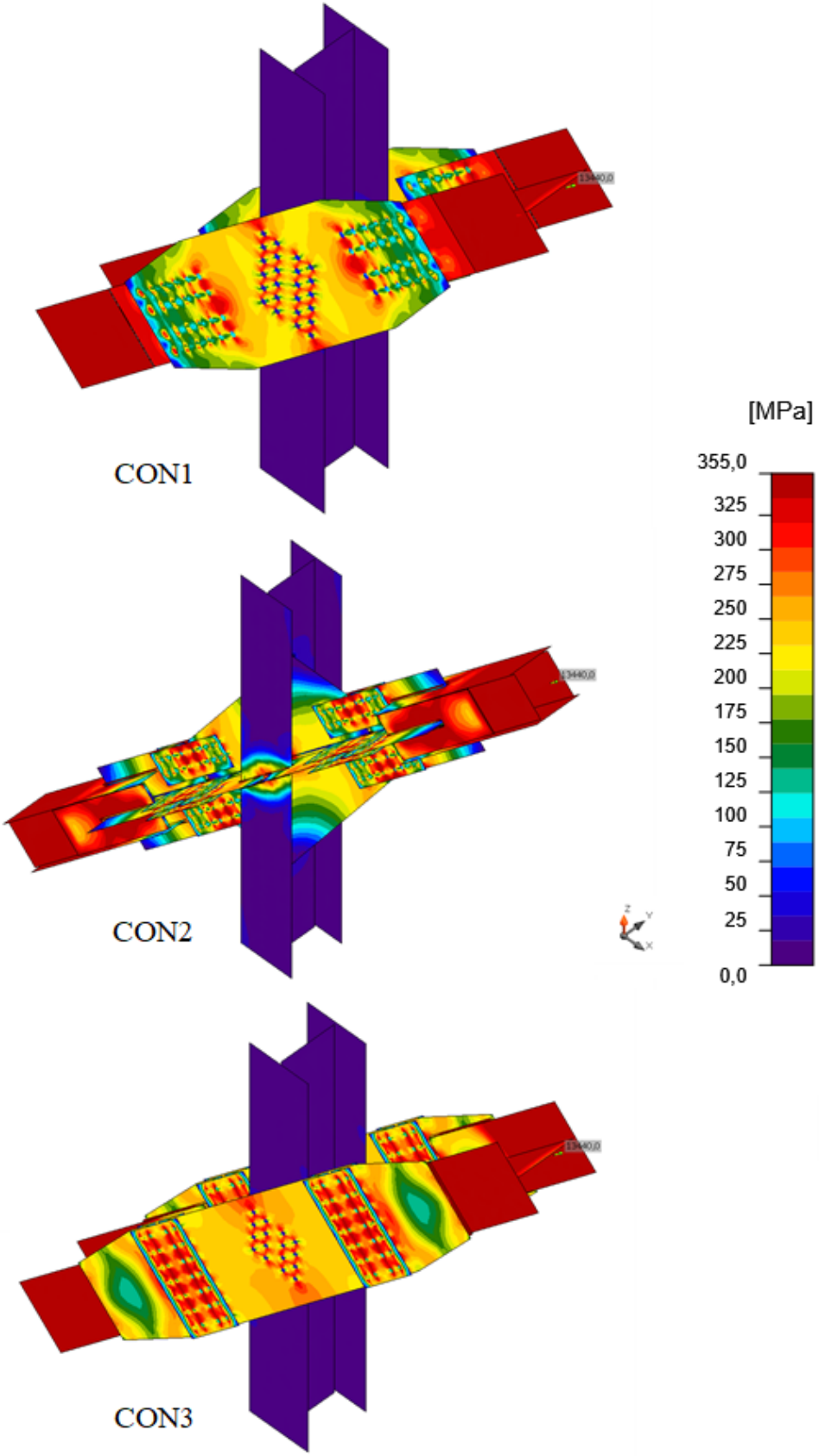

Figure 40. Equivalent stress (Von Mises) in connections CON1, CON2 and CON3 when subjected to tensile force equal to the nominal yield capacity of the brace.

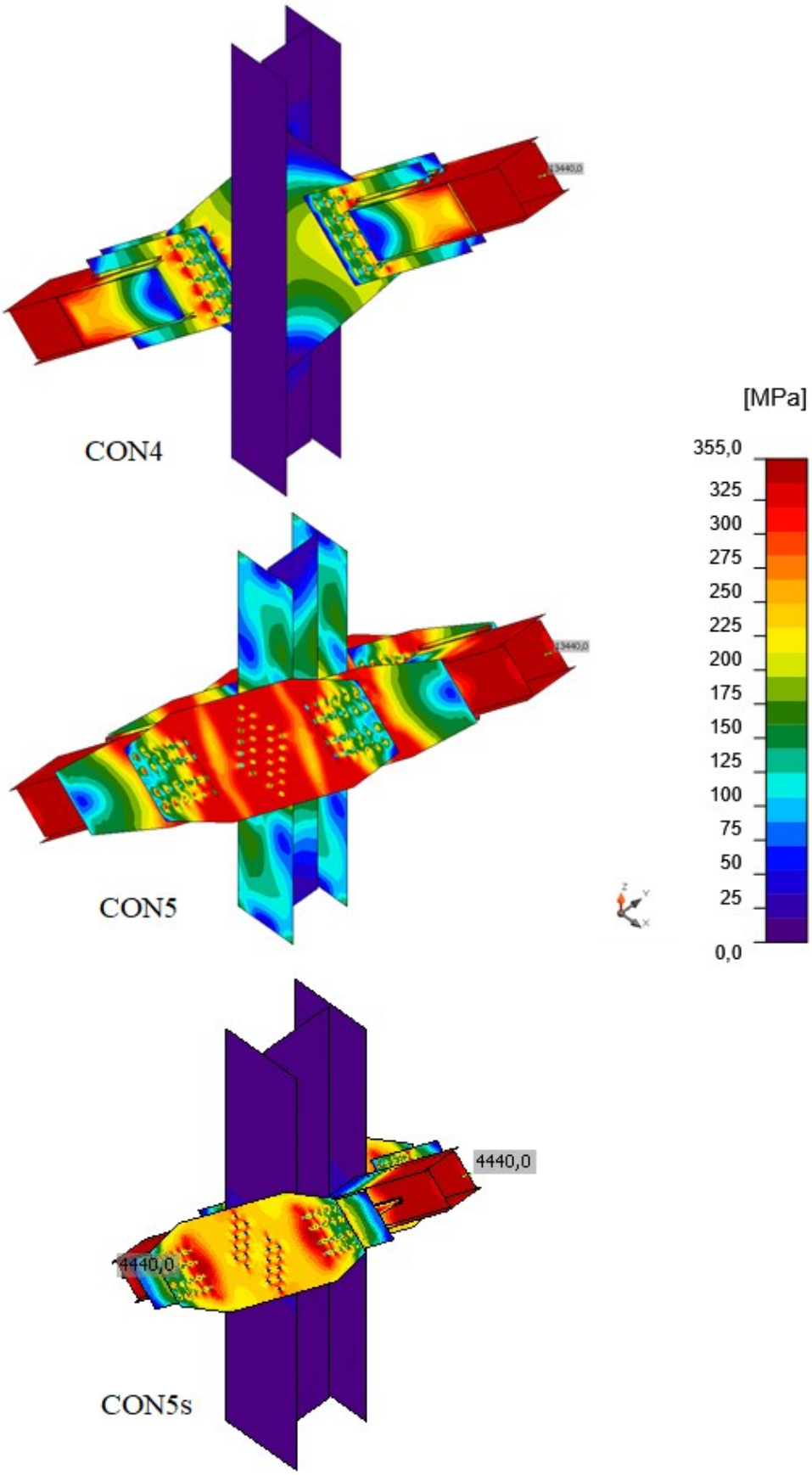

Figure 41. Equivalent stress (Von Mises) in connections CON4, CON5 and CON5s when subjected to tensile force equal to the nominal yield capacity of the brace.

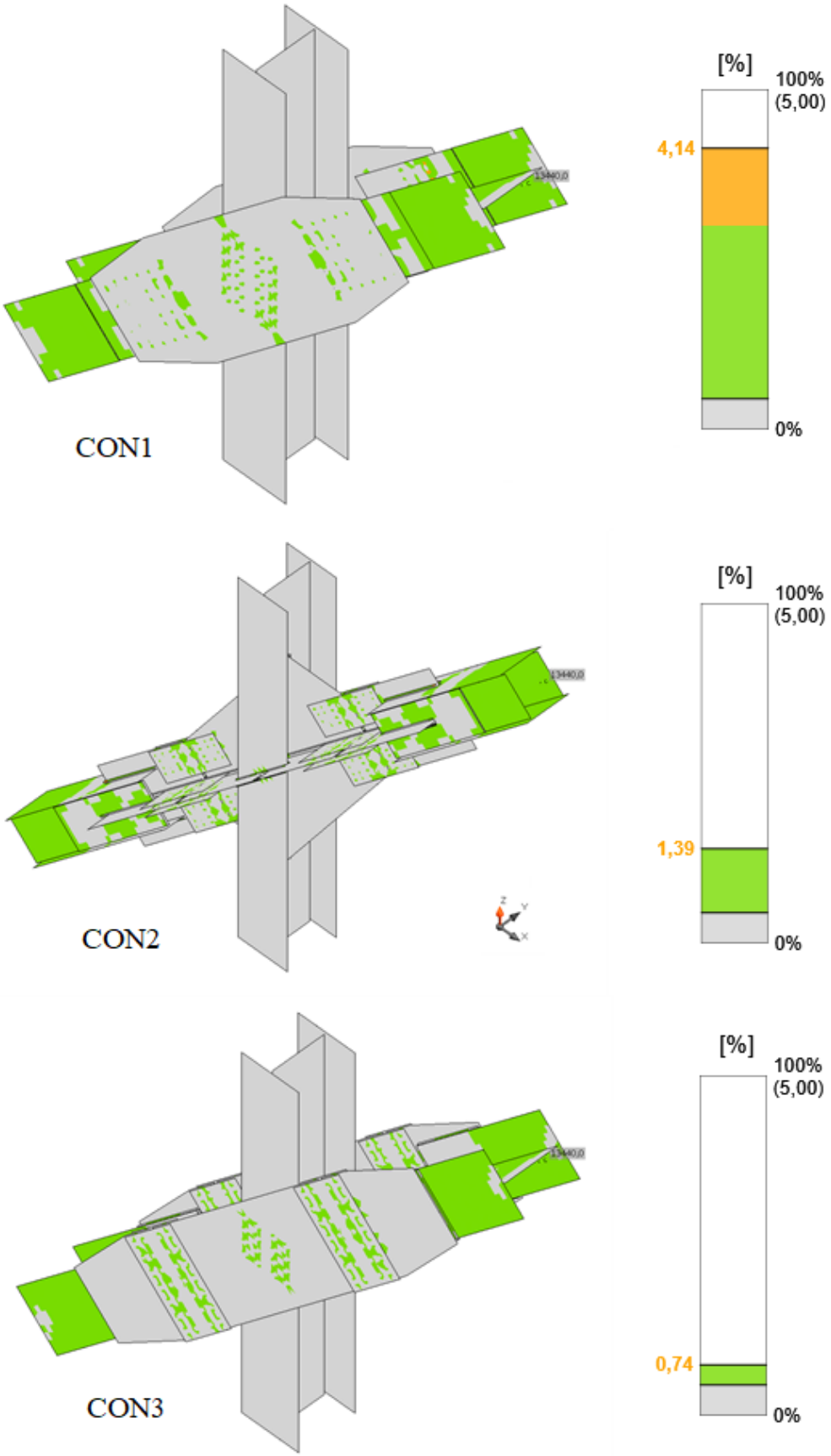

Figure 42. Plastic membrane strain in connections CON1, CON2 and CON3 when subjected to tensile force equal to the nominal yield capacity of the brace.

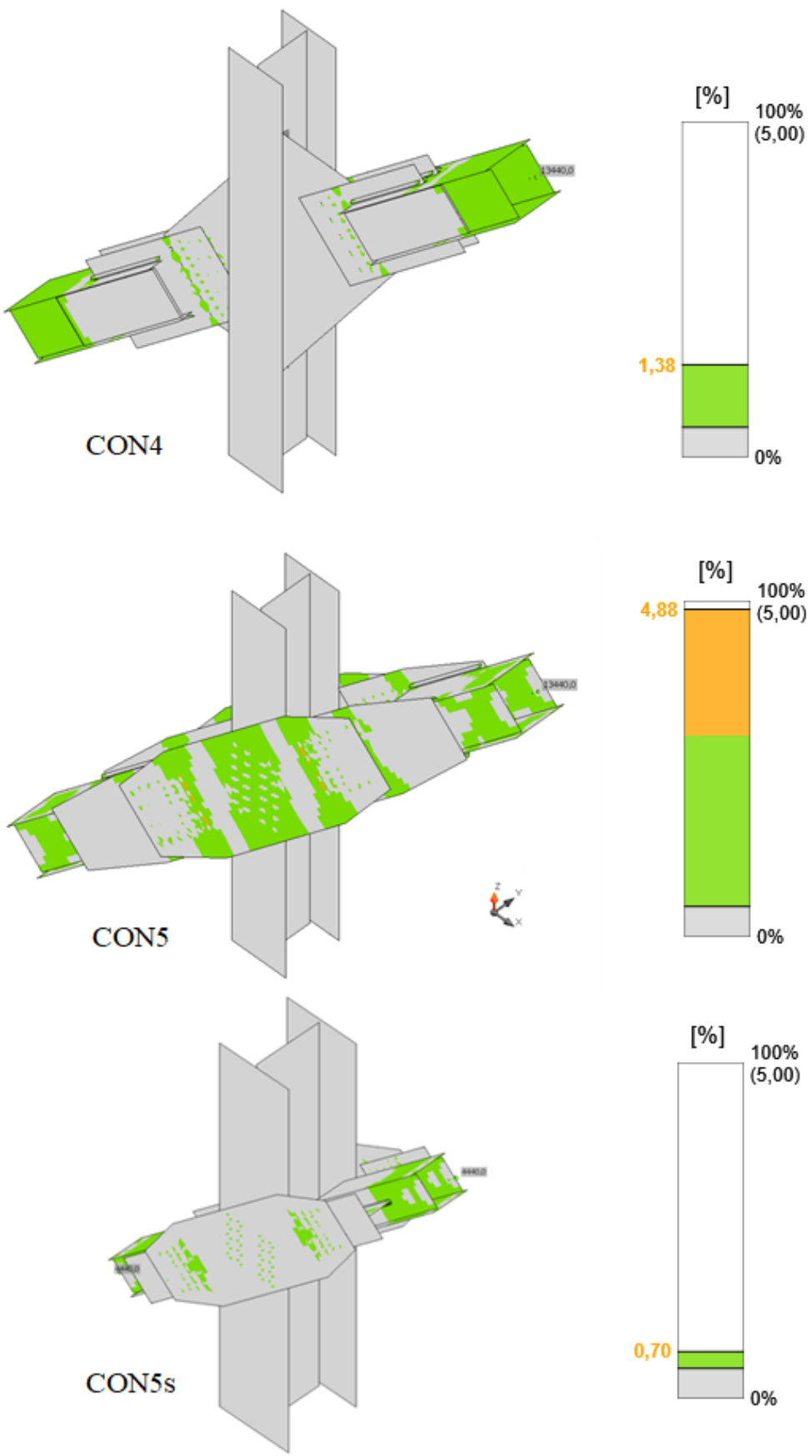

Figure 43. Plastic membrane strain in connections CON4, CON5 and CON5s when subjected to tensile force equal to the nominal yield capacity of the brace.

Connection CON5 features a long connection area, which is not particularly stiff in the out-of-plane direction. Figure 41 shows stresses being transferred from the braces to the column in a way that is not seen in the other connections. The deformed view of the connection shown in Figure 44 shows how the gusset plates and connection plates are bent inwards when the braces are pulled outwards. The deformations are exaggerated by a factor of 10. The bending plates are connected to the flanges of the column, and thus flexion can be seen in the column flanges as well. Such behavior of the connection is not desirable, and a web connecting the connection plates should be provided as a stiffener. Similar issues are not found in CON5s, where the web of the I-beam section used in the connection prevents out-of-plane bending of the plates. Largest plastic strains are still found at the connection plate net cross sections in both CON5 and CON5s.

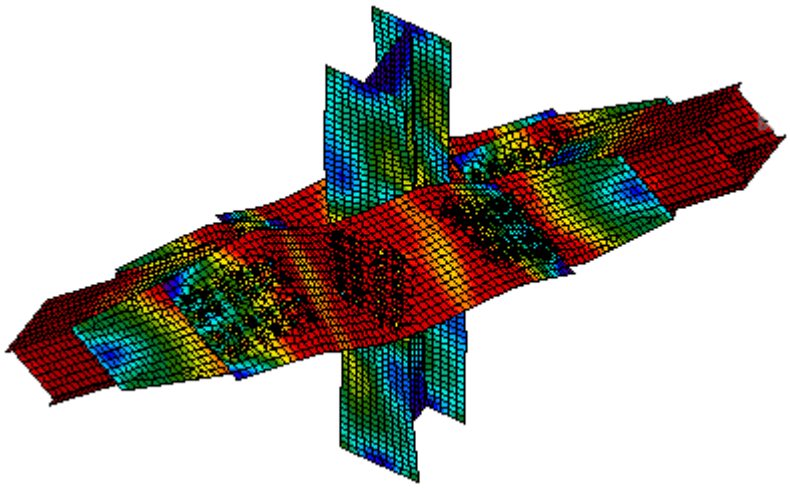

Figure 44. Deformed (x10) view and equivalent stress of CON5.

When the design of the brace connection is made according to ASIC 341, sufficient brace end rotation capacity should be provided. Otherwise, the connection must be able to resist the flexure forces defined in equation 35. Interestingly, the brace end rotation demands set in Eurocode 8 and NCh2369 are not as strict as in AISC 341. When flexure resistance is however necessary, it can be achieved by increasing plate thicknesses or by using stiffeners where needed.

In many practical applications, the determination of the buckling length of the brace will be based on an estimate chosen by the designer. The rotational stiffness of the connection can, however, be calculated in IDEA StatiCa to estimate its rigidity (see Table 14). A graph is generated in IDEA StatiCa for each connection type to evaluate the bending stiffness in the in-plane and out-of-plane directions. The graphs are not generated for the small versions of the connections, except for CON5s, since their behavior is expected to be similar to that of the larger connection. An example of this graph is shown in Figure 45, and the rest of the graphs can be found in Appendix 2.

Table 14. Connection properties in bending.

In-plane bending								
	$S_{j,ini}$ (MNm/rad)	$S_{j,R}$ (MNm/rad)	$S_{j,P}$ (MNm/rad)	Support classification	ϕ_c (mrad)	$M_{j,Rd}$ (kNm)	$M_{c,Rd}$ (kNm)	k_{cr} (-)
CON1	∞	123.8	7.7	Rigid	411.4	1357.7	1321.6	0.50
CON2	769.9	185.4	11.6	Rigid	17.4	1296.3	1874.8	0.53
CON3	∞	123.8	7.7	Rigid	390.6	1357.7	1321.6	0.50
CON4	∞	185.4	11.6	Rigid	289.9	1921.2	1874.8	0.50
CON5	∞	191.3	12.0	Rigid	281.3	1975.8	1928.1	0.50
CON5s	10.8	21.8	1.4	Semi-rigid	205.6	217.6	373.9	0.69
Out-of-plane bending								
	$S_{j,ini}$ (MNm/rad)	$S_{j,R}$ (MNm/rad)	$S_{j,P}$ (MNm/rad)	Support classification	ϕ_c (mrad)	$M_{j,Rd}$ (kNm)	$M_{c,Rd}$ (kNm)	k_{cr} (-)
CON1	∞	381.0	23.8	Rigid	294.0	2842.0	2849.4	0.50
CON2	∞	145.1	9.1	Rigid	34.0	1298.5	1676.0	0.50
CON3	2185.8	381.0	23.8	Rigid	288.8	2916.2	2849.4	0.53
CON4	9.0	145.1	9.1	Pinned	219.5	582.7	1676.0	0.92
CON5	∞	161.4	10.1	Rigid	299.4	1797.6	1783.7	0.50
CON5s	∞	15.7	1.0	Rigid	274.0	326.4	320.2	0.50

where $S_{j,ini}$ is the initial rotational stiffness of the connection calculated at 2/3 of the limit capacity
$S_{j,R}$ is the limit for rigid connection classification
$S_{j,P}$ is the limit for nominally pinned connection classification
ϕ_c is the ultimate rotation capacity of the connection
$M_{j,Rd}$ is the ultimate limit bending resistance of the connection at 5% plastic strain
$M_{c,Rd}$ is the design bending resistance of the brace (SFS-EN 1993-1-1 2005, p. 50)

By using the approximate expression for critical buckling force presented by Brush and Almroth (1975, p. 26), the effective buckling length factors can be solved for the different connections:

$$N_{cr} = \frac{(\lambda_1 + 0.4)(\lambda_2 + 0.4)}{(\lambda_1 + 0.2)(\lambda_2 + 0.2)} \pi^2 \frac{EI}{L^2} \tag{46}$$

where $\lambda_1 = \frac{EI}{S_{j,ini,1}L}$ is a rotation stiffness parameter for the first end of the compressed bar
$\lambda_2 = \frac{EI}{S_{j,ini,2}L}$ is a rotation stiffness parameter for the second end of the compressed bar

By considering this critical buckling force (equation 46) equal to the classical representation (equation 43), the effective buckling length factor can be solved as

$$k_{cr} = \sqrt{\frac{(\lambda_1 + 0.2)(\lambda_2 + 0.2)}{(\lambda_1 + 0.4)(\lambda_2 + 0.4)}} \tag{47}$$

The effective buckling length factor k_{cr} presented in Table 14 is calculated according to equation 47. Theoretically, a compressed bar with rigid supports at both of its ends should have an effective buckling factor of 0.5, while a bar with pinned supports at both of its ends should have an effective buckling factor of 1.0. In practical applications, the rotation stiffnesses of the connections are neither completely rigid nor nominally pinned, and as such the values of k_{cr} will vary between 0.5 and 1.0. It should be noted, that the infinite initial stiffnesses reported for most of the connections in Table 14 are a result of inaccuracy of the numerical calculation utilized by IDEA StatiCa, and practically no stiffness should be infinite. In the calculation of k_{cr}, the infinite values are replaced with very high constant values, which produce results corresponding to rigid connections. The results obtained through this analysis show that the support classification per Eurocode gives a rather good estimate on the buckling length of the braces. It is noteworthy, that the analyzed connections are assumed to be a part of a braced frame with little horizontal displacement. Realistically, the horizontal displacement of a frame can be quite significant in an earthquake, causing the effective buckling lengths of the braces to increase.

From an ease of design point of view, all used connections should be either rigid or nominally pinned. Nominally pinned connections transfer the internal forces without developing significant bending moments. Rigid connections are assumed to have sufficient rotational stiffness to justify analysis based on full continuity between the connected members. Semi-rigid connections lie between the two aforementioned classes. They transfer bending moments but do not provide enough rotational stiffness to be considered continuous. Using semi-rigid connections in design usually requires additional stiffness calculations to be made, which complicates the overall process of structural analysis. However, Eurocode allows connections to be classified based on experimental evidence and previous satisfactory performance, which might allow semi-rigid connections to be classified as either rigid or nominally pinned in some situations. (SFS-EN 1993-1-8 2005, p. 54.)

The classification of the connections by their stiffness and the corresponding limit values for rigid and nominally pinned joints are calculated in IDEA StatiCa based on Eurocode formulae (Theoretical background n.d., SFS-EN 1993-1-8 2005 pp. 54–55). For the purposes of the stiffness calculations as per Eurocode 3, the connections are assumed to be a part of a frame where the bracing system reduces the horizontal displacement by at least 80%, and the span length of each brace is 8 m. The corresponding settings are used in IDEA StatiCa calculations, as those settings affect the limit values of connection stiffness classification.

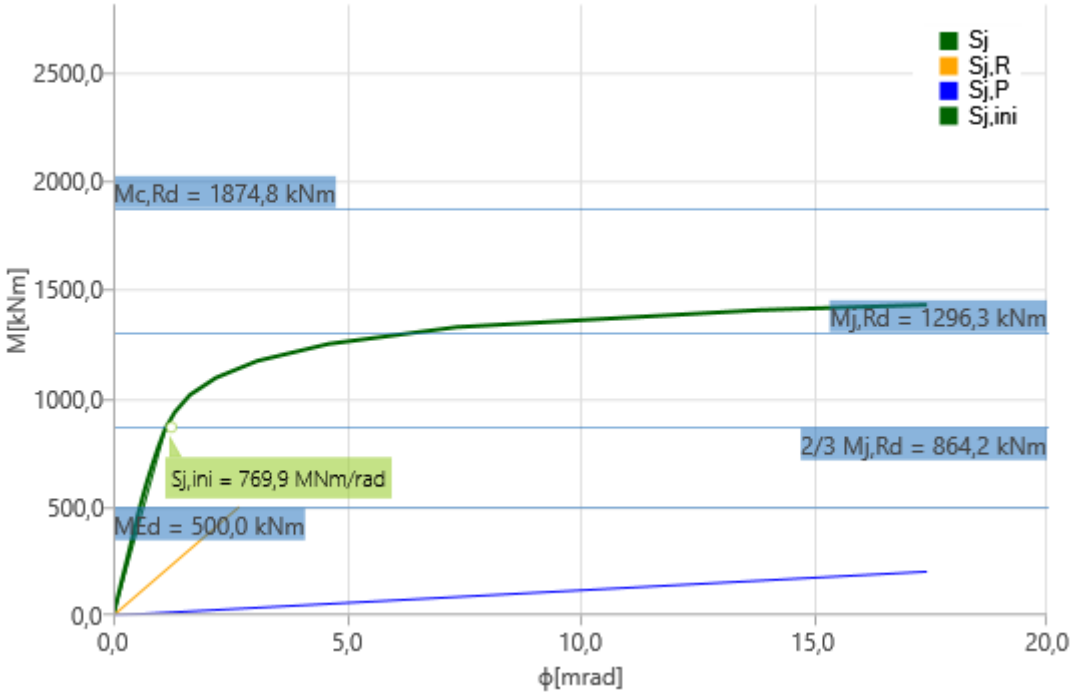

Figure 45. In-plane bending stiffness diagram for rigid connection CON2.

The following notation is used in the figure above:

- S_j is the rotational stiffness of the connection
- M_{Ed} is an arbitrary design bending moment used to control the direction of analyzed stiffness
- ϕ is the rotation of the brace end.

The only connection type that can be classified as nominally pinned in one direction is CON4. Featuring only a single gusset plate, CON4 bends relatively freely in the out-of-plane direction (Figure 46). Whether or not such behavior is desirable depends on the conceptual design of the braced frame.

Connections CON1, CON3, CON4 and CON5 are all rigid connections that can also withstand bending moment equal to the design bending moment capacity of the brace in the in-plane direction. In the out-of-plane direction, only connections CON3 and CON5 can resist such forces. Such bending moment resistance is, however, not always necessary, provided that sufficient brace end rotation capacity is available. Rotation capacities vary from 205 to 411 milliradians (11.7–23.6 degrees) for most of the connections, except for CON2 which has barely any rotation capacity. As such, the resistance of CON2 to buckling needs further design considerations. It should however be noted, that even the connections with a larger rotation capacity seem to remain rigid until close to their ultimate resistance. Thus, their rotation capacity comes from yielding of the connection plates, and their resistance in cyclic loading is an important design consideration. The rotation capacities required from the connections depend on the expected story drift of the structure, as larger drifts cause larger transverse displacements of the diagonal braces.

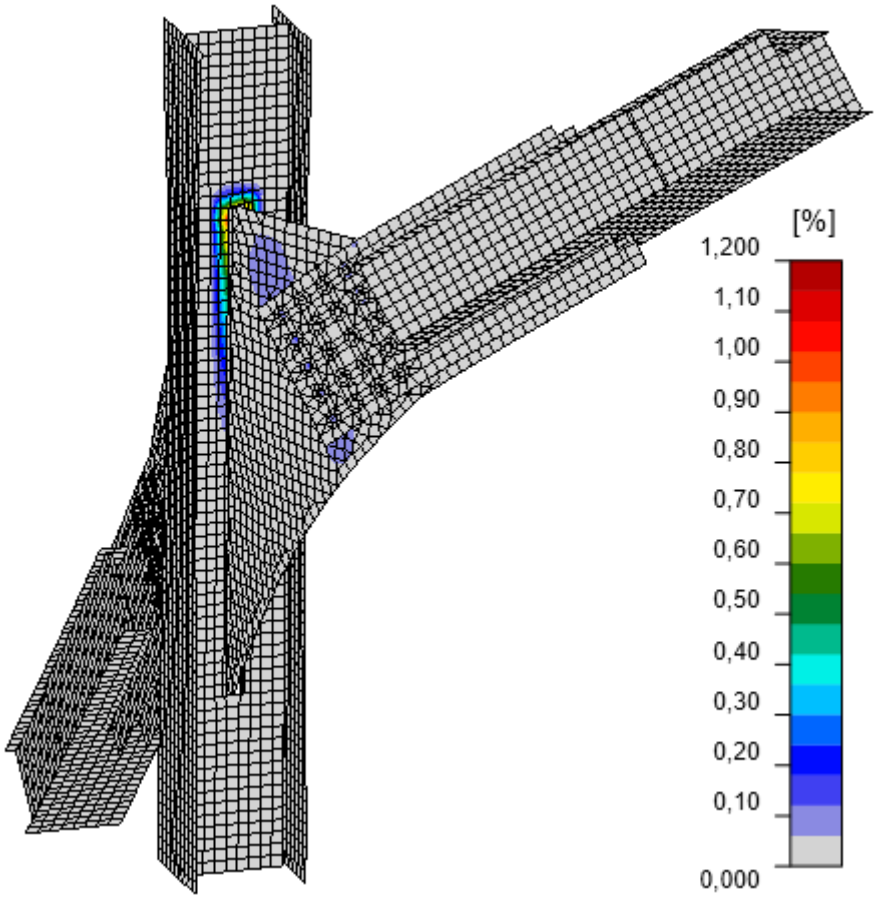

Figure 46. CON4 exhibits nominally pinned behavior in out-of-plane bending. The plastic strains and deformation (exaggerated by a factor of 10) are displayed for a design bending moment of 500 kNm.

Compressed diagonal braces might experience buckling in several modes. In-plane and out-of-plane flexural buckling are the most common buckling modes which are also discussed in previous chapters. Depending on the shape of the brace cross section, they might also experience torsional and flexural-torsional buckling, with open cross sections being more susceptible than closed cross section shapes. Buckling modes including torsion of the diagonal brace are however typically not problematic, and do not require special consideration in the design process.

When the braces transmit compression forces to the connection, buckling of connection plates is possible. Using a compressive normal force of 10750 kN, which produces stress equal to 80% of the yielding stress of the brace as per NCh2369, the linear buckling analysis is performed for the large version of each connection. The relevant buckling mode in the scope of global stability is considered for each connection. The buckling factors and the critical buckling shapes resulting from the analysis are shown in Figure 47. The lower the buckling factor, the more susceptible the connection is to buckle, which might cause global instability. Perhaps surprisingly, connection CON4 is not the most vulnerable to buckling. This might be explained by the very large thickness of the gusset plate and zero-eccentricity normal force transfer from the knife plates. Connections featuring large, unsupported, relatively slender plates, such as CON3 and CON5, perform relatively poorly under compression.

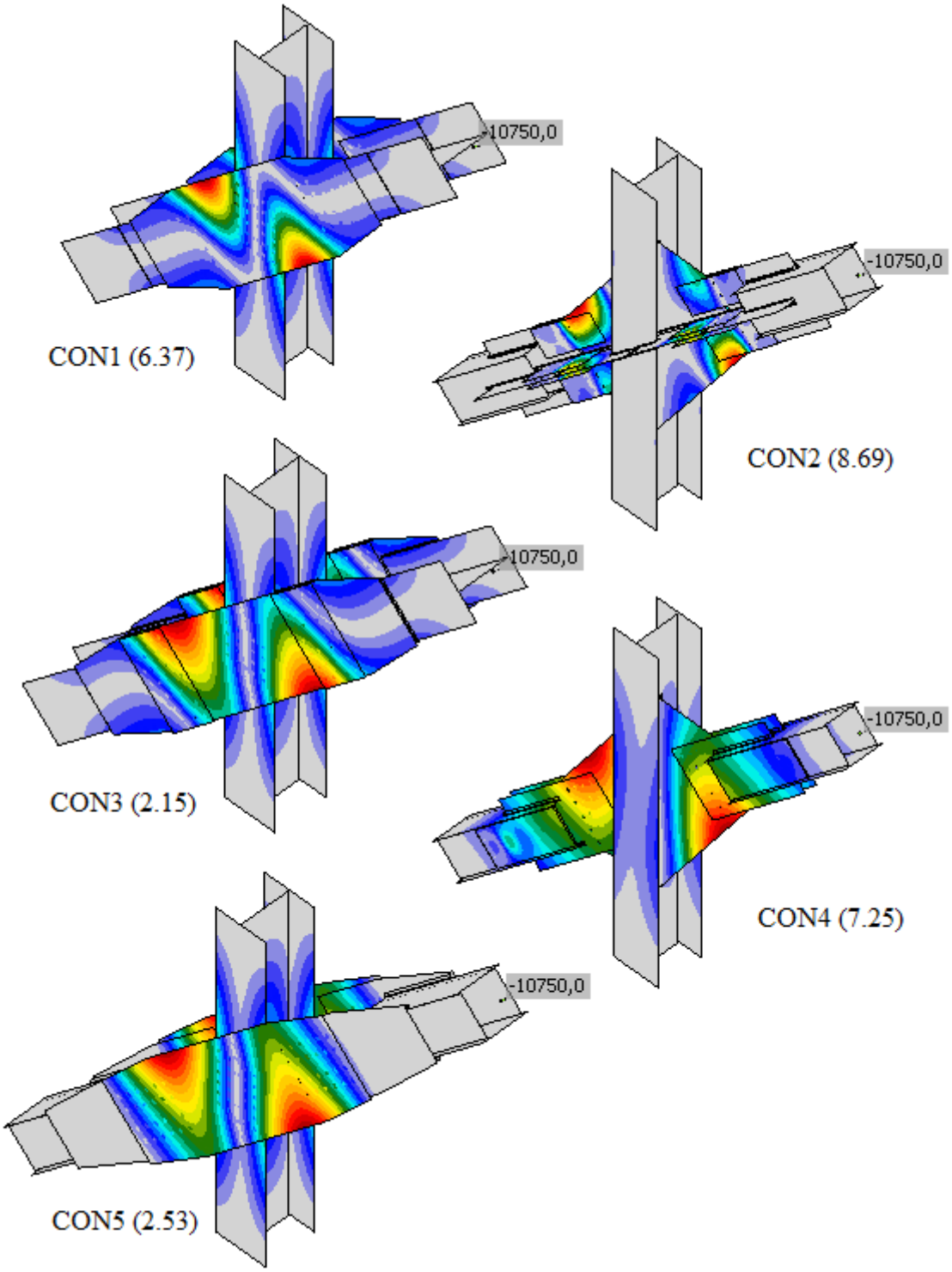

Figure 47. Visual representation of critical buckling modes. Red color represents the areas most susceptible to buckling. Buckling factor is given in parenthesis for each connection.

5.2 *Cost analysis*

The results of the weight and cost comparison are shown in Table 15 and Table 16, separately for the large and the smaller versions of the connections, respectively. In the large category, connection CON3 is the lightest and least expensive option, while CON5 is both the heaviest

and the most expensive option. A similar trend can be found when comparing the smaller connections, where the lightest option, CON1s, is also the least expensive. However, here the heaviest connection, CON4s, is not the most expensive option, and that title is rather taken by CON2s. In the analyzed connections, the weight does not always directly correlate with their cost.

In the large brace category, the most expensive connection is almost 53% more expensive than the least expensive one. The difference in their weight is however only 23%. Similarly, the cost difference between the most and the least expensive design in the smaller brace category is 47%, with their weight difference being only 17%. The largest weight difference between two designs is found between CON4s and CON1s at around 27%.

Table 15. Summary of mass and costs of the large connections and braces.

	Mass (kg)	Estimated cost (€)
CON1	4288.0	8686.6
CON1b	4057.1	9423.6
CON2	4483.6	9761.8
CON3	**3985.1**	**6840.3**
CON4	4682.3	8673.8
CON5	4888.9	10463.1

Table 16. Summary of mass and costs of the small connections and braces.

	Mass (kg)	Estimated cost (€)
CON1s	**1022.6**	**2130.4**
CON2s	1202.4	3136.9
CON3s	1059.6	2354.3
CON4s	1296.1	2730.2
CON5s	1202.4	2438.0

5.3 *Specialist survey*

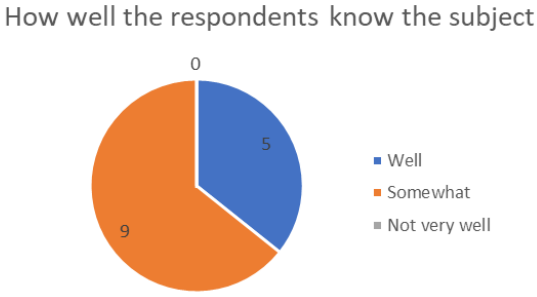

Figure 48. The respondents' competence with the subject based on self-evaluation.

Out of the 24 people the questionnaire was sent to 14 responded, out of which 13 people responded to the multiple-choice questions and 9 gave open feedback. The overall response percentage was therefore 58%, which can be considered quite good for internal surveys. The results of the multiple-choice questions are shown in Figure 49. As is evident from the spread of the results, there are no clear answers to the questions. General trends can however be seen in many of the answers, which will become clearer with the quantifying analysis

performed later in this section. The competence of the people answering the survey is quite good based on their self-evaluation, as shown in Figure 48.

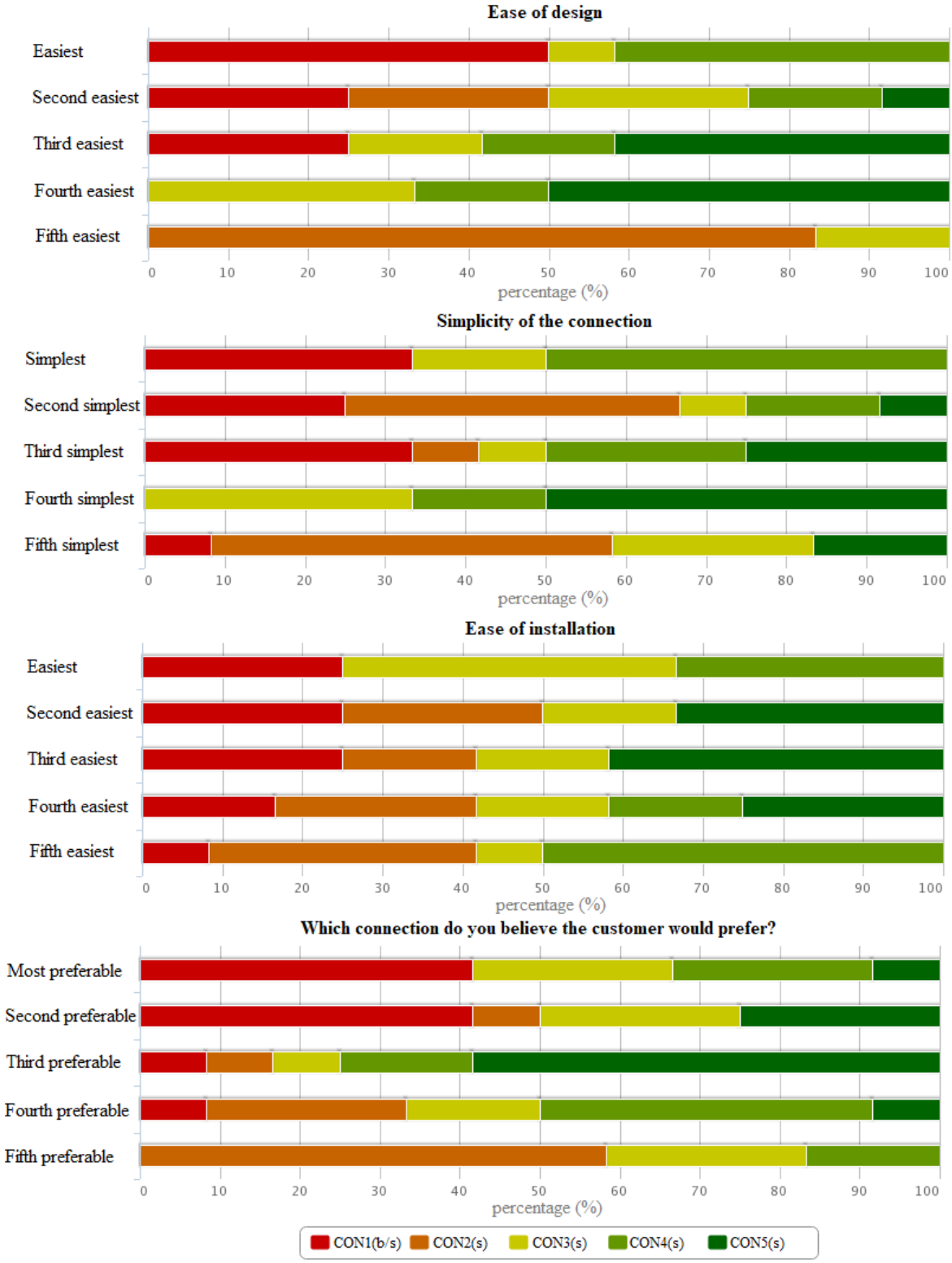

Figure 49. The questionnaire results shown as a percentage for each connection.

A scoring system awarding the two best connections and punishing the two worst connections in each category is devised. The best and second-best options are scored +2 and

+1, respectively, while the worst and the second worst options are scored -2 and -1, respectively. The scoring is done individually for each survey response, after which the mean of all the results is used for scoring each connection. The large and the small versions are ranked independently from each other in the total comparison, although the questionnaire considered them as the same connection and thus awarded them the same score. The reason to separate the large and the small versions from each other is to be able to include the calculated mass and cost estimates in the comparison, as those differ depending on the size of the connection. The mass and the estimated cost of each connection is linearly scaled such that the best option (lowest mass or cost) is assigned value 2 and the worst option is assigned value -2. All intermediate results are linearly interpolated between those limit values. The determination of the mass and the cost of each connection is not a part of the survey but they are presented together with the survey results. The results of this quantifying analysis are shown in Table 17.

Table 17. Quantifying analysis of the survey results and the mass and cost calculations. The mass and cost scores are scaled linearly from -2 to 2, independently for the small and the large connections. The questionnaire results are scored from -2 to 2 in each category and averaged over all the answers. A positive score implies good results.

Connection	Ease of design	Mechanical simplicity	Ease of installation	Customer preference	Low mass	Low cost
CON1	1.15	0.69	0.46	1.15	0.66	-0.04
CON1b	1.15	0.69	0.46	1.15	1.68	-0.85
CON2	-1.23	-0.46	-0.77	-1.38	-0.21	-1.23
CON3	-0.31	-0.46	0.62	0.08	2.00	2.00
CON4	0.92	1.08	-0.31	-0.08	-1.09	-0.02
CON5	-0.54	-0.85	0.00	0.23	-2.00	-2.00
CON1s	1.15	0.69	0.46	1.15	2.00	2.00
CON2s	-1.23	-0.46	-0.77	-1.38	-0.63	-2.00
CON3s	-0.31	-0.46	0.62	0.08	1.46	1.11
CON4s	0.92	1.08	-0.31	-0.08	-2.00	-0.38
CON5s	-0.54	-0.85	0.00	0.23	-0.63	0.78

The numerical results are displayed graphically in Figure 50 and Figure 51 for the large and the small connections, respectively. A radar chart is chosen to be able to distinguish the performance of each connection individually in each of the categories. Furthermore, superimposing the results in the same graph allows for easy direct comparison.

Judging by the radar chart results only, CON1, CON1b and CON3 seem like the best large connection options, depending on what the most important criteria are. In the small connection category, CON1s is the best option in 4 of the 6 categories. Essentially, the bigger the enclosed area in the plot, the better the connection is overall. However, the methods by which this data was collected and analyzed might not provide unambiguous, directly comparable results. Therefore, the open feedback is analyzed for a more complete breakdown of the connection properties.

The open feedback contained many different viewpoints considering connection design, sometimes contradicting with other respondents' answers. Some reoccurring themes were, however, identified through coding of the open feedback. Most of the open feedback contained a notion, that the ranking of a connection in any category is dependent on many

different criteria and the current project. As such, strict ranking of the connections is a difficult task, and might not be accurate.

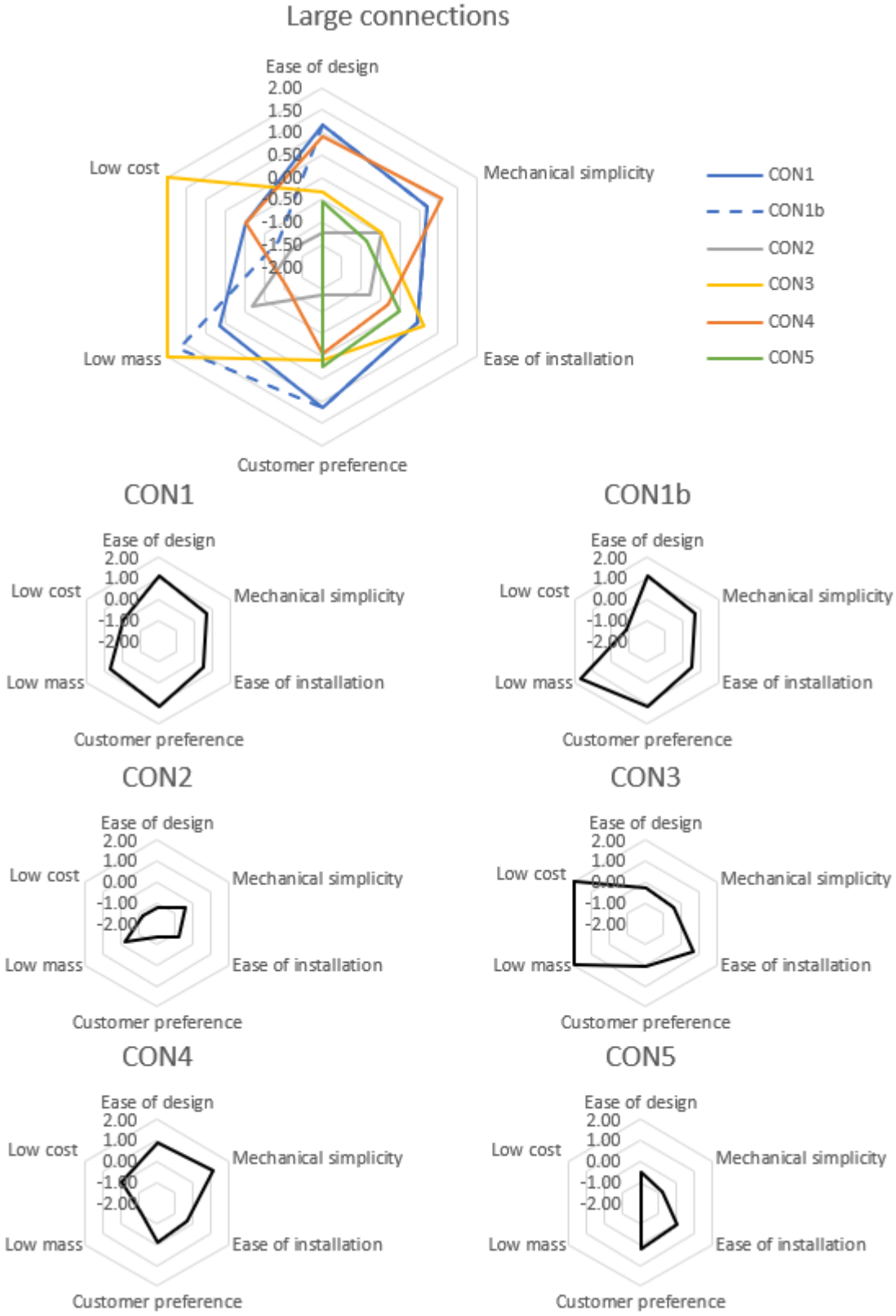

Figure 50. Radar chart representation of properties of the large connections. The results are displayed individually for every connection in the bottom part and overlaid in the same chart in the top part of the figure.

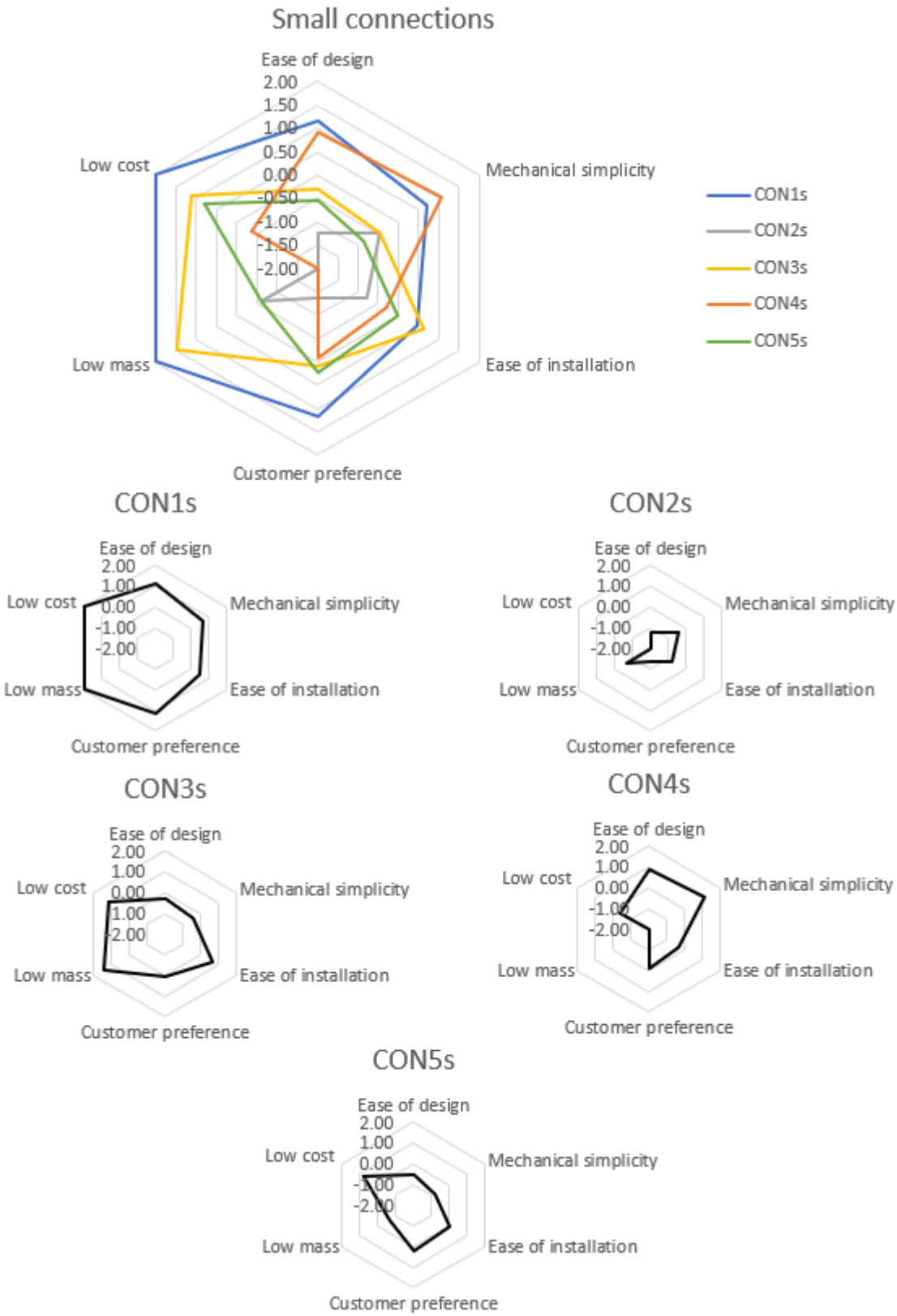

Figure 51. Radar chart representation of properties of the small connections. The results are displayed individually for every connection in the bottom part and overlaid in the same chart in the top part of the figure.

The most prevalent feedback considering the connections dealt with the demands of friction connections, which are typically required in seismic areas. Connections featuring a clearance between plates to facilitate installation, i.e., CON4, are difficult to use as a slip-critical friction connection. Friction connections rely on flush contact between plates fastened by pretensioned bolts. A friction connection might not be possible to implement in a connection where the initial clearance between plates can be several millimeters.

Another identified theme considered the question regarding the customers preference in connection selection. It was reminded that the customer does not often have the expertise to provide relevant feedback considering connection design, and as such that might not be a relevant factor in selecting the most suitable connection. The customer's opinion might, however, be guided by the total mass or the estimated cost of the solution, as is expected. Sometimes they might also prefer designs that take the least amount of space in the structure. In cases where the customer is responsible for the installation of the connections, they might also prefer designs featuring fewer parts and bolts.

According to one responder connections CON1, CON3 and CON5 become complex to design when more braces and beams are added to them. This comment is probably related to the fact that connecting I-beams to the connection plates such that they carry gravity loads about their strong axis is not readily possible. Some design options for connecting multiple members in the connections are shown in section 5.4.

Conflicting feedback was received concerning the buckling resistance of connection CON4. With the connection featuring only a single gusset plate, it might be susceptible to buckling in the out-of-plane direction. On the other hand, it was pointed out that the buckling problem might be avoided by dimensioning the gusset plate such that its slenderness is sufficiently low. When the connections are designed for the plastic capacity of the brace, plate thicknesses tend to be high, and as such the buckling might not become a problem. This notion is supported by the linear buckling analysis results shown in Figure 47.

Ease of installation was another category that was deemed difficult evaluate. Oftentimes the feedback received from the construction site regarding the ease of installation has been dependent on the party conducting the installation, i.e., the same connection might receive both positive and negative feedback depending on who does the installation. Specific feedback was received regarding the installation of connections CON1 and CON5. Braced frames in industrial structures are typically installed in blocks, such that the lower diagonal braces are a part of the lower block, while the upper braces belong to the upper block. Therefore, installation of the upper braces becomes impossible if both connection plates are bolted already in the earlier stage. One solution is to rely on only the connection plate on one side of the column during the construction stage, which might last several weeks. The second connection plate would be installed together with the upper block. The strength of a single connection plate during the installation stage must be verified if such practice is used.

Potential issues were identified with connections featuring parts outside the column flanges, i.e., CON1, CON3 and CON5. Plates and bolts protruding further than the column in the out-of-plane direction might become cumbersome when designing wall and plane structures. Design of the connections of possible horizontal beams in the out-of-plane direction requires acknowledgement of the brace connections. Furthermore, connections featuring braces with variable cross sections were criticized as complex.

General feedback on the selection of optimal connections was also received from a responder with extensive experience in designing industrial structures. Despite the design being dependent on multiple factors, the solutions most preferred by the customer have been those that feature a low total mass. Even though the mass of the structure does not always correlate with its cost, as shown in section 5.2, the option with the lowest mass has been deemed the best by the customer. An important factor in the price of the connection is also the location of manufacturing, as labor tends to be expensive in Europe, and those values were used in the cost estimation. Sometimes the cost of the structure might also be entirely based on its weight, depending on the outsourcing contract.

5.4 *Other design considerations*

The possibility to connect other members, such as beams, to the same connection is desirable. This can be done for each of the connection options by extending the gusset plates or connection plates out towards the location of the brace. Similar bolted connection can then be used for the beam, as is used for the braces. However, the orientation of the connected beams in CON1 and CON3 will have them bending around their weaker axis. The width of the beam must also be equal to that of the brace and the column. When it is necessary to orient the beam in another configuration, or to use another profile size, a different connection must be designed. Such a configuration is still possible with little to no eccentricities. The members in CON3 might need to be moved back to allow room for adjacent sandwich plates of the brace and the beam. Connections CON2 and CON4 show probably the most versatility out of the different options, with easy connection of beams of various sizes, however preferring rectangular hollow cross sections.

Each of the connections are modeled for two diagonal braces only, to keep the calculations and comparison as simple as possible. Practically though, horizontal beams are almost always connected to the same node as the braces, and the number of diagonal braces can be up to four. Thus, the possibility to connect additional members to the same connection is considered. Connections CON1, CON3 and CON5 are similar enough to be considered together. Connections CON2 (Figure 54) and CON4 (Figure 55) are considered separately due to their different geometries. The examples of the connections featuring multiple members as shown below have not been verified by calculations and are modeled for illustration purposes only.

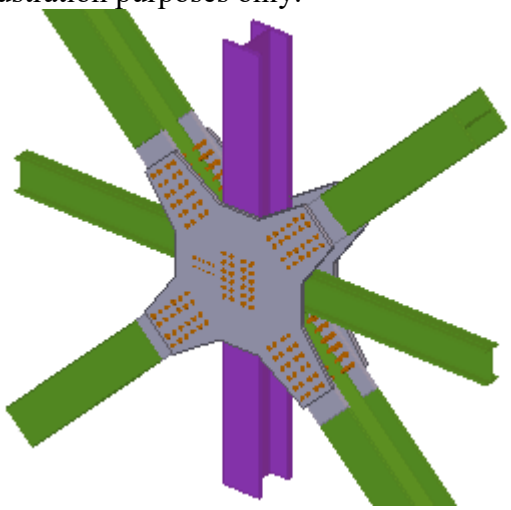

Figure 52. Connection CON1 modified to fit multiple beams and braces.

Adding more braces to CON1, CON3 and CON5 can be accomplished by simply expanding the connection plates (Figure 52). However, connecting beams to the connection requires special consideration. It is possible to connect the beams in the same way as the braces, but that would have them carry loads about their weak axis, unless an adapter such as that in CON5 is used. Furthermore, large eccentricities in beam connections might impose bending moment on the column. Therefore, two alternative beam connection options are shown in Figure 53.

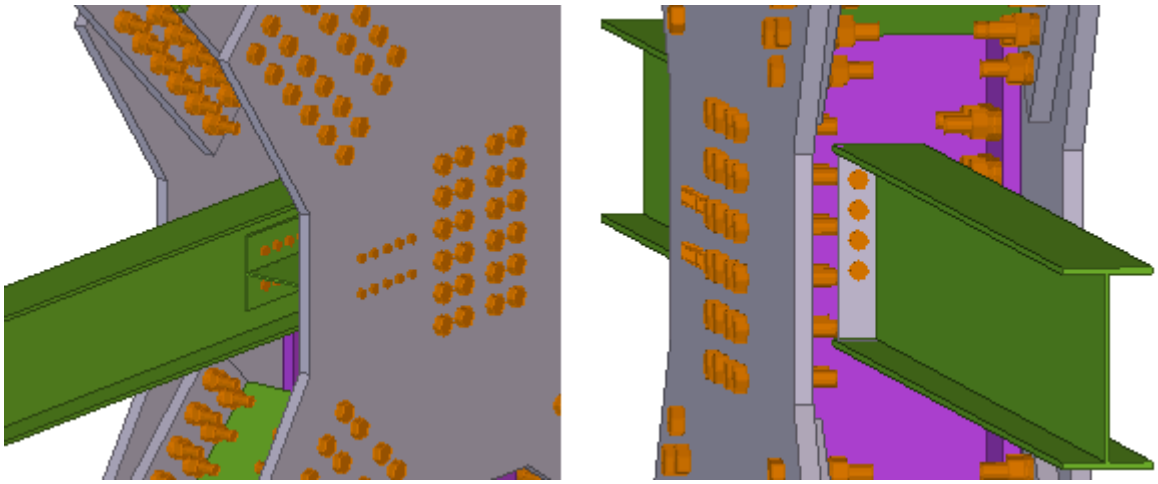

Figure 53. Beam connection options to be used in CON1, CON3 and CON5.

Perhaps the simplest option for a beam connection is a bolted end plate connection between the beam and column web (Figure 53, right). This practically zero eccentricity connection can be used on many different I-beam sizes, and the same bolts can be used to connect another beam on the other side of the column. If a stiffer connection is needed, the end plate and the bolts can be placed above and below the profile. The I-beam has to be of such size though, that it does not collide with the bolts of the brace connection. Furthermore, this option might not be as suitable in a seismic application as friction connections, as the bolts under tension are more prone to brittle failure.

Another way to connect a beam to the brace connection is to bolt short I-beam sections to either side of the end of the beam (Figure 53, left). This option is not as simple or lightweight, but it provides a way to connect a variety of different sizes of beams to the brace connection without the risk of bolt collision. The short I-beam sections can also be welded to the beam already in the workshop instead of bolting them at site. Web stiffeners can also be welded to the beam when necessary. This connection features a larger eccentricity than the previous option, but it is still smaller than those shown for connections CON2 and CON4. Furthermore, this connection provides a more ductile fracture mechanism due to the bolts being subjected mainly to shear forces.

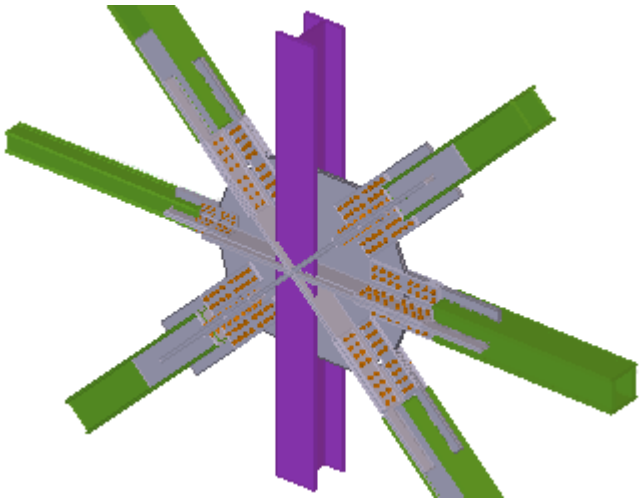

Figure 54. Connection CON2 modified to fit multiple beams and braces.

Connecting additional beams and braces to CON2 does not require any special considerations, as the same type of connection can be used for each member. The horizontal connection plates in the beams might also be omitted, as they do not significantly increase the shear force carrying capacity of the connection. Members of different sizes can be easily connected. However, to fit all connections, the eccentricities from the center of the connection are quite significant, which might create unwanted bending moments at the column. Large connections also increase the total weight, which in turn increases the total costs.

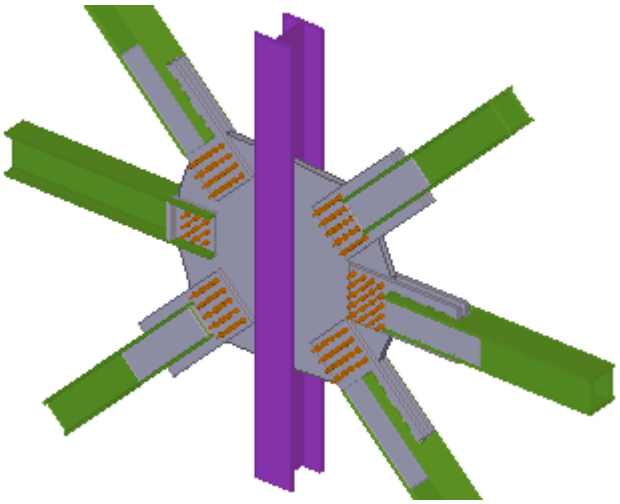

Figure 55. Connection CON4 modified to fit multiple beams and braces.

When beams and additional diagonal braces are added to CON4, the size of the gusset plate becomes very large. Such gusset plates might be prone to buckling in compression, and they add a lot of weight to the connection. The size of the gusset plate can be reduced in cases where it is possible to push the beams closer to the column. The connection type does, however, add a lot of versatility in terms of members that can be connected. As can be seen in Figure 55, it is possible to connect both I-beams and box profiles with similar connections.

General design objectives were described for concentric brace connections in Chapter 2.4.3. These objectives are based on relatively recent literature, which is backed up by practical research. Much of the research has been performed in association with American researchers

and as such made from that perspective. Therefore, the connection types used in the research are those commonly used in North America, i.e., welded gusset plate connections, and the design considerations are related to those connections. These objectives can, however, be partly generalized to evaluate the performance of the connections included in this thesis.

First, the connections are required to be strong enough to allow the brace to yield or buckle before rupturing. All the connections are dimensioned according to the design tensile force to ensure that the connection never fails before the brace, fulfilling the first requirement. The buckling of the brace happens at forces lower than the yielding of the brace, but it induces bending moments in the connections. This bending moment needs to be either resisted by the connection, or brace end rotations must be allowed. These properties of the connections were discussed in section 5.1 and summarized in Table 14. The strength of the connections in repeated cyclic loading is not verified in this thesis and should be considered in design.

The strength of the connections was verified via Eurocode-based calculations as well as the CBFEM analysis. The specific failure mechanisms considered in the initial analysis are discussed in chapter 4. Although the strength of the connections surpasses the nominal tensile strength of the brace, the failure mechanism through which the system eventually fails was not studied. The bolted connections do, however, show capacity for developing plastic deformations near the bolt holes, as can be seen in Figure 42 and Figure 43, which is a sign of ductile behavior. The available strength in different failure mechanisms should be evaluated and balanced to ensure ductility of the connections.

The location where plastic hinging might occur in a brace connection is also typically of interest, as that can be used to estimate the buckling length of the brace. The effective buckling length of a member affects the critical compressive force at which it buckles (see equations 43 and 46). The locations where plastic hinges might form in the connections are not entirely clear, but the buckling effective buckling length factors were calculated by utilizing the initial stiffnesses of the connections instead. Most of the connections can be classified either rigid or pinned in a given direction, which makes them simple to use in design. Only CON5s of the studied connections is classified as semi-rigid, which makes it a less preferable option.

Connections CON1, CON3 and CON5s are expected to buckle in the plane of the frame, since they have lower bending resistance in that direction, making them less likely to cause damage to surrounding structures in an earthquake. However, buckling direction of the braces might not be important in the design of an industrial structure, depending on the application. Furthermore, most of the connections provide rigid end supports for the braces, reducing their buckling lengths and transverse displacements. Connection CON4 is the only connection studied in this thesis that buckles in the out-of-plane direction with pinned end supports. As such, it will need the most transverse clearance to allow for buckling.

5.5 *Reliability analysis*

The reliability of the presented results is analyzed in this section. Possible sources for inaccuracies and errors are identified. Each of the utilized analysis methods is examined individually in the following sections.

5.5.1 Connection modeling

The concepts for the different connections were chosen based on solutions that have been used in brace connections in past projects worldwide. The small versions of each connection were designed separately, as they required the use of an adapter piece in many of the connections. Design calculations according to Eurocode were used for the initial dimensioning of the connections, after which they were modeled in Tekla Structures.

The strength of the connections was then verified in IDEA StatiCa using Eurocode-based design checks. The connection geometries were then iterated to find solutions where their utilization ratio was within the set limits. However, the connections can sometimes be fairly complex, and optimization of their geometry would require extensive testing. In this analysis, each of the connections was deemed satisfactory when they passed the IDEA StatiCa design checks when the braces were subjected to their nominal plastic tensile capacity.

As bending and compression design checks were omitted in this initial stage, the connection geometries were not optimized for resisting those phenomena. As such, e.g. purpose specific stiffeners were not modeled and thus their cost and weight were not taken into account. The buckling behavior of many of the connections could also be improved by smart design of stiffeners.

The connections were designed in two different sizes to evaluate their versatility. Including more braces of different size in the analysis would have provided more data, which might have been useful in evaluating the overall performance of the connections. Furthermore, many different design solutions could have been made especially for the small versions of the connections than what were presented in this thesis. The design force used in connection design depends on the design code. The dimensions of the connections will naturally depend directly on the design forces, and therefore the comparison might yield different results depending on where the structure is built, and which standards must be used. Furthermore, AISC 341 sets specific brace end rotation capacity requirements which are not fulfilled by most of the studied connections. Special consideration would therefore have to be made when such brace connections are used in destinations where compliance with AISC 341 is required.

The braces were connected to the frame at a 45-degree angle. However, it is common to have braces in many different angles connected to the same joint. Braces connected at a low angle (measured from horizontal level) leave less space for the beam connection, which increases the eccentricity of the beam connection. In some cases, it might even prevent the types of beam connections discussed in previous chapter. Large connection areas also increase the overall mass of the connections, which might influence their ranking.

5.5.2 Component-based finite element method

The largest limitation considering the CBFEM software IDEA StatiCa is the lack of control given to the user. While the minimum and maximum element sizes as well as the default mesh density can be controlled, the element shape and type cannot be changed. The 3D geometries of the connections are always modeled by 2D shell elements. Thus, the stress distribution might not be properly simulated, especially in thicker plates under flexure. The simplifications will, however, allow for simple and quick calculation of results, which should be adequate in most design cases.

The effects of brace buckling cannot be accurately modeled either, as the software does not support large displacements or input of initial imperfections, and the model is geometrically linear. Furthermore, the linear buckling analysis can only be used to estimate the severity of the buckling effects of compressed parts. Therefore, the realistic behavior of the brace and the connection in earthquakes cannot be accurately estimated. The verification of the connection's performance is based on Eurocode design checks, which are however assumed to be conservative.

The chosen element sizes were those set as default in the software and recommended by the IDEA StatiCa user manual. The default size elements allow for quick calculation of results, but some inaccuracy can be expected. The resistance of the connections to design loads might be 5% more than those received by more accurate models. Therefore, a lower utilization ratio might be preferable in design. However, the material model fails to account for effects of strain hardening, and therefore the connections might possess extra strength that is not accounted for in the design checks, especially when yielding of the material is expected. The amount of error caused by these two inaccuracies is assumed to be moderate.

Overall, the component-based finite element method is presumed to produce reliable results in connection modeling. The accuracy of CBFEM has been tested with both laboratory experiments as well as analytical methods. Verifications of the CBFEM with Eurocode-based component method and more accurate research FEM models are presented in the IDEA StatiCa website (Verification examples EN, n.d.). Therefore, the quality of the results obtained by the CBFEM analysis is assumed to be acceptable.

5.5.3 Feature-based costing method

The feature-based costing method has been shown to be accurate in estimating manufacturing costs in European workshops. The unit prices used in this analysis were those applicable for the Finnish fabrication industry. Furthermore, the unit costs were based on four years old information at the time of writing. The cost of labor represents a significant portion of the total cost of a connection, whereas that share would be much smaller in a country with cheaper labor.

As was discovered through the open feedback of the survey, the costs of the connections also depend on the contract with the workshop. Especially when the fabrication takes place in a country with inexpensive labor, the cost of the connection is almost entirely based on its weight. Whereas European workshops tend to include a large variety of fabrication features in the cost estimation, it might be based on only the weight elsewhere.

The feature-based cost estimation was also not entirely accurate, as all possible fabrication features were not considered. For example, the cost of painting and weld inspection were not included in the estimation, as those might be dependent on the project. Cost of transportation and erection was also omitted. The cost of plate parts was also somewhat exaggerated, as their cost included cutting around their perimeter. This would not be necessary for plates of standard size, that could simply be sawed from a flat bar stock.

5.5.4 Survey

Two comments in the open feedback considered it of critical importance to evaluate the connections when they feature more than two diagonal braces and horizontal beams. The simplification to only feature two diagonal members in the connection in the preliminary

analysis was intentional, although it might have affected the questionnaire results. Although no pictures of connections featuring multiple braces and beams were provided, many responders were able to evaluate how well a connection can be applied in such cases.

One responder noted, that answering to the questionnaire was impossible with only pictures of the connections provided. According to them, more detailed information on e.g. dimensioning would have been required. Ideally, a 3D model should have been provided to be able to properly evaluate the connections. However, 93% of responders were able to answer to the questionnaire having only received pictures of the connections as background information. It is still acknowledged that providing more detailed information about the connection types might have yielded somewhat different results.

It is also acknowledged, that evaluating the large and the small connections together in the questionnaire was not ideal, as their geometries might differ significantly. The reasoning for this decision was to keep the questionnaire as short as possible in order to maximize the amount of responses. Evaluation of 11 connections in one questionnaire might have been too time consuming for some responders. The scoring method based on the ranking of the connections is also not accurate in cases where all options are close to equal, as the ranking system used does not account for the magnitude of the difference between options. Furthermore, according to the open feedback, it was sometimes difficult to rank the connections from best to worst, as there are many factors involved in the evaluation. However, it is expected that using the average values of the responses provides useful data that is viable when comparing the connection designs.

6 Conclusions

Earthquakes are destructive natural phenomena, the effects of which must be taken into account in structural design in seismic areas. In the scope of industrial structures, continuity of operation and damage limitation are important objectives of structural design, in addition to protection of human life.

In order to provide safety and to limit the economic losses in strong earthquakes, the structures must be designed according to approved design codes. Design codes are based on decades of research and experience, and they provide a robust basis for structural design. However, the structural designer has a lot of influence on the cost and the weight of connection and bracing design. Therefore, the characteristics of different solutions were compared.

The primary objective of this thesis was to find a diagonal brace connection that could be used as universally as possible in concentrically braced frames built according to different design codes. As was presented in this thesis, the design codes might be based on somewhat different principles. In practical design, the main differences concern the design forces and allowable stresses in the braces. The connections themselves can, however, be somewhat similar between structures designed according to different design codes.

Connections of I-profile braces were found to be generally more lightweight and less expensive compared to the connections of box-profile braces featured in this thesis. The connection type featuring a single gusset plate and two knife plates welded to the brace (CON4(s), see Figure 34) was, however, found to be a simpler design that is sometimes no more expensive than the connection of an I-profile brace. However, they can be significantly heavier than I-profile brace connections due to the large gusset plates.

The survey results reinforc the common conception that different projects require different connection solutions. Especially the open feedback showed that there are many criteria to be considered in selecting the optimal connection. The radar charts created based on the survey results and calculated weight and cost estimates (Figure 50 and Figure 51) can be used to compare the characteristic features of different connections.

Traditionally, the cost effectiveness of the steel frame has been evaluated by its weight, by both the customer and the designer. Therefore, design options featuring low mass have been deemed as good solutions. In such a scenario, connections bolted to the outside of the column flanges featuring either an I-profile or a built-up brace profile (CON1(b/s) and CON3(s), see Figure 30, Figure 31 and Figure 33) could be chosen as the best options in both the small and the large connection categories. Furthermore, their estimated costs are also the lowest in their respective categories. However, adding beams to either of those connection types can be complex and requires extra considerations. Furthermore, frame installation by blocks might be troublesome for CON1, while special attention might be necessary to prevent buckling in CON3.

Where different sized profiles are used, and where simple connection of beams is desired, gusset plate connections and box-profile (or rectangular HSS) braces (CON2(s) and CON4(s), see Figure 32 and Figure 34) are a good option. Both designs have been used in previous projects and deemed satisfactory. The largest disadvantage of both of those connections is their heavy weight. Furthermore, using connection CON4 as a friction-type

connection might not be possible, and therefore it cannot be used in all projects, depending on the friction connection requirements.

Bolted connections used in other brace configurations are of interest in the future. Especially braces in X- and V-configurations are commonly used in the industry. Therefore, finding a connection solution to be used in those scenarios would be useful. Connections of eccentrically braced frames and buckling restrained concentrically braced frames will also need to be studied separately. Furthermore, other types of bolted CBF brace connections than those presented in this thesis can be studied.

Since more recent research has shown that brace connections do not always behave as intended, more testing could be done on the selected connection design. A more sophisticated finite element analysis utilizing solid elements and cyclic loading can be used to verify ductile behavior of the connection. Full-scale frames have also been built and tested in previous studies, although such endeavors require special equipment and funding.

To facilitate the design process of the connections, calculation templates and spreadsheet tools can be used. Such templates typically automatically perform design calculations per applied design codes based on geometry and design load input from the user. Parametric components can also be created and used in Tekla Structures to expedite the modeling of the connection. The development of such tools could be a useful task in future theses or research.

Bibliography

ANSI/AISC 341-16. 2016. Seismic provisions for structural steel buildings. Chicago, Illinois, USA: American institute of steel construction. 480 p.

ANSI/AISC 360-16. 2016. Specification for structural steel buildings. Chicago, Illinois, USA: American institute of steel construction. 620 p.

ASCE/SEI 7-10. 2010. Minimum design loads for buildings and other structures. Reston, Virginia, USA: American Society of Civil Engineers. 595 p.

Bruneau, M. & Uang, C. M. & Sabelli, R. 2011. Ductile design of steel structures. 2nd ed. New York, New York, USA: McGraw-Hill Education. 928 p. ISBN 978-0-07-162523-4.

Brush, D. O. & Almroth, B. O. 1975. Buckling of bars, plates and shells. New York, New York, USA: McGraw-Hill Education. 379 p. ISBN 978-0070085930.

Charney, F. A. 2015. Seismic loads: guide to the seismic load provisions of ASCE 7-10. Reston, Virginia, USA: American Society of Civil Engineers. 272 p. ISBN 978-0-7844-7839-4.

Chen, L. & Tirca, L. 2013. Simulating the seismic response of concentrically braced frames using physical theory brace models. Open journal of civil engineering. Vol. 3:2A. P. 69-81. ISSN 2164-3164.

Chopra, A. K. 2011. Dynamics of structures. 4th ed. New Jersey, USA: Prentice Hall. 992 p. (Prentice-hall international series in civil engineering and engineering mechanics). ISBN 0-13-285803-7.

Costanzo, S. & Raffaele, L. 2017. Concentrically braced frames: European vs. North American seismic design provisions. The open civil engineering journal. [Electronic journal]. Vol. 11:1-11. P. 453-463. [Cited 1 Feb 2019]. ISSN 1874-1495. DOI: 10.2174/1874149501711010453.

Duggal, S. K. 2013. Earthquake-resistant design of structures. 2nd ed. Oxford, United Kingdom: Oxford University Press. 528 p. ISBN 978-0-19-808352-8.

Elnashai, A. S. & Di Sarno, L. 2008. Fundamentals of earthquake engineering. Chichester, United Kingdom: John Wiley & Sons. 366 p. ISBN 978-0-470-02483-6.

Fell, B. V. 2008. Large-scale testing and simulation of earthquake-induced ultra low cycle fatigue in bracing members subjected to cyclic inelastic buckling. [online]. Dissertation. University of California. California. 264 p. [Cited 29 Mar 2019]. Available at: https://datacenterhub.org/resources/1223.

Haahtela, Y. & Kiiras, J. 2015. Talonrakennuksen kustannustieto 2015. Helsinki, Finland: Haahtela-kehitys. 390 p. ISBN 9789525403237.

Haapio, J. 2012. Feature-based costing method for skeletal steel structures based on the process approach. Doctoral dissertation. Tampere University of Technology. Tampere. 99 p. ISBN 978-952-15-2795-1.

Hsiao, P.-C. 2012. Seismic performance evaluation of concentrically braced frames. [online]. Dissertation. University of Washington, department of civil and environmental engineering. [Cited 22 January 2019]. Available at: http://hdl.handle.net/1773/21983.

Hsiao, P.-C. & Lehman, D. E. & Roeder, C. W. 2012. Improved analytical model for special concentrically braced frames. Journal of constructional steel research. Vol. 73. P. 80–94. ISSN 0143-974X.

JouCO2 & COSTi. Metallirakentamisen tutkimuskeskus. [Cited 8 Mar 2019]. Available at: http://metallirakentamisentutkimuskeskus.fi/jouco2-amp-costi.

KH X1-00244. 1998. Kiinteistön ylläpidon kustannuksia ja menekkejä. Helsinki, Finland: Rakennustieto Oy. 8 p.

KH X1-00291. 2001. Kiinteistön ylläpidon kustannuksia ja menekkejä. Helsinki, Finland: Rakennustieto Oy. 7 p.

KH X1-00379. 2006. Kiinteistön ylläpidon kustannusindeksin käyttö. 2000 = 100. 2005, 4. neljännes. Helsinki, Finland: Rakennustieto Oy. 8 p.

Krumpen, R. P. & Carrato, P. J. 2009. Comparative study of bolted versus welded SCBF connections. Proceedings of the 2009 Structures Congress. Austin, Texas, USA. 30.4.–2.5.2009. Reston, Virginia, USA: ASCE. 2012. P. 1-7. ISBN 9780784410318. (DOI: 10.1061/41031(341)148).

Kurejková, M. 2017. Laboratory validation of IDEA StatiCa steel connections and details. [online]. Czech technical university in Prague. [Cited 11 Feb 2019]. Available at: https://resources.ideastatica.com/Content/02_Steel/Verifications/Articles/LABORATORY_VALIDATION_OF_IDEA_STATICA_STEEL_CONNECTIONS_AND_DETAILS.pdf.

Lehman, D. & Roeder, C. & Yoo, J. H. & Johnson, S. 2004. Seismic response of braced frame connections. 13th world conference on earthquake engineering. Vancouver, B.C., Canada. 1.–6.8.2004. Paper No. 1459.

Lumpkin, E. J. & Hsiao, P.-C. & Roeder, C. W. & Lehman, D. E. & Tsai, C.-Y. & Wu, A.-C. & Wei, C.-Y. & Tsai, K.-C. 2012. Investigation of the seismic response of three-story special concentrically braced frames. Journal of constructional steel research. Vol. 77. P. 131–144. ISSN 0143-974X.

Nascimbene, R. & Rassati, G. A. & Wijesundara, K. K. 2012. Numerical simulation of gusset plate connections with rectangular hollow section shape brace under quasi-static cyclic loading. Journal of constructional steel research. Vol. 70. P. 177-189. ISSN 0143-974X.

Nazarko, N. 2018. Kattilalaitoksen teräsrungon suunnittelun tehostaminen aikaisempien projektien avulla. Master's thesis. Tampere university of technology. Tampere. 59 p. Available at: http://www.urn.fi/URN:NBN:fi:tty-201811212663.

Peña, C. & Medalla, M. & López-García, D. & Illanes, R. 2017. NCh2369 vs ASCE7 – Strength vs ductility? Industrial steel braced frames. 16th world conference on earthquake engineering. Santiago, Chile. 9.–13.1.2017.

Roeder, C. W. & Lehman, D. E. & Johnson, S. & Herman, D. & Yoo, J. H. 2006. Seismic performance of SCBF braced frame gusset plate connections. 4th international conference on earthquake engineering. Taipei, Taiwan. 12.–13.10.2006.

Roeder, C. W. & Lehman, D. E. & Lumpkin, E. & Hsiao, P.-C. & Palmer, K. 2008. SCBF gusset plate connection design. North American steel construction conference NASCC. New Orleans, Louisiana, USA. 18.–21.4.2007. Chicago, Illinois, USA: American institute of steel construction AISC. P. 266-282. ISBN 9781604239041.

Roeder, C. W. & Lehman, D. E. & Yoo, J. H. 2005. Improved seismic design of steel frame connections. International journal of steel structures. Vol. 5:2. P. 141–153. ISSN 2093-6311.

Roeder, C. W. & Lumpkin, E. J. & Lehman, D. E. 2011. A balanced design procedure for special concentrically braced frame connections. Journal of constructional steel research. Vol. 67:11. P. 1760–1772. ISSN 0143-974X.

Šabatka, L. & Wald, F & Kabeláč, J. & Gödrich, L. & Navrátil, J. 2014. Component based finite element model of structural connections. [online]. 12th international conference on steel, space and composite structures. Prague, Czech Republic. 28-30.5.2014. [Cited 11 Feb 2019]. Available at: https://resources.ideastatica.com/Content/02_Steel/Verifications/Articles/11_CVUT_Sabatka_SS14_CBFEM_v7_SM.pdf.

Sabelli, R. & Roeder, C. W. & Hajjar, J. F. 2013. Seismic design of steel special concentrically braced frame systems: a guide for practicing engineers. NEHRP seismic design technical brief No. 8. Gaithersburg, Maryland, USA: National Institute of Standards and Technology. [Cited 4 Feb 2019]. Available at: https://www.nehrp.gov/library/techbriefs.htm.

Sen, A. D. & Sloat, D. & Ballard, R. & Johnson, M. M. & Roeder, C. W. & Lehman, D. E. & Berman, J. W. 2016. Experimental evaluation of the seismic vulnerability of braces and connections in older concentrically braced frames. Journal of structural engineering. Vol. 142:9. P. 04016052 (1–15). ISSN 0733-9445.

SFS-EN 1090-2. 2018. Execution of steel structures and aluminium structures. Part 2: Technical requirements for steel structures. Helsinki: Suomen standardoimisliitto SFS. 204p.

SFS-EN 1993-1-1 + AC. 2005. Eurocode 3: Design of steel structures. Part 1-1: General rules for buildings. Helsinki: Suomen standardoimisliitto SFS. 91 p.

SFS-EN 1993-1-8 + AC. 2005. Eurocode 3: Design of steel structures. Part 1-8: Design of joints. Helsinki: Suomen standardoimisliitto SFS. 133 p.

SFS-EN 1998-1. 2004. Eurocode 8: Design of structures for earthquake resistance. Part 1: General rules, seismic actions and rules for buildings. Helsinki: Suomen standardoimisliitto SFS. 229 p.

Shen, J. & Seker, O. & Akbas, B. & Seker, P. & Momenzadeh, S. & Faytarouni, M. 2017. Seismic performance of concentrically braced frames with and without brace buckling. Engineering structures. Vol. 141. P. 461–481. ISSN 0141-0296.

Soules, J. G. & Bachman, R. E. & Silva, J. F. 2016. Chile earthquake of 2010: assessment of industrial facilities around Concepción. Reston, Virginia, USA: American Society of Civil Engineers. [cited 31 Jan 2019]. ISBN 9780784478592 (electronic). Available at: http://dx.doi.org/10.1061/9780784413647.

Strømmen, E. N. 2014. Structural dynamics. Cham, Switzerland: Springer International Publishing. 510 p. (Springer series in solid and structural mechanics 2). ISBN 978-3-319-01801-0.

Sucuoğlu, H. & Akkar, S. 2014. Basic earthquake engineering: from seismology to analysis and design. Cham, Switzerland: Springer International Publishing. 288 p. ISBN: 978-3-319-01025-0.

Tamboli, A. R. 2016. Handbook of structural steel connection design and details. 3rd ed. New York, New York, USA: McGraw-Hill Education. 652 p. ISBN: 978-1-25-958552-4 (electronic).

Tapan, K. S. 2009. Fundamentals of seismic loading on structures. Chichester, United Kingdom: John Wiley & Sons. 406 p. ISBN 978-0-470-01755-5.

Theoretical background. IDEA StatiCa. [Cited 11 Feb 2019]. Available at: https://resources.ideastatica.com/Content/02_Steel/Theoretical_background/1_General.htm

Thornton, W. A. & Muir, L. S. 2009. Design of vertical bracing connections for high seismic drift. Modern steel construction. March 2009. ISSN 0026-8445.

Verification examples EN. IDEA StatiCa. [Cited 17 May 2019]. Available at: https://resources.ideastatica.com/Content/02_Steel/Verifications/EN/EC.htm?tocpath=Connection%7CVerification%20and%20articles%7CVerification%20examples%20%20EN%7C_____0.

Appendices

Appendix 1. Drawings of the connections. 6 pages.
Appendix 2. Bending stiffness diagrams. 4 pages.
Appendix 3. Connection cost calculations. 4 pages.
Appendix 4. Questionnaire translation. 2 pages.

Appendix 1. Drawings of the connections

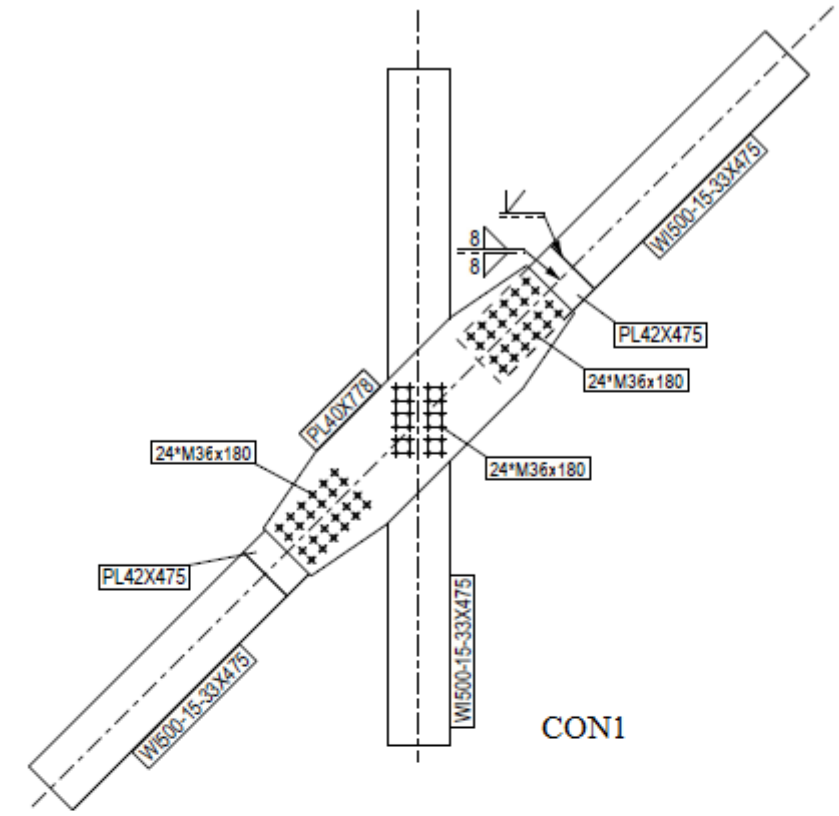

CON1

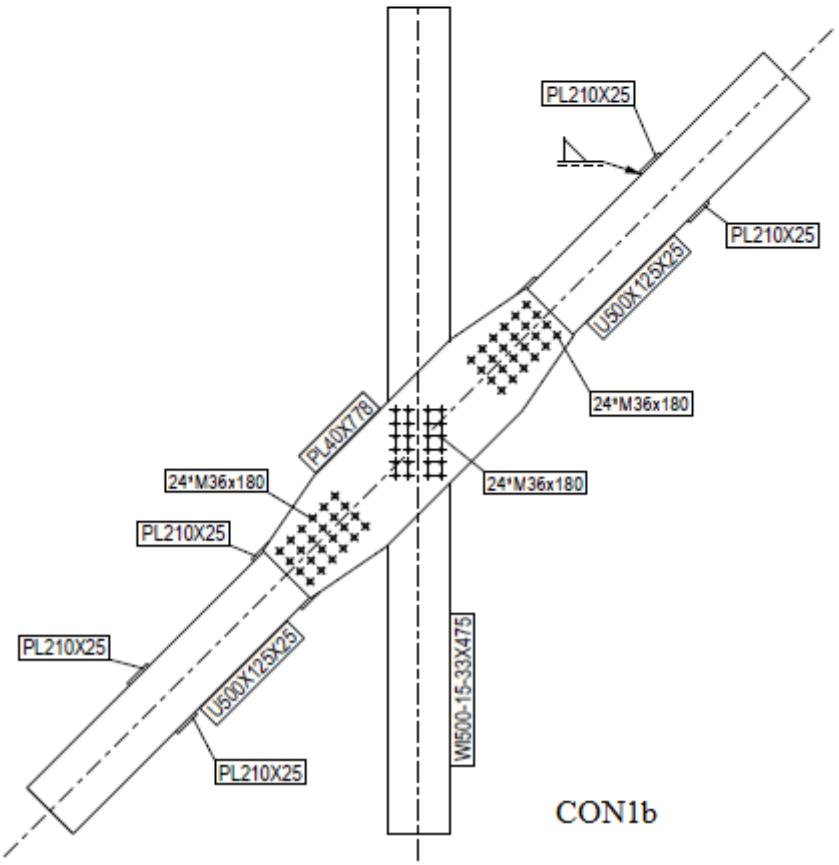

CON1b

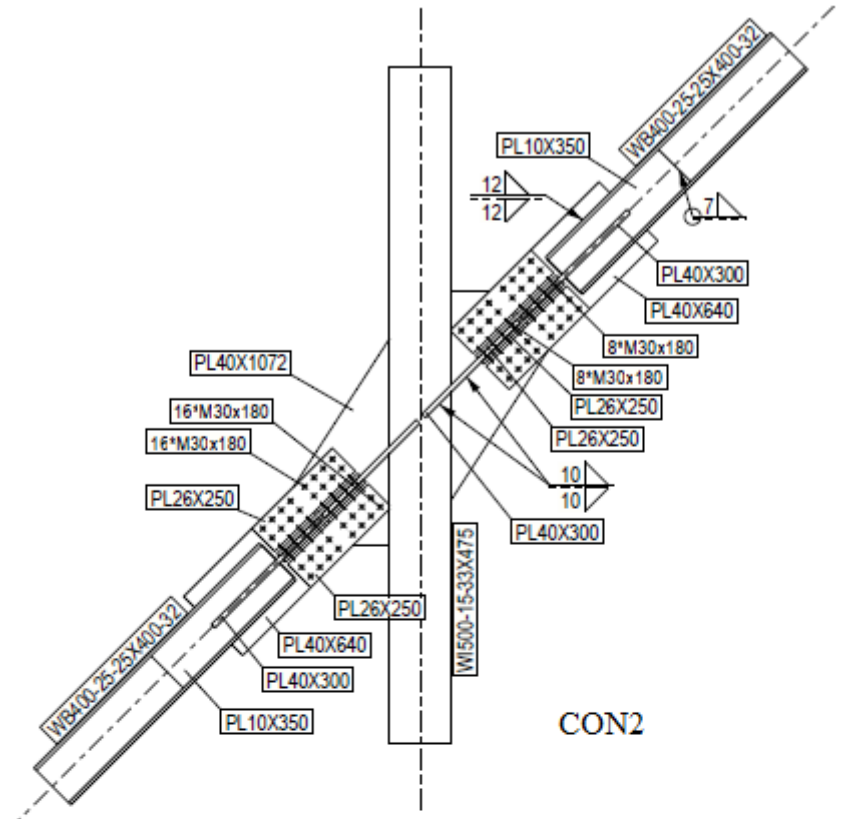
WB400-25-25X400-32
PL10X350
12
12
7
PL40X300
PL40X640
8*M30x180
8*M30x180
PL26X250
PL26X250
10
10
PL40X300
PL40X1072
16*M30x180
16*M30x180
PL26X250
PL26X250
PL40X640
PL40X300
PL10X350
WB400-25-25X400-32
WI500-15-33X475
CON2

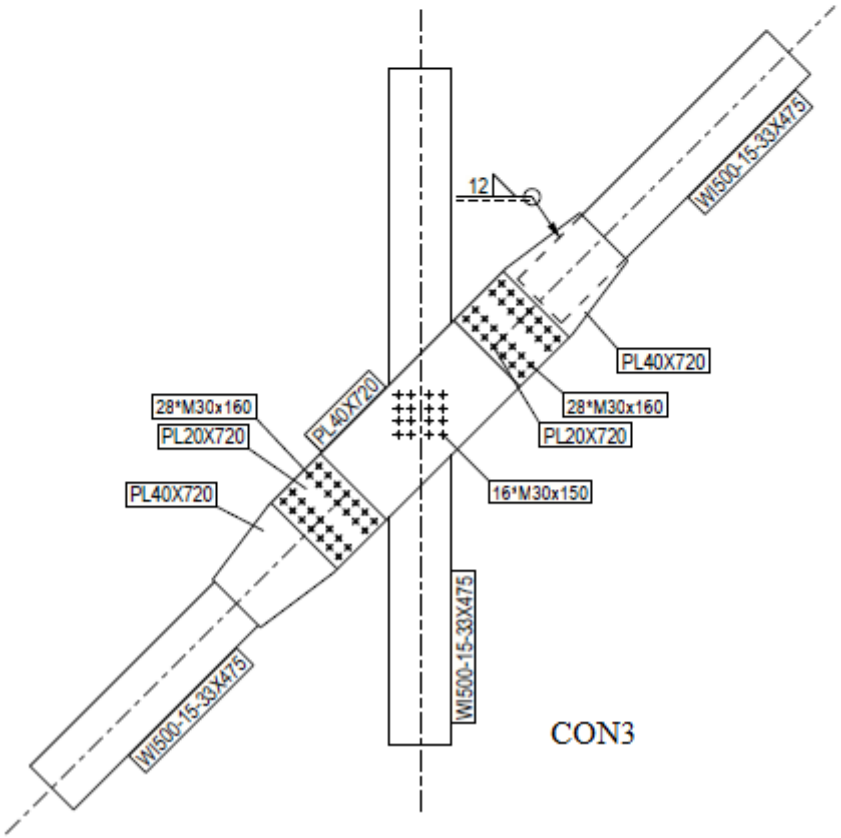
12
WI500-15-33X475
PL40X720
28*M30x160
PL20X720
PL40X720
28*M30x160
PL20X720
16*M30x150
PL40X720
WI500-15-33X475
WI500-15-33X475
CON3

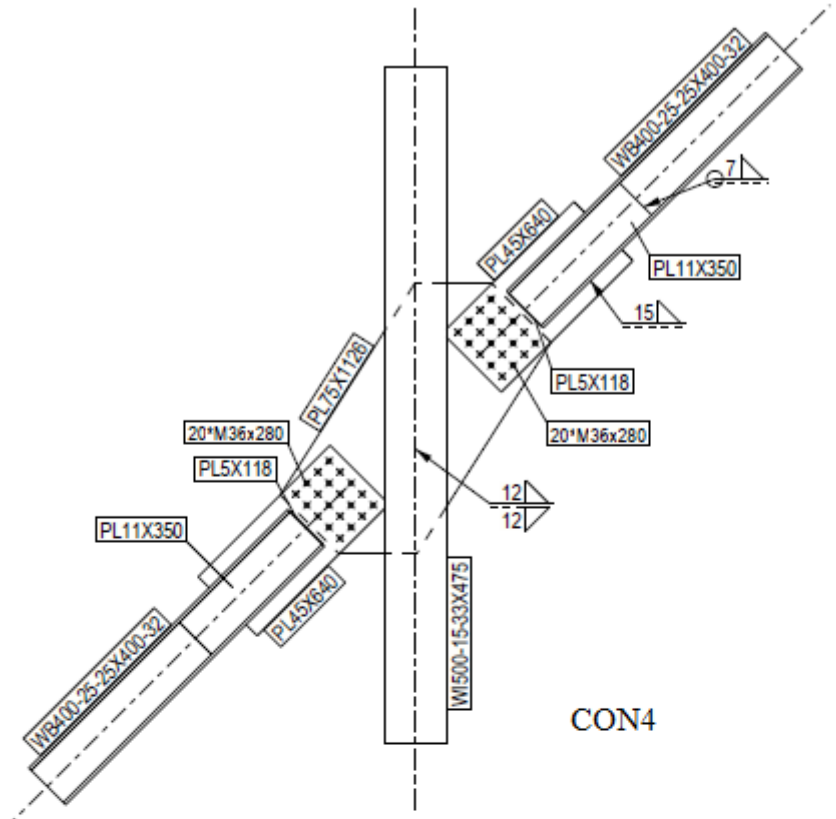
WB400-25-25X400-32
7
PL45X640
PL11X350
15
PL5X118
PL75X1126
20*M36x280
20*M36x280
PL5X118
12
12
PL11X350
PL45X640
WB400-25-25X400-32
WI500-15-33X475

CON4

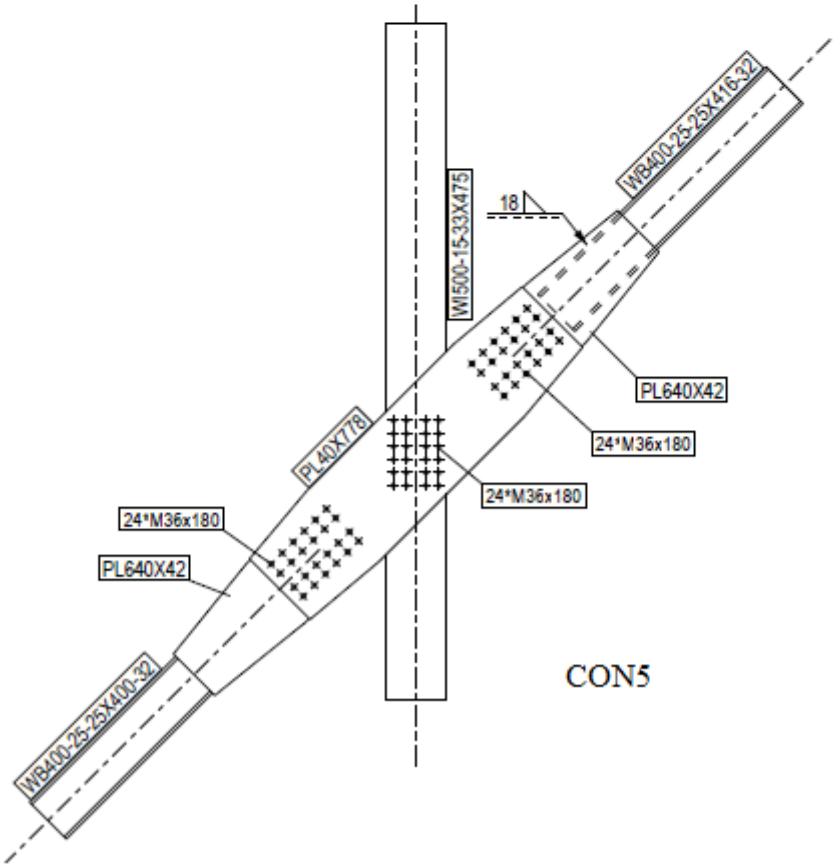
WB400-25-25X416-32
18
WI500-15-33X475
PL640X42
24*M36x180
PL40X778
24*M36x180
24*M36x180
PL640X42
WB400-25-25X400-32

CON5

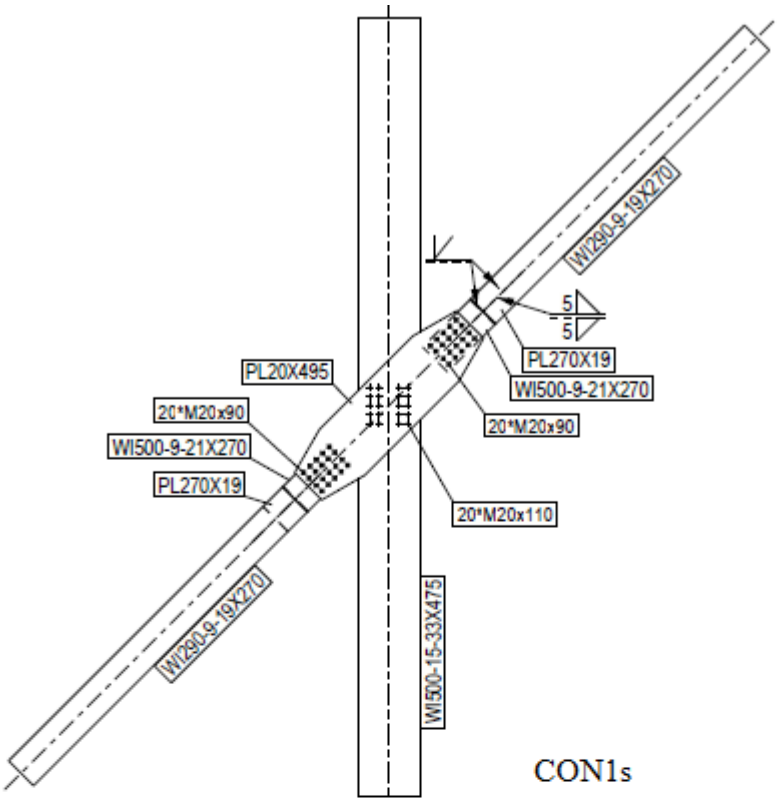
WI290-9-19X270
5
5
PL270X19
WI500-9-21X270
20*M20x90
PL20X495
20*M20x90
WI500-9-21X270
PL270X19
20*M20x110
WI290-9-19X270
WI500-15-33X475

CON1s

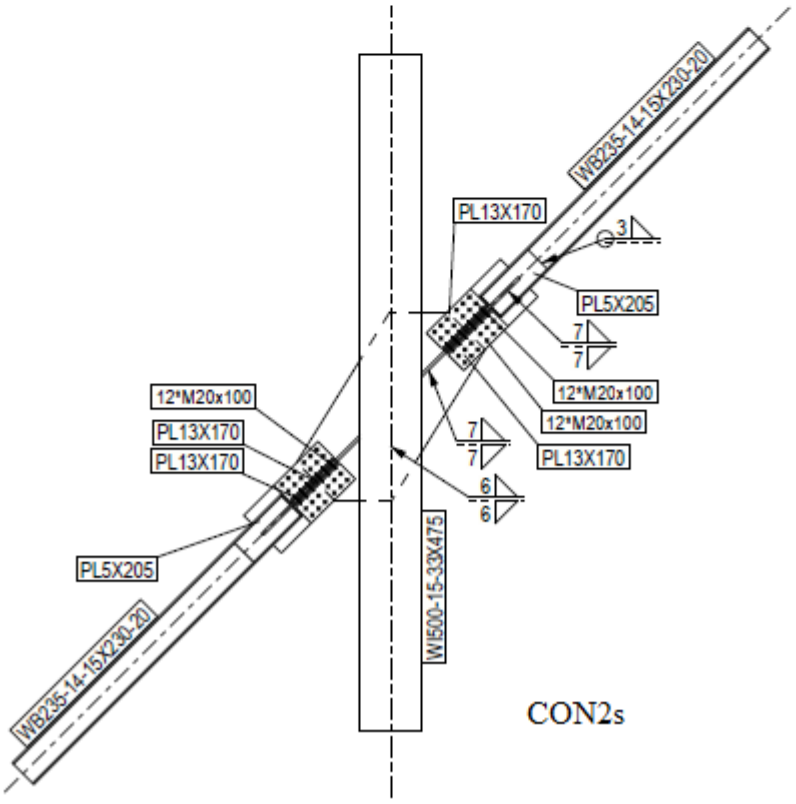
WB235-14-15X230-20
PL13X170
3
PL5X205
7
7
12*M20x100
12*M20x100
PL13X170
7
7
6
6
12*M20x100
PL13X170
PL13X170
PL5X205
WB235-14-15X230-20
WI500-15-33X475

CON2s

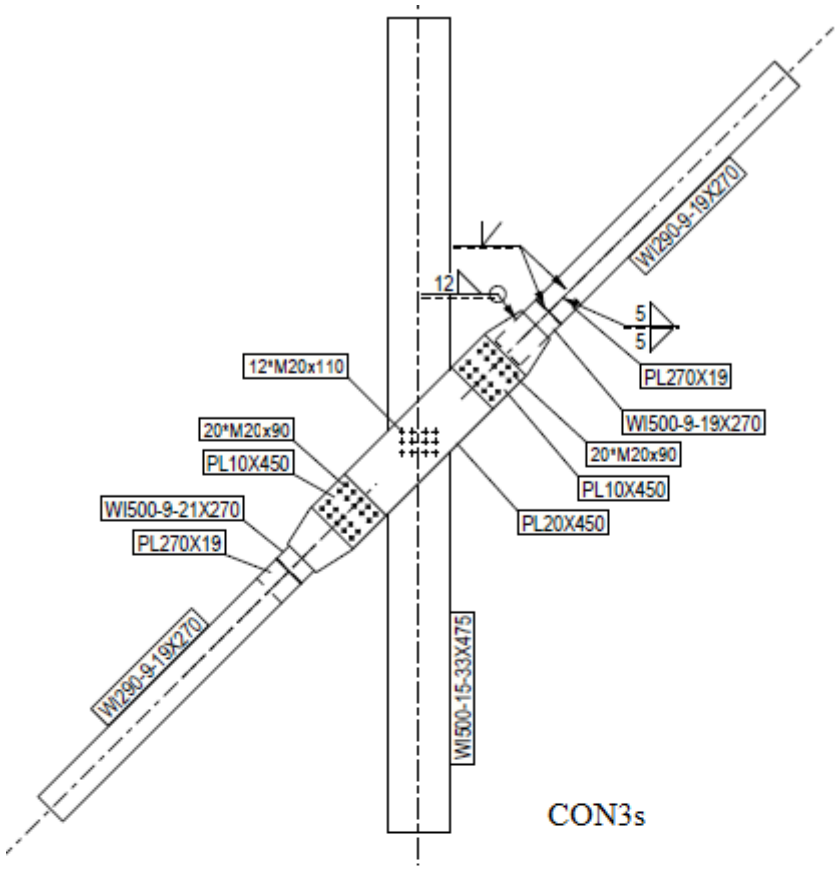
WI290-9-19X270
12
5
5
PL270X19
12*M20x110
WI500-9-19X270
20*M20x90
PL10X450
20*M20x90
PL10X450
WI500-9-21X270
PL20X450
PL270X19
WI290-9-19X270
WI500-15-33X475

CON3s

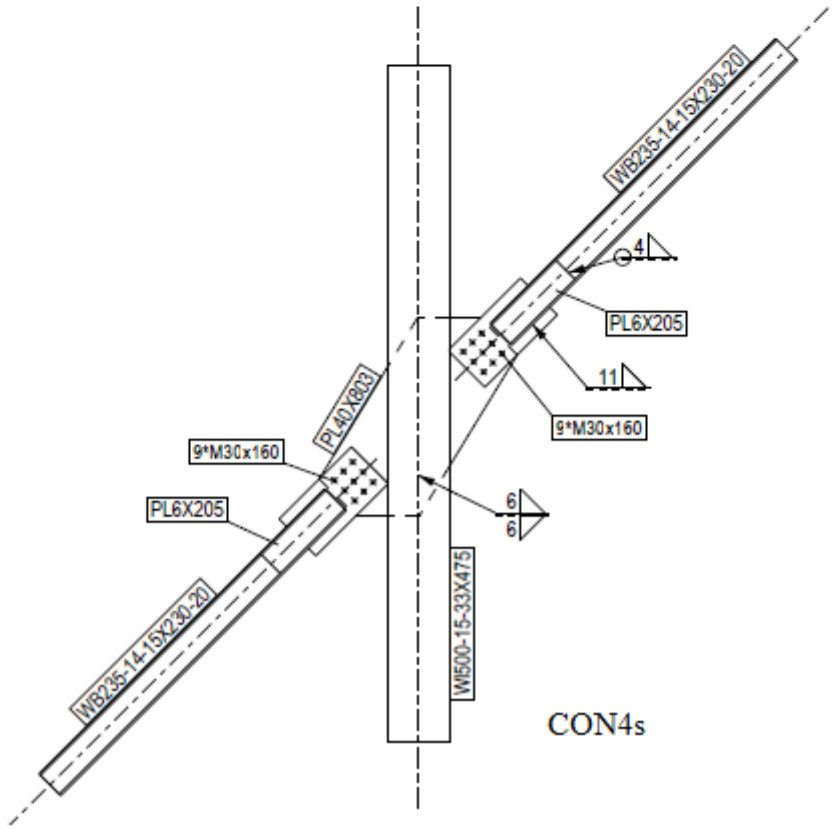
WB235-14-15X230-20
4
PL6X205
11
PL40X803
9*M30x160
9*M30x160
6
6
PL6X205
WB235-14-15X230-20
WI500-15-33X475

CON4s

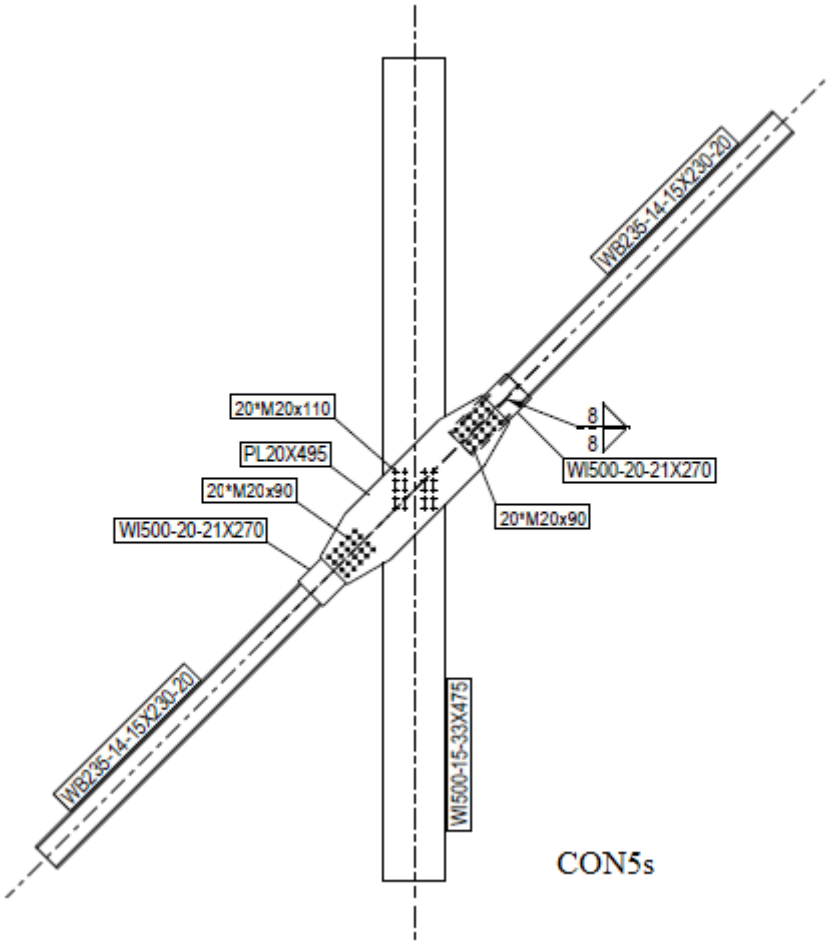
WB235-14-15X230-20
20*M20x110
PL20X495
20*M20x90
WI500-20-21X270
8
8
WI500-20-21X270
20*M20x90
WB235-14-15X230-20
WI500-15-33X475

CON5s

Appendix 2. Bending stiffness diagrams

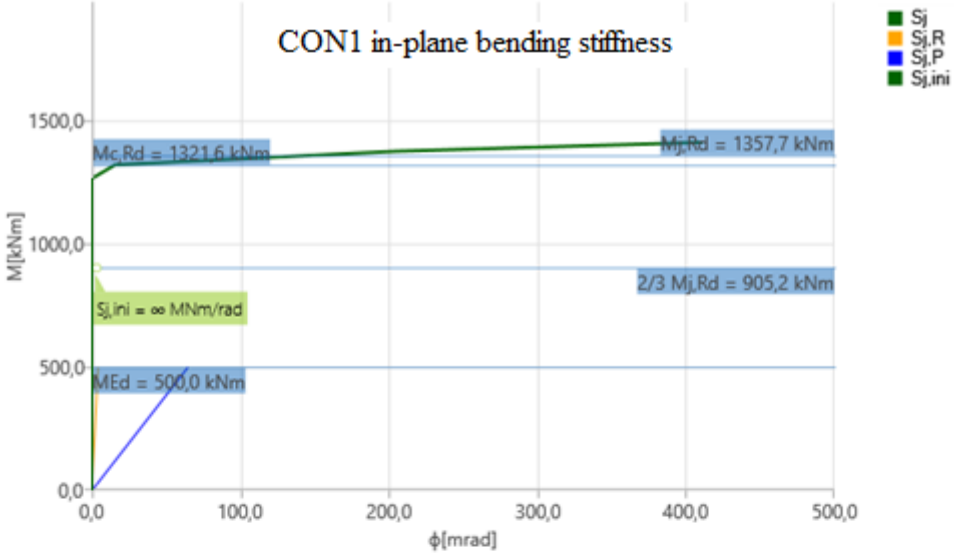

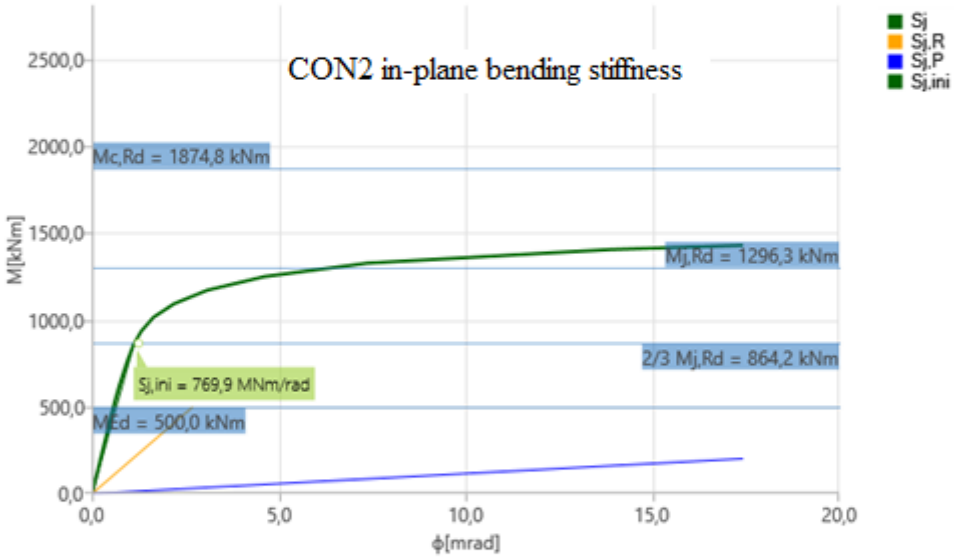

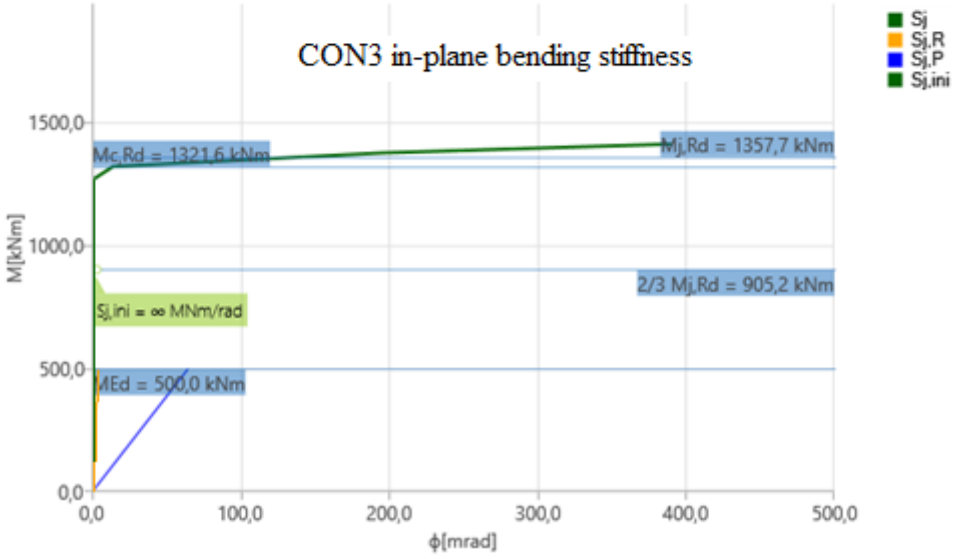

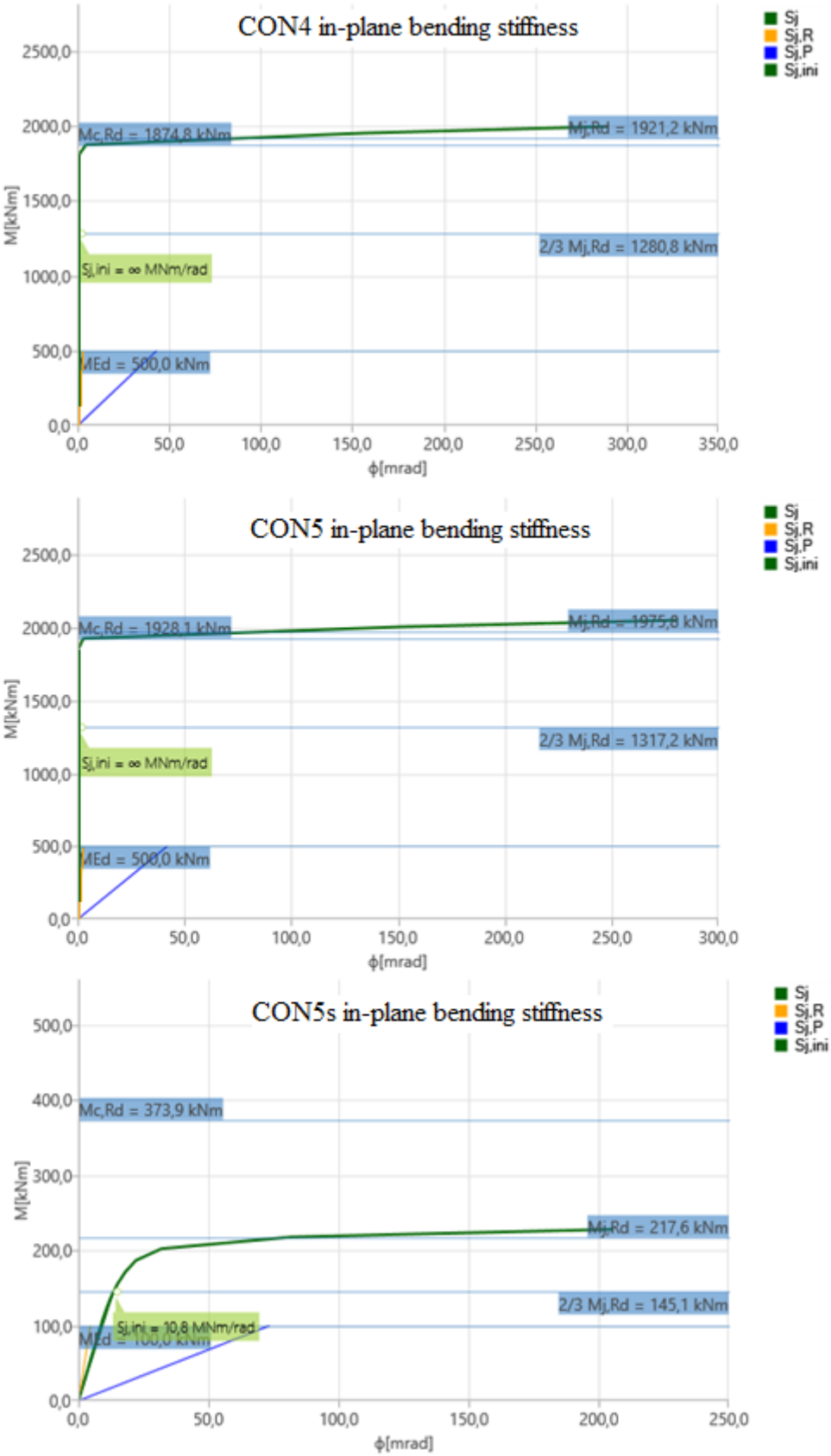
CON4 in-plane bending stiffness
Sj
Sj,R
Sj,P
Sj,ini
M[kNm]
ϕ[mrad]
Mc,Rd = 1874,8 kNm
Mj,Rd = 1921,2 kNm
2/3 Mj,Rd = 1280,8 kNm
Sj,ini = ∞ MNm/rad
MEd = 500,0 kNm
CON5 in-plane bending stiffness
Mc,Rd = 1928,1 kNm
Mj,Rd = 1975,8 kNm
2/3 Mj,Rd = 1317,2 kNm
Sj,ini = ∞ MNm/rad
MEd = 500,0 kNm
CON5s in-plane bending stiffness
Mc,Rd = 373,9 kNm
Mj,Rd = 217,6 kNm
2/3 Mj,Rd = 145,1 kNm
Sj,ini = 10,8 MNm/rad

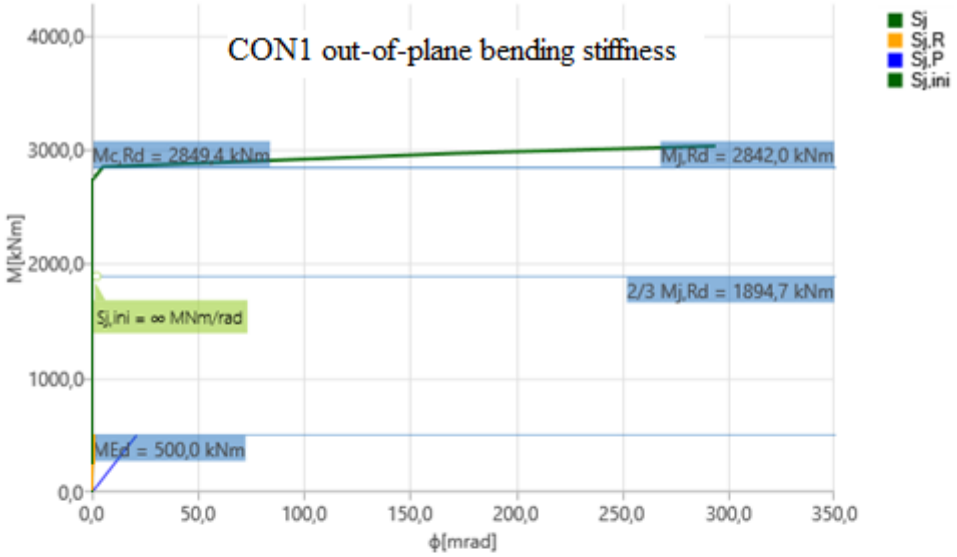
CON1 out-of-plane bending stiffness
Sj
Sj,R
Sj,P
Sj,ini
4000,0
3000,0
2000,0
1000,0
0,0
M[kNm]
Mc,Rd = 2849,4 kNm
Mj,Rd = 2842,0 kNm
2/3 Mj,Rd = 1894,7 kNm
Sj,ini = ∞ MNm/rad
MEd = 500,0 kNm
0,0
50,0
100,0
150,0
200,0
250,0
300,0
350,0
ϕ[mrad]

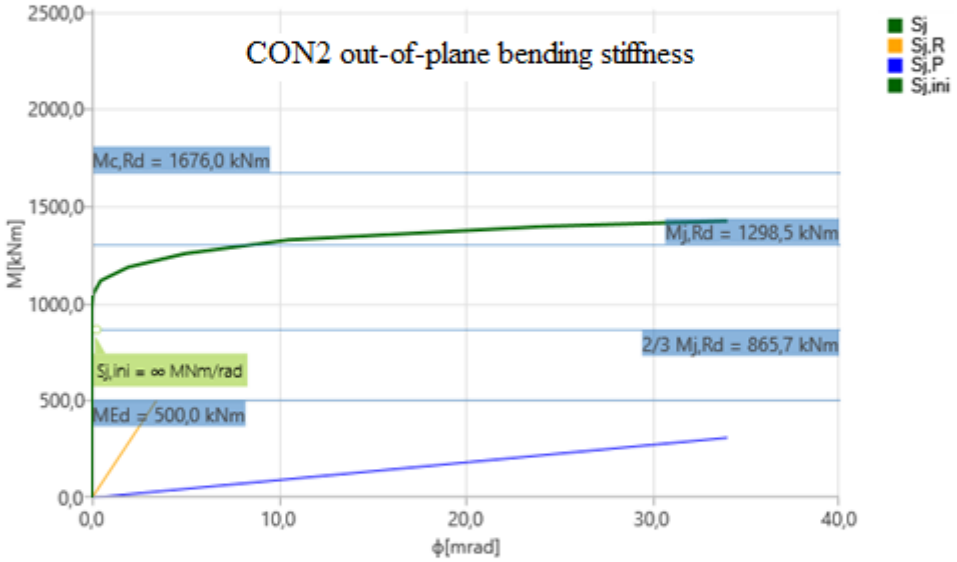
CON2 out-of-plane bending stiffness
Sj
Sj,R
Sj,P
Sj,ini
2500,0
2000,0
1500,0
1000,0
500,0
0,0
M[kNm]
Mc,Rd = 1676,0 kNm
Mj,Rd = 1298,5 kNm
2/3 Mj,Rd = 865,7 kNm
Sj,ini = ∞ MNm/rad
MEd = 500,0 kNm
0,0
10,0
20,0
30,0
40,0
ϕ[mrad]

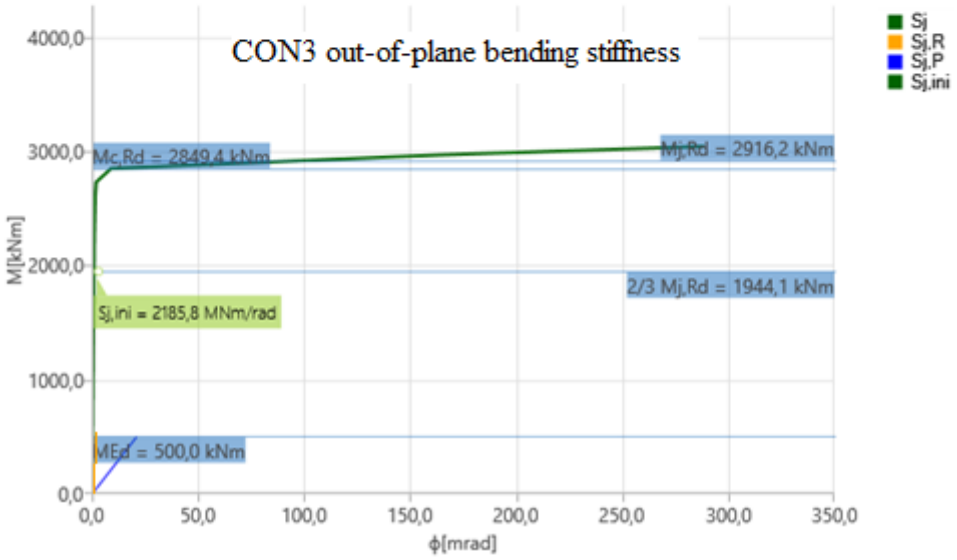
CON3 out-of-plane bending stiffness
Sj
Sj,R
Sj,P
Sj,ini
4000,0
3000,0
2000,0
1000,0
0,0
M[kNm]
Mc,Rd = 2849,4 kNm
Mj,Rd = 2916,2 kNm
2/3 Mj,Rd = 1944,1 kNm
Sj,ini = 2185,8 MNm/rad
MEd = 500,0 kNm
0,0
50,0
100,0
150,0
200,0
250,0
300,0
350,0
ϕ[mrad]

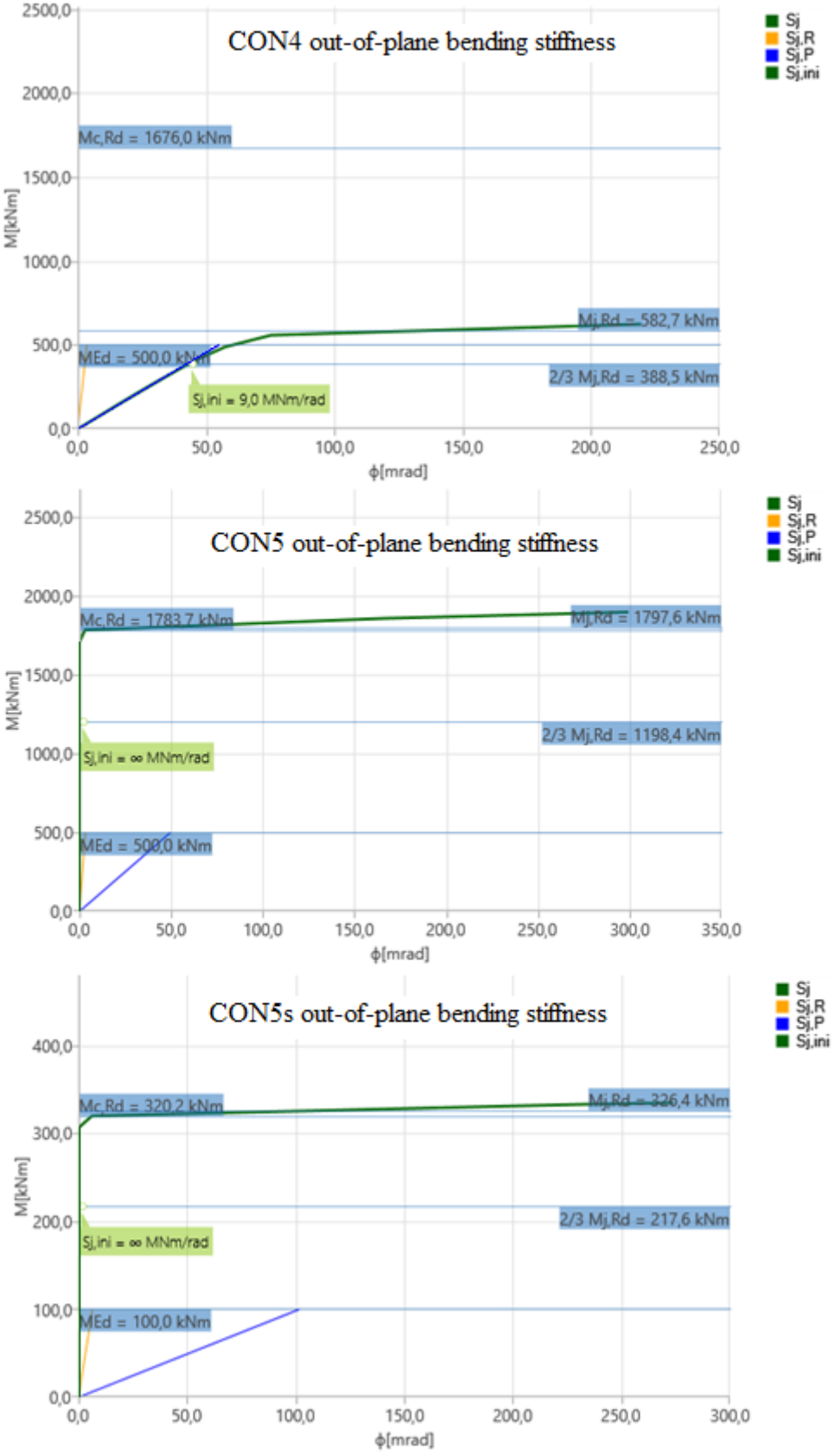
CON4 out-of-plane bending stiffness
Sj
Sj,R
Sj,P
Sj,ini
Mc,Rd = 1676,0 kNm
Mj,Rd = 582,7 kNm
MEd = 500,0 kNm
2/3 Mj,Rd = 388,5 kNm
Sj,ini = 9,0 MNm/rad
M[kNm]
ϕ[mrad]
CON5 out-of-plane bending stiffness
Mc,Rd = 1783,7 kNm
Mj,Rd = 1797,6 kNm
2/3 Mj,Rd = 1198,4 kNm
Sj,ini = ∞ MNm/rad
MEd = 500,0 kNm
CON5s out-of-plane bending stiffness
Mc,Rd = 320,2 kNm
Mj,Rd = 326,4 kNm
2/3 Mj,Rd = 217,6 kNm
Sj,ini = ∞ MNm/rad
MEd = 100,0 kNm

Appendix 3. Connection cost calculations

Connection	Part or fastener	Length (mm)	Net weight (kg)	Material (€)	Cutting (€)	Deburring (€)	Welding (€)	Drilling (€)	Blasting (€)	Assembly (€)	Quantity (-)	Total weight (kg)	Total cost (€)
CON1	Plate PL40X778	2860.0	642.1	849.6	35.9	2.3		97.3	1.2		2	1284.2	1972.5
	Plate PL42X475	1020.0	159.7	194.2	17.8	1.0	178.9	27.4	0.4		4	638.8	1679.1
	Beam WI500-15-33X475	6700.0	1991.2	2417.3	166.7	13.6	251.8				1	1991.2	2849.4
	Bolt + Nut M36, grade 8.8	180.0	2.1	6.3						0.5	144	305.6	971.2
	Washer M36		0.1	2.3							528	68.2	1214.4
											Sum:	4288.0	8686.6
CON1b	Plate PL25X210	420.0	17.3	21.1	6.3	0.4	37.2				8	138.5	519.6
	Plate PL20X450	1020.0	72.1	87.6	7.7	0.9	196.8	20.5	0.4		4	288.2	1255.9
	Plate PL40X778	2860.0	642.1	849.6	35.9	2.3		97.3	1.2		2	1284.2	1972.5
	Beam U500X125X25	6700.0	986.2	1199.2	69.0	13.2	418.2	44.6	0.9		2	1972.4	3490.0
	Bolt + Nut M36, grade 8.8	180.0	2.1	6.3						0.5	144	305.6	971.2
	Washer M36		0.1	2.3							528	68.2	1214.4
											Sum:	4057.1	9423.6
CON2	Plate PL26X250	875.0	44.7	54.3	7.7	0.7		15.6	0.4		16	715.2	1258.2
	Plate PL40X300	1030.0	97.0	118.0	23.5	1.1	133.4	13.1	0.9		4	388.0	1159.7
	Plate PL40X300	1160.0	109.3	132.9	17.2	0.9	167.8	13.1	1.0		4	437.2	1331.7
	Plate PL40X640	1160.0	233.1	283.5	20.1	1.1	155.2	19.4	1.0		2	466.2	960.6
	Plate PL40X1072	2207.0	675.9	903.4	39.5	3.0	299.7	32.2	1.9		1	675.9	1279.6
	Plate PL10X350	1200.0	30.8	40.1	11.6	1.4	54.5				4	123.2	430.6
	Plate PL5X155	180.0	1.1	1.5	4.9	0.2	2.2				8	8.8	70.2
	Beam WB400-25-25X400-32	4890.0	1439.5	1750.4	94.1	17.0	400.4				1	1439.5	2262.0
	Bolt + Nut M30, grade 8.8	180.0	1.4	2.0						0.5	128	178.5	323.2
	Washer M30		0.1	1.3							512	51.1	686.1
											Sum:	4483.6	9761.8
CON3	Plate PL20X720	535.0	60.5	73.5	7.3	0.8		20.2	0.3		8	484.0	817.3
	Plate PL40X720	985.0	200.7	270.8	19.3	1.1	130.4	17.1	0.4		4	802.8	1756.5
	Plate PL40X720	1950.0	440.9	536.1	27.6	1.7		59.8	0.8		2	881.8	1251.9
	Beam WI500-15-33X475	5410.0	1607.9	1951.8	115.4	11.2	207.2				1	1607.9	2285.6
	Bolt + Nut M30, grade 8.8	160.0	1.3	1.9						0.5	112	143.8	269.4
	Bolt + Nut M30, grade 8.8	150.0	1.2	1.8						0.5	32	39.3	73.7
	Washer M30		0.1	1.3							288	25.6	385.9
											Sum:	3985.1	6840.3

Connection	Part or fastener	Length (mm)	Net weight (kg)	Material (€)	Cutting (€)	Deburring (€)	Welding (€)	Drilling (€)	Blasting (€)	Assembly (€)	Quantity (-)	Total weight (kg)	Total cost (€)
CON4	Plate PL11X350	1200.0	36.3	44.1	6.3	1.0	64.2				4	145.1	462.2
	Plate PL20X77	400.0	4.8	5.9	5.7	0.3	16.0				2	9.7	55.7
	Plate PL45X640	1430.0	323.3	393.1	23.6	1.3	147.3	25.2	0.6		4	1293.2	2364.4
	Plate PL75X1126	2384.0	1435.8	1994.5	61.8	3.6	319.3	61.7	2.0		1	1435.8	2442.9
	Plate PL5X118	360.0	1.7	2.2	5.0	0.3	4.3				4	6.6	47.5
	Beam WB400-25-25X400-32	5620.0	1654.4	2011.7	94.9	17.2	457.2				1	1654.4	2581.0
	Bolt + Nut M36, grade 8.8	280.0	2.9	8.3						0.5	40	116.9	352.0
	Washer M36		0.1	2.3							160	20.7	368.0
											Sum:	4682.3	8673.8
CON5	Plate PL40X778	2960.0	696.8	879.3	36.7	2.4		97.3	1.3		2	1393.7	2033.8
	Plate PL25X416	990.0	80.8	98.3	8.4	0.9	220.2				4	323.3	1310.9
	Plate PL42X640	1710.0	333.0	438.8	25.3	1.5	154.2	28.4	0.7		4	1331.8	2595.6
	Plate PL5*286	350.0	3.9	5.3	5.1	0.4	5.4				2	7.8	32.4
	Beam WB400-25-25X400-32	4955.0	1458.6	1773.7	92.2	17.1	421.8				1	1458.6	2304.7
	Bolt + Nut M36, grade 8.8	180.0	2.1	6.3						0.5	144	305.6	971.2
	Washer M36		0.1	2.3							528	68.2	1214.4
											Sum:	4888.9	10463.1

Connection	Part or fastener	Length [mm]	Net weight [kg]	Material [€]	Cutting [€]	Deburring [€]	Welding [€]	Drilling [€]	Blasting [€]	Assembly [€]	Quantity [-]	Total weight [kg]	Total cost [€]
CON1s	Plate PL9X210	458.0	5.3	8.3	5.3	0.4	22.0				2	10.5	72.1
	Plate PL20X495	1760.0	125.21	166.3	9.3	1.4		49.1	0.8		2	250.4	453.9
	Plate PL19X270	234.0	9.4	11.4	5.7	0.3	38.3				4	37.8	222.5
	Beam WI290-9-19X270	5540.0	544.8	658.2	41.8	11.0	89.2				1	544.8	800.3
	Beam WI500-9-21X270	520.0	63.1	76.9	18.4	1.6	26.8	31.1	0.5		2	126.2	310.6
	Bolt + Nut M20, grade 8.8	90.0	0.3	0.8						0.5	80	27.2	106.9
	Bolt + Nut M20, grade 8.8	120.0	0.4	1.0						0.5	40	16.5	60.8
	Washer M20		0.0	0.4							240	9.2	103.2
											Sum:	1022.6	2130.4
CON2s	Plate PL5X103	105.0	0.4	0.6	4.8	0.1	2.5				8	3.4	64.0
	Plate PL5X205	510.0	3.9	5.5	10.1	0.7	7.7				4	15.4	95.6
	Plate PL13X170	480.0	8.3	10.0	5.5	0.4		10.8	0.2		16	133.3	431.2
	Plate PL20X195	555.0	17.0	20.7	6.2	0.5	57.7	9.6	0.5		4	68.0	380.8
	Plate PL20X195	820.0	25.1	30.5	6.8	0.6	51.8	9.6	0.7		4	100.4	400.3
	Plate PL20X410	555.0	35.7	43.4	6.7	0.6	39.4	12.5	0.4		2	71.5	206.0
	Plate PL20X775	1690.0	186.1	250.1	16.6	2.5	55.4	17.5	0.7		1	186.1	342.7
	Beam WB235-14-15X230-20	5830.0	578.5	696.5	60.6	17.0	183.5				1	578.5	957.5
	Bolt + Nut M20, grade 8.8	100.0	0.4	0.9						0.5	96	34.9	135.0
	Washer M20		0.0	0.4							288	11.0	123.8
											Sum:	1202.4	3136.9
CON3s	Plate PL9X210	458.0	5.3	8.3	5.3	0.4	22.0				2	10.5	72.1
	Plate PL10X450	360.0	12.7	15.5	5.5	0.5		13.4	0.2		8	101.8	280.3
	Plate PL20X450	500.0	31.9	43.0	6.6	0.6	64.9	10.9	0.4		4	127.7	505.8
	Plate PL20X450	1500.0	106.0	128.9	8.7	1.2		32.6	1.3		2	212.0	345.3
	Plate PL19X270	234.0	9.4	11.4	5.7	0.3	43.8				4	37.8	244.6
	Beam WI290-9-19X270	4760.0	468.1	565.6	38.1	9.6	79.5				1	468.1	692.7
	Beam WI500-9-19X270	450.0	50.9	61.7	17.6	1.5	25.9				2	101.8	213.4
	Bolt + Nut M20, grade 8.8	90.0	0.3	0.8						0.5	80	27.1	106.9
	Bolt + Nut M20, grade 8.8	110.0	0.4	1.0						0.5	24	9.3	35.4
	Washer M20		0.0	0.4							256	9.8	110.1
											Sum:	1059.6	2354.3

Connection	Part or fastener	Length [mm]	Net weight [kg]	Material [€]	Cutting [€]	Deburring [€]	Welding [€]	Drilling [€]	Blasting [€]	Assembly [€]	Quantity [-]	Total weight [kg]	Total cost [€]
CON4s	Plate PL5X73	215.0	0.6	0.8	4.9	0.2	3.0				4	2.5	35.6
	Plate PL6X205	700.0	6.8	8.7	5.3	0.6	13.0				4	27.0	110.3
	Plate PL10X42	235.0	0.8	0.9	4.9	0.2	9.9				2	1.5	31.8
	Plate PL22X400	785.0	54.2	65.9	7.4	0.8	71.6	12.1	0.3		4	216.9	632.6
	Plate PL40X803	1795.0	408.2	550.4	33.2	2.4	238.2	17.6	1.5		1	408.2	843.3
	Beam WB235-14-15X230-20	6200.0	615.2	740.7	66.2	17.4	193.8				1	615.2	1018.1
	Bolt + Nut M30, grade 8.8	160.0	1.3	1.9							18	23.1	34.4
	Washer M30		0.1	1.3							18	1.6	24.1
											Sum:	1296.1	2730.2
CON5s	Plate PL20X495	1760.0	125.2	166.3	9.3	1.4		49.1	0.8		2	250.4	453.9
	Plate PL5X165	210.0	1.4	1.8	4.9	0.2	3.6				2	2.7	21.2
	Beam WB235-14-15X230-20	7000.0	694.6	836.3	66.8	19.9	216.2				1	694.6	1139.2
	Beam WI500-20-21X270	630.0	101.4	123.3	20.2	1.8	99.9	31.5	0.5		2	202.8	554.7
	Bolt + Nut M20, grade 8.8	90.0	0.3	0.8						0.5	80	27.1	106.9
	Bolt + Nut M20, grade 8.8	110.0	0.4	1.0						0.5	40	15.5	58.8
	Washer M20		0.0	0.4							240	9.2	103.2
											Sum:	1202.4	2438.0

Appendix 4. Questionnaire translation

Survey of concentric brace connections in earthquakes

This questionnaire is a part of a Master's thesis study by Sebastian Muuronen conducted together with Sweco. The object of the questionnaire is to rank the enclosed industrial seismic brace connections from best to worst. The connections have been designed for the nominal plastic normal force capacity of the brace.

Link to pictures of the connections (large and small versions)

How well do you believe to be able to evaluate seismic brace connections of steel structures?

	Well
	Somewhat
	Not very well

Ease of design (how long it takes to perform calculations and model)

	CON1(b/s)	CON2(s)	CON3(s)	CON4(s)	CON5(s)
Easiest					
Second easiest					
Third easiest					
Fourth easiest					
Fifth easiest					

Simplicity of the connection (conceptual simplicity and unambiguity of mechanical performance)

	CON1(b/s)	CON2(s)	CON3(s)	CON4(s)	CON5(s)
Simplest					
Second simplest					
Third simplest					
Fourth simplest					
Fifth simplest					

Ease of installation

	CON1(b/s)	CON2(s)	CON3(s)	CON4(s)	CON5(s)
Easiest					
Second easiest					
Third easiest					
Fourth easiest					
Fifth easiest					

Which connection do you believe the customer would prefer?

	CON1(b/s)	CON2(s)	CON3(s)	CON4(s)	CON5(s)
Most preferable					
Second preferable					
Third preferable					
Fourth preferable					
Fifth preferable					

Open feedback
